NIGERIAN MINING JOURNAL

ISSN 1117 - 4307

Volume 17 Number 1 November 2019

A Publication of

NIGERIAN SOCIETY OF MINING ENGINEERS

NIGERIAN MINING JOURNAL

Volume17 - Number 1 - November 2019

Table of Contents

NIGERIAN MINING JOURNAL

ISSN 1117-4307

Volume 17 | Number 1 | November 2019

A PUBLICATION OF THE NIGERIAN SOCIETY OF MINING ENGINEERS

Editor-in-Chief

I. S. Amoka

Publisher

Nigerian Society of Mining Engineers (NSME)
NSME Secretariat, Bukuru,
P.M.B. 2036,Jos, Plateau State, Nigeria

(c) Nigerian Society of Mining Engineers

All rights preserved. No part of this publication may be reproduced, stored, in a retrieval system or transmitted in any form or by any means without the prior permission of the Nigerian Society of Mining Engineers

Cover Page

Sluice box operation at AAY International Company gold mining site Popo Niger, Borge Local Government of Niger Ste.

Editorial Address

Gems Mining & Geoexploration Consult,
P. O. Box 9489, Kaduna
Tel: +2348062262221, +2348023636689
Email: nigerianminingjournal@gmail.com
Website: www.nsme.org.ng

NIGERIAN MINING JOURNAL
Editorial Board

Editor-in-Chief
Engr. Dr. I. S. Amoka
Gems Mining & Geoexploration Consult, Kaduna, Nigeria

Editors
B.M. Olaleye, Federal University of Technology, Akure

E.O.A. Damisa, Kaduna Polytechnic, Kaduna

B.S. Jatau, Nasarawa State University, Keffi

B.O. Nwude, National Steel Raw Materials Agency, Kaduna

John A. Ajayi, Federal University of Technology, Akure

S.A. Yaro, Ahmadu Bello University, Zaria

J. S Mallo University of Jos, Jos

D.G. Thomas, Ahmadu Bello University, Zaria

P.I. Olasehinde, Federal University of Technology, Minna

J. M. Akande, University of Namibia, Namibia

J. I. Nwosu, University of Port Harcourt, Port-Harcourt

O. A. W. Oyeladun, Kaduna Polytechnic, Kaduna

L. K. Salati, Kaduna Polytechnic, Kaduna

Editorial Advisers
Musa Nashuni
Nuru A. Yakubu
G.M. Sheikh
M.K. Amate

NIGERIAN SOCIETY OF MINING ENGINEERS (NSME)
Council

Executive Members

President:
Engr. Dr. E.O.A. Damisa, FNSME

1st Vice President:
Engr. Prof. B. M. Olaleye, FNSME

2nd Vice President:
Prof. B. S. Jatau, FNSME

Secretary-General
Engr. U. A. Hassan, FNSME

Assistant Secretary:
Engr. Omoruyi, John Bull

Treasurer:
Engr. John Marshall

Financial Secretary:
Engr. Adigun Fatai

Publicity Secretary:
Engr. A. D. Bida

Social Secretary:
Engr. A. O. Adetunji, FNSME

Auditor:
Engr. Anthony U. Ojile, FNSME

Editor- in-Chief:
Engr. Dr. I. S. Amoka, FNSME

Members-in-Council
Engr B.O. Nwude, FNSME, IPP
Engr. Princess (Mrs,) Florence Diejomaoh
Engr. Dr. Luqman K. Salati
Engr. Adeyemo Jacob Titilope
Engr. Oyebola A. W. Oyeladun
Engr. Dr. Dungka G. Thomas

Fellows - in - Council
Engr. S.O. Oladipo, FNSME.
Engr. M. Sanusi Jibril, FNSME

Institutional Members in Council
Julius Berger
Shell Petroleum Development Company

Yashe, et al (2019) Nigerian Mining Journal, (16) 1 - 11
© Nigerian Society of Mining Engineers, ISBN 1117 - 4307

Geology and Geochemistry of Ilmenite Mineral in Malumfashi Schist Belt

*Yashe J. H., *Ibrahim A. A. and **Bello A.
*Department of Geology, Ahmadu Bello University, Zaria.
**Department of Petroleum & Mineral Resources Engineering, Kaduna Polytechnic, Kaduna.
Jyhalliru81@gmail.com, alykazy@gmail.com and abubakardtm@gmail.com,

Abstract
The geology, geochemistry and the economic potential of Ilmenite occurrence in sheet 79 Malumfashi NW is presented in this study. The field and petrographic studies revealed that, the area consists of largely muscovite and carbonaceous schist together with Granite as major rocks. Tourmalinites and quartzite as minor rocks. Numerous quartz veins of various sizes trending NS parallel to the foliation of the schist are present throughout representing a silicification episode. The outcrop contains quartz veins which may be the possible host of the mineralization (Ilmenite). The mineralization occurs in nodules within the quartz veins and it also comes in nuggets and in some places as a smaller fragment scattered within the quartz veins. They show lack of cleavage and have a buggy texture. Based on the major oxide geochemistry, the schist in the study area have high silica (SiO_2) composition of (95.49 – 97.21 wt. %). Titanium oxide (TiO_2) is (73.73 – 82.71 wt. %) and Iron oxide (Fe_2O_3) composition of (14.51 – 75.23 wt. %). The fact that Fe_2O_3 and TiO_2 forms Ilmenite rather than any other mineral indicates that the hydrothermal solution is oxidizing,and related to dehydration related to prograde metamorphism of shale. Ilmenite is a primary source of titanium metal, which when combined with other metals produces durable high strength light weight alloys. These alloys are used to manufacture a wide variety of high performance tools. A form of titanium dioxide is used to produce white high refractive pigments.
Keywords: Geology, Geochemistry, Ilmenite, prograde, titanium.

Introduction

Ilmenite is a primary metal in mafic igneous rock. It is often concentrated into layers by process called Magmatic Segregation. Through these processes ilmenite crystals are then formed by crystallizing out of magma relatively early before most of the other minerals and as a result, the most heavier crystals of ilmenite fall into bottom of the magma chamber and then readily collected in layers.

It can also be found occurring in pegmatite and in some metamorphic rock as well as in the sedimentary rocks that are formed from the weathering and erosion of them. The best field indicators of mineral ilmenite usually include crystal habit, lack of cleavage, streak association, density and lustre. In this study, the field occurrence, petrography and geochemistry of ilmenite in the area east of Malumfashi town is studied. This is necessary because this is the first-time ilmenite occurrence is reported in the area.

The Nigerian Basement

The Nigerian basement lies in the area east of the West African Craton and northwest of the Congo Craton, and south of the Tuareg shield (Hoggar massif (Fig. 2). The region was affected by the Pan-African orogeny about 600 Ma. It is believed that the Pan-African belt evolved by plate tectonics processes which involved collision between the passive margin of West African Craton and the active margin of the Tuareg shield about 600 Ma (Black *et al*., 1979; Ajibade*et al*., 1987). The collision at the cratonic margin led to the reactivation of the internal region of the Pan African belt.

The geology of the basement rocks of Nigeria has been described and reviewed by many workers including Oyawoye (1970); McCurry (1976); Rahaman (1976); Turner (1983); Fitches *et al*. (1985) and Ajibade*et al*., (1987); McCurry (1976); Garba (2003); Dada (2006, 2008); Baba *et al*. (2006), developed a general geochronological classification of the Precambrian basement complex rocks of Nigeria, shown in Table 1 (Ibrahim, 2010). The Nigerian Pan-African basement is (Fig. 2), on the basis of rock types, divided into three units (Fitches *et al*., 1985; Ajibade*et al*., 1987), thus:

i. Polymetamorphic Migmatite-Gneiss Complex.
ii. The schist belt (Metasediments)
iii. Older Granite suite

The area of study is located within the Federal Survey of Nigeria sheet 79 Malumfashi NW situated within Malumfashi Local Government Area of Katsina State which shears boundaries with Kankara. Musawa. Bakori. Kafur, and Dutsinma Local Government Areas. And the study area is about 40km^2 bounded by latitude 11°47'00"N and 11°46'00"N, and longitude 7°37'55"E and 7°42'00"E (Figure1).

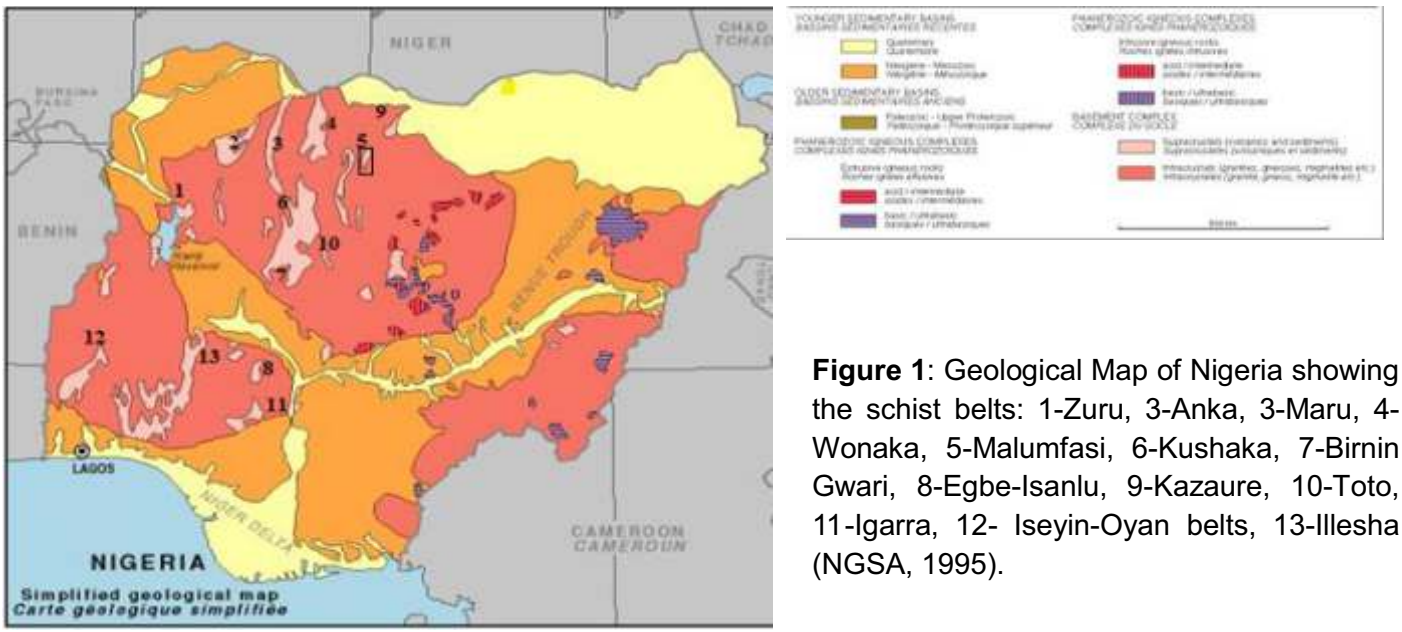

Figure 1: Geological Map of Nigeria showing the schist belts: 1-Zuru, 3-Anka, 3-Maru, 4-Wonaka, 5-Malumfasi, 6-Kushaka, 7-Birnin Gwari, 8-Egbe-Isanlu, 9-Kazaure, 10-Toto, 11-Igarra, 12- Iseyin-Oyan belts, 13-Illesha (NGSA, 1995).

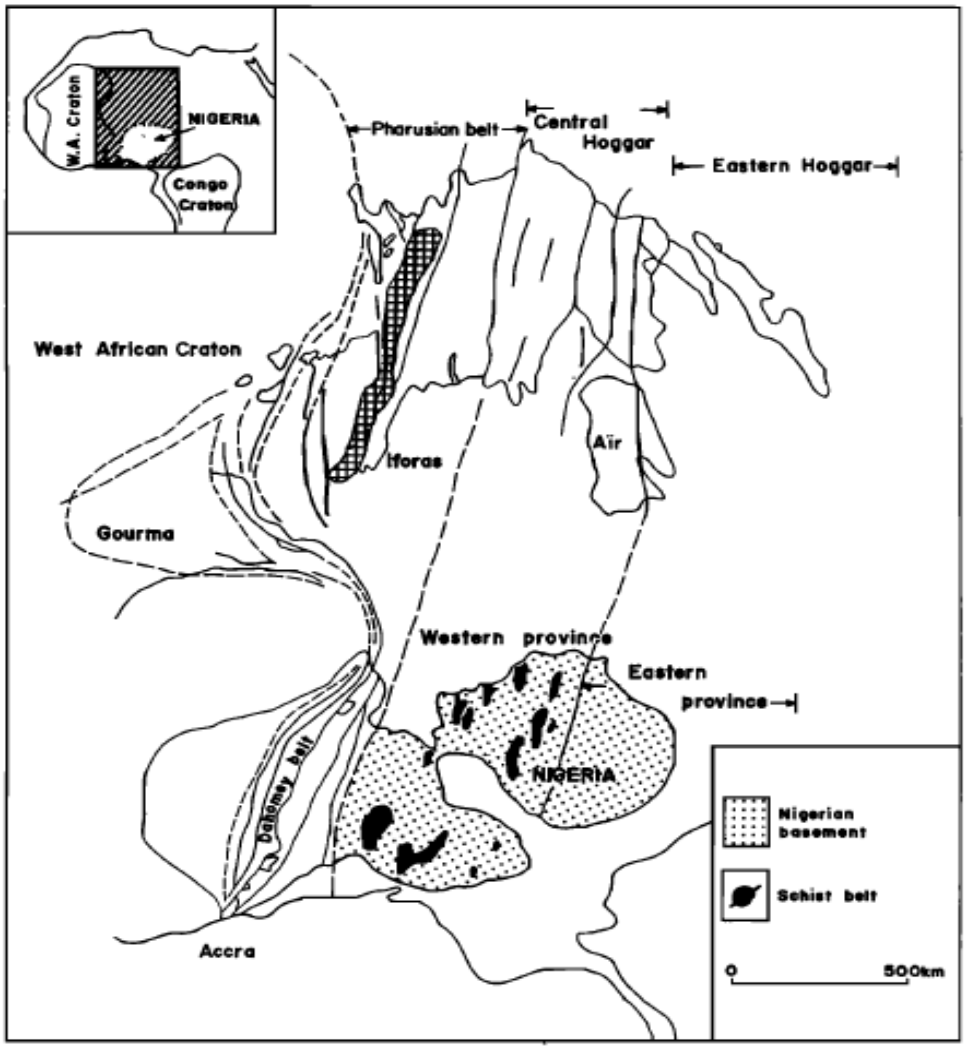

Figure 2. Location of the Nigerian Basement Complex (After Ajibade *et al*., 1987)

The Schist Belts

The Nigerian schist belts occur in a 300 to 400 km wide zone, and predominantly west of longitude 8º E, which trends NNE, parallel to the boundary between the Pan-African province and the West African Craton (Turner, 1983; Fitches *et al*., 1985; Ajibade *et al*., 1987; Adekoya, 1996). These schist belts are believed to belong to the Pan-African marginal basin development (Turner, 1983; Fitches *et al*., 1985). However, the Nigerian schist belts are believed to have evolved by plate tectonic processes. They are described as having been deposited on a back – arc basin, which developed after the onset of subduction at the cratonic margin at about 1000Ma. Closure of the ocean at the cratonic margin about 600Ma and crustal thickening to the east led to the deformation and metamorphism of the sediments (Ajibade *et al*., 1987).

Methodology

The work was carried out with the use of a topographic base map of Sheet 79 (Malumfashi) NW, which was gridded to aid locating positions, and mark places where lithological units were identified using Global Positioning System (GPS). Photographs and rock samples were

taken back for use in the laboratory. Identification and study of minerals, microstructures, and geochemical analysis of the samples collected, from the study area was first carried out by visual observation and then using transmitted light microscopy. Petrographic study of thin sections was carried out to identify the mineral constituents and composition in each type. This was done by the aid of using a transmitted light microscope here in Geology Department, Ahmadu Bello Univesity, Zaria. Geochemical analysis was carried out using the X-ray Fluorescence (XRF) technique to determine the major and trace elements at Multi User Science Research Laboratory A.B.U Zaria and Kano State University of Science and Technology Wudil.

Geology of the Study Area

The major lithological units observed in the study area are mainly schist of different types and granite. The minor lithology is quartzite and tourmalinites. Figure 3 is the geological map of the study area.

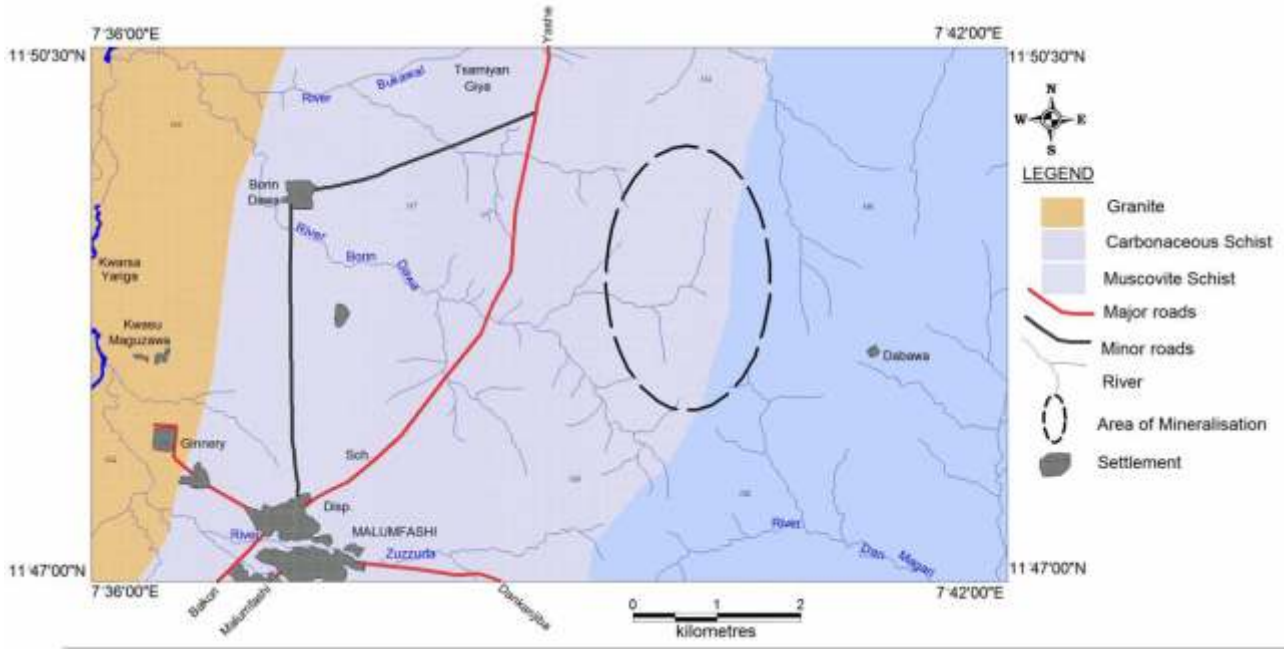

Figure 3: The geological map of the study area.

Major Rock Types

Schist

Schist dominate the study area; it occurs as lateritic ridges. It occupies about 80% of the study area, the different types of schist in the study area are named after the dominant mafic mineral comprising the rocks. These include:

Muscovite Schist

Muscovite schist is a crystalline metamorphic rock mostly composed of muscovite (more than 50%) as tabular and elongated minerals which is formed from the metamorphism of shale, it occupies about 45% of the study area.

The muscovite schist occurs as low-lying ridge irregular in outline and shows intense chemical weathering and are largely composed of

muscovite and other minerals such as quartz, orthoclase feldspar and ferromagnesian minerals.

The rock is light grey in colour and quartz shows up in some shades of grey, and on close inspection the colours are found to be dark brownish-green due to the arrangement of darker coloured minerals (Biotite, hornblende). The crystals are of medium to fine grain as shown in Plate 1.

Plate 1: A hand specimen of muscovite schist

Carbonaceous Schist

The carbonaceous schist consists mostly of the carbonaceous minerals. It occupies about 35% of the study area. They come in boulders and also in ridges. They also undergo intense chemical weathering and largely composed of micas and feldspars. In hand specimen the rock is dark grey in colour, the quartz shows up as some shiny shades of grey but on closer inspection, there are lighter coloured minerals. The crystals texture is of medium to fine grain as shown in Plate 2.

Granites

The granites outcropped around the North western part of the study area. The exposure occurs as domes while some occur as boulders with irregular outline. The rock covers almost 10% of the study area, mostly in the N.W part of the area. The granites are porphyritic and most of the exposures are affected by physical weathering such as exfoliation and biological weathering like root penetration through fractures. The rock is greyish in colour and the texture is medium to coarse. The mineral that constitute the rock are mainly quartz, biotite and plagioclase feldspars. The feldspars occur as phenocryst and is weakly foliated Plate 3.

Plate 2: Carbonaceous schist

Plate 3: An outcrop of granite.

Minor Lithology

Quartzite

Quartzite is non-foliated metamorphic rock composed of quartz. and it forms when a quartz rich sandstone is altered by heat pressure and chemical activity of metamorphism. This condition recrystallizes the sand grain and the silica cement that bind them together. The result is network of interlocking quartz grains of incredible strength.

In the study area, it comprises of > 80% quartz. The rock occupies about 5% of the study area and it occurs in hills, boulders and in some places in smaller fragments trending NS as shown in Plate 4.

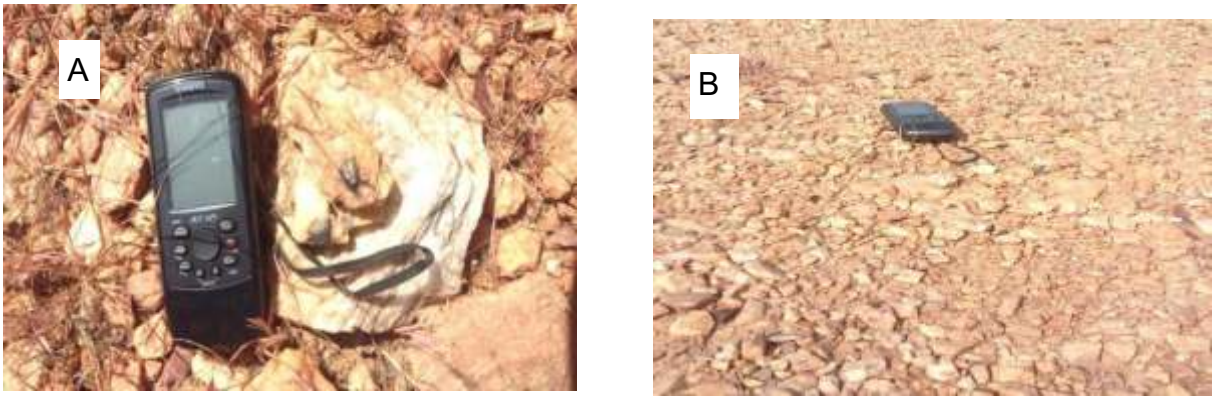

Plate 4: A boulder (A) and fragments (B) of Quartzite in the study area.

Toumalinite

Tourmalinite as the name implies is a metasomatic rock containing excess of 15% tourmaline, it covers almost 5% of the study area occurring as veins and interlayered beds, boulders and in some places as small fragments.

Tourmalinisation is the metasomatic replacement of feldspar and micas by the mineral tourmaline. The reaction is complex but involve the circulation of hydrothermal fluid in both the element boron and fluorine. This process is wide spread in the variety of igneous intrusions and if allowed to go completion will form rock of granite origin where all the feldspars and micas have been replaced forming a rock containing quartz and tourmaline only.

Field Occurrence of Ilmenite in the Study Area

The whole area under study is a silicified muscovite schist ridge containing numerous quartz vein of various size trending North South (NS), which is the same direction of the foliation of the schist.

Ilmenite here occurs as a disseminated nodular mineralization within the quartz vein that is highly weathered with a thickness of about 0.5m trending (NS) direction. The nature of the structure within the study area shows lack of cleavage as well as the boggy texture. Also, the mineralization occurs as nuggets and in some places as smaller fragments scattered within the quartz vein. All types were found within Loc 3, 3a, 3b, 3c, and Loc 6 as shown in Plate 7.

Ilmenite is often found exhibiting dichroic colours from dark brown to pinkish brown when viewed under polarising microscope as best mineral that shows strong shades of gray when viewed under petrographic polarizing light. Although ilmenite has no cleavage it has visible partings associated with twining. Partings are generally not observed in thin section or fragments. However, the simple opaque ilmenite is most common associated with other interesting mineral including olivine, zircon, hematite, quartz, rutile etc.

Ilmenite mineral is sometimes magnetic and will actually always become magnetic if

heated and viewed closely with the aid of polarizing light microscope it can be found having granular and massive forms. It can also occur as grain in placer sands the detrital grains are more or less equant.

Geochemistry

Geochemical analysis for major elements in the schist is presented in Table 1 below. This method is chosen to determine the background contents of Fe and Ti within the rocks in order to constrain the sources of the two-element necessary for the formation of ilmenite.

Loc. 3

Loc. 3a

Loc. 3b

Loc. 3c

Loc. 6

Plate 7. Ilmenite samples of different shapes and sizes recovered from the study area.

Plate. 6: A nugget of ilmenite found within the study area.

Table 1. Major element composition in the schist from the study area (all values are in wt. %).

MAJOR ELEMENTS IN WT%								
Muscovite schist					Carbonaceous schist			
Elements (Oxide)	**LOC 2a**	**LOC 4**	**LOC 5a**	**LOC 5b**	**LOC 3**	**LOC 3a**	**LOC 3b**	**LOC 6**
SIO_2	17.52	95.49	4.37	92.12	2.62	3.76	97.21	3.8
TiO_2	0.6	0.2	73.73	3.22	79.74	82.71	0.23	82.82
Al_2O_3	5.31	1.54	1.84	1.55	1.17	1.27	1.24	2.08
Cr_2O_3	0.06	0.00	0.23	0.03	0.37	0.28	0.00	0.05
Mn_2O_3	0.1	0.05	1.25	0.09	0.49	0.44	0.05	0.48
Fe_2O_3	75.23	0.34	18.12	1.91	14.51	11.27	0.16	10.28
Na_2O	0.00	0.84	0.00	0.00	0.00	0.00	0.41	0.00
K_2O	0.00	0.59	0.08	0.05	0.15	0.19	0.25	0.01
Ca_2	0.62	0.00	0.1	0.08	0.5	0.08	0.05	0.09
P_2O	0.43	0.34	0.03	0.27	0.31	0.03	0.32	0.03
MgO	0.13	0.19	0.27	0.18	0.14	0.02	0.18	0.13
TOTAL	100	100	100.2	99.5	100	100	100	99.82

Silica (SiO_2) content ranges from 95.49 - 17.52% in Muscovite schist, 97.21 -2.62wt% in Carbonaceous schist and 82.71-0.23wt% in Carbonaceous schist. (Al_2O_3) ranges from 5.31-1.54wt% in Muscovite schist and 2.08-1.17wt% in Carbonaceous schist; (Cr_2O_3) is 0.23-0.00wt% in Muscovite schist, 0.37-0.00wt% in Carbonaceous schist. (Mn_2O_3) ranges from 1.25-0.1wt% in Muscovite schist, and then 0.49 - 0.05wt% in Carbonaceous schist. (Fe_2O_3) is 75.23-0.34wt% in Muscovite schist, and also 14.51-0.16wt% in carbonaceous schist. (N_2O) is 0.84-0.00wt% in Muscovite schist and 0.41-0.00wt% in carbonaceous schist. (K_2O) is 0.59-0.00wt% in Muscovite schist and 0.25-0.01wt% in carbonaceous schist. (Ca0) shows 0.62-0.00wt% in Muscovite schist and 0.09-0.05wt% in Muscovite schist, while 0.32 -0.03wt% in carbonaceous schist. (MgO) is ranging from 0.19-0.13wt% in Muscovite schist and 0.41-0.02wt% in carbonaceous schist.

The major element analysis shows that the muscovite schist generally has higher SiO_2 content than the carbonaceous schist. The muscovite schist also has a higher Al_2O_3 content than the carbonaceous schist, thus indicating a peraluminous protolith. The samples generally have a low Na_2O and K_2O concentration with averages of O.15wt % and 0.16wt % indicating that the rocks were derived from an alkaline deficient source. The concentration of Fe_2O_3 tend to increase with increasing TiO_2, this is observed as the samples with the lowest TiO_2 concentration (loc 4 and Loc 3b) have the lowest Fe_2O_3 content 0.34 and 0.16 wt. % respectively. The TiO_2 and Fe_2O_3 rich rocks are SiO_2 deficient and vice versa. The carbonaceous schists which are interpreted to be of igneous origin are more enriched in TiO_2 (with an average TiO_2 of 61.37wt %) more than the muscovite schists (with an average TiO_2 of 19.43wt %) suggesting that their protolith exerts very strong influence on their mineralogy. They generally have a low magnesium concentration with an average of 0.188 wt %.

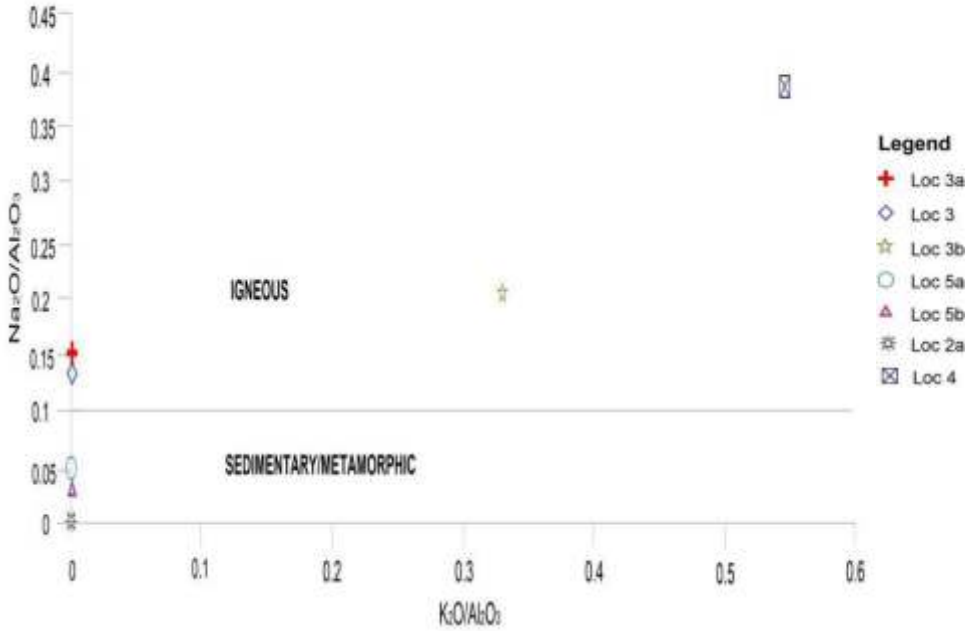

Figure 4: Plot of Na_2O/Al_2O_3 vs. K_2O/Al_2O_3 (Wt. %) showing variation diagram for the field of Igneous and Metasedimentary rocks (Oyebamiji, 2014).

Plot of Na_2O/Al_2O_3vs. K_2O/Al_2O_3 (Wt. %) (Fig 4) shows that the schist are all of igneous origin, this may be the cause of their relatively lower concentration in alkaline elements. All the carbonaceous schists (Loc 3a, 3, 3b, and 4) plotted in the region indicating igneous protolith while the muscovite schist (Loc 2a, 5a and 5b) all plotted in the region of sedimentary or metamorphic origin. From these results it can be inferred that the metamorphism of the protolith to the schist was accompanied by mobile fluid generation and the fluid is likely going to be hydrothermal fluid related to the metamorphic breakdown of hydrous minerals. The high iron and titanium oxide content of the fluid were sourced from the schist and allows for the formation of ilmenite ($FeTiO_2$).

Uses of Ilmenite

Ilmenite is a primary source of titanium metal. Small amount of titanium combined with metal will produce durable high strength high weight alloys. These alloys are used to manufacture a wide variety high performance tools. e.g. air craft parts, artificial joints for human and sporting equipment such as bicycle frames. About 5% of ilmenite are used to produce synthetic rutile form of titanium dioxide used to produce white high refractive pigments.

These pigments produces a white color and brightness in paints, papers, abrasives, plastics, Tooth paste and even food. Titanium dioxide used to make powder with a highly controlled

particle size ranges. These powders are inexpensive polishing abrasive in a variety of lapidary work that includes rock tumbling, lapping, cabbing and sphere making. Titanium dioxide abrasive is used in many other industries.

Conclusion

In this study occurrences of ilmenite have been established in the quartz veins associated with schists in the area east of Malumfashi, in the Malumfashi schist belt. The source of the fluids has tentatively been constrained to metamorphic fluids associated with metamorphic breakdown of hydrous minerals during prograde of shale. The fact that the minerals occur as nuggets indicate the likelihood of finding economic deposits when systematic exploration is conducted.

It is therefore recommended that further exploration and studies of this deposit is required to establish the grade and tonnage of the deposit and an assessment of its suitability for industrial use.

Acknowledgements

Contributions from colleagues at the Department of Geology, Ahmadu Bello University Zaria, are hereby acknowledged. We remain grateful.

References

Ajibade, A. C. 1(988): Structural and tectonic evolution of the Nigerian basement with special reference to NW Nigeria. *In* International Conference on Proterozoic Geology Tectonics High-Grade Terrains (Ife, Nigeria), pp. 42-129

Ajibade, A. C. (1976): Provisional classification of the Schists Belts of North Western Nigeria In: C. A. Kogbe "Geology of Nigeria" 2nd revised edition *Rock View Nigeria limited, jos,* pp. 85-90.

Ajibade. A. C., and Wright. J. B., (1989): The Togo-Benin-Nigeria Shield: evidence of crustal aggregation in the Pan-African belt, *Tectonophysics*, 165: pp. 125–129.

Ajibade. A. C, Woakes, M., and Rahaman Nigeria" 2nd revised edition *Rock View Nigeria limited, Jos,* pp. 57-69M.A (1987): Proterozoic Crustal Development in the Pan-African Regime of Nigeria. In: C. A. Kogbe (edition) "Geology of

Danbatta, U.A. (1991): Geological Investigation of the SW Portion of the Zuru Schist Belt, NW Nigeria. Unpublished M.Sc. Thesis, A.B.U Zaria, pp. 146-150

Danbatta U.A., (1999): Geotectonic evolution of the Kazaure Sciest Belt in the Precambrian Basement of NW Nigeria. Unpublished PhD Thesis, Ahmadu Bello University Zaria, pp. 279-286

Danbatta U.A., (2001): Tectono-Metamorphic evolution of the Kazaure Schist Belt, NW Nigeria. Paper presented at the-37" Annual Conference of Nigerian Mining and Geoscience Society. NMGS Abstract, 33: pp. 56-109

Danbatta, U.A. (2003): The lithogeochemical framework underlying the geotectonic evolution of the Kazaure Schist Belt, NW Nigeria. The Nigerian Journal of Scientific Research, 4(1):1-13.

Danbatta, U.A. (2008): A Review of the Evolution and Tectonic Framework of the Schist Belts of Western Nigeria, West Africa. *Africa geoscience review*15 **(**2**):** pp. 145-158.

Elatikpo S.M. Danbatta U.A and Najime T. (2013): Geochemistry and Petrogenesis of Gneisses around Kafur-Yari Bori-Tsiga area within Malumfashi Schist Belt, Northwestern Nigeria. *Journal of Environmental Earth Scie*nce 4 (7): pp.171-180.

Falconer, J. D. (1911): The geology and geography of northern Nigeria. Macmillan Publishers, London pp. 289-295

Fitches, W.R., Ajibade A. C., Egbuniwe I.G., Holt R. W., and Wright J.B. (1985): Late Proterozoic Schist Belts and Plutonism in NW Nigeria', *Geological Society of London*, 142: pp. 319- 337.

McCurry, P. (1971): Pan-African Orogeny in Northern Nigeria. *Geological Society of America Bulletin,* 82: pp. 3251–3263.

McCurry, P. (1976): Pan-African Orogeny in Northern Nigeria. *Geological Society of America Bulletin* 82*:* pp. 3251-3263.

McCurry, P. and Wright, J.B. (1977): Geochemistry of calc-alkaline volcanic in northwestern Nigeria, and possible Pan-African suture zone. *Earth and Planetary ScienceLetters*.37: pp. 90-96

Oyawoye, M. O. (1964): The Geology of the Nigerian Basement Complex - a Survey of our Present Knowledge of them. *Journal of Metallurgy* 1(2): pp. 87-102.

Oyawoye, M. O. (1972): The basement complex of Nigeria. *In* Dessauvagie, T. F., and Whiteman, A. J., eds. African geology. Ibadan, Geology Department, University of Ibadan, pp. 42-98

Rahaman, M. A. (1976): Progressive polyphase metamorphism in pelitic schists around Aiyetoro, Oyo State, Nigeria. *Journal of Mineralogy and Geology*. 13:pp. 33-44.

Rahaman, M. A. (1988): Recent Advances in the Study of the Basement Complex of Nigeria in: Geological Survey of Nigeria (ed.) *Precambrian Geology* of Nigeria, pp. 11-41.

Rahaman, M. A., Ekwere, S. J., Azmatullah, M. and Ukpong, E. E. (1988): Petrology and geochemistry of granitic intrusive rocks from the western part of the Oban Massif, southeastern Nigeria. *Journal African Earth*

Truswell, J. F., and Cope, R. N. (1963): The geology of parts of Niger and Zaria provinces, northern Nigeria. *Geological Survey of Nigeria Bulletin,* 29: pp. 26- 53

Turner D. C. (1983): Upper Proterozoic Schist Belts in the Nigerian Sector of the Pan-African Province of West-Africa. In: C. A. Kogbe “Geology of Nigeria” 2nd Revised Edition, *Rock View Publication Company, Jos,* Nigeria. pp. 93-109

Jibril and Ibrahim (2019) Nigerian Mining Journal, (16) 13 - 20
© Nigerian Society of Mining Engineers, ISBN 1117 - 4307

Nickel (Ni) Mineralization Potential in the Mallam Tanko Serpentinite, North Western Nigeria

***Jibril, I. B. and **Ibrahim, A. A.**
*Department of Mineral Resources Engineering, Kaduna Polytechnic
**Department of Geology, Ahmadu Bello University Zaria.

Abstract
The Mallam Tanko serpentinite forms a discontinuous north-south trending body with sharp contacts against vertically foliated and finely banded biotite-rich gneisses and schists, which pass rapidly outwards to more massive quartz, feldspathic, gneisses and migmatites. Two blocks of potential ore body have been defined, comprising 29million tonnes of nickeliferous serpentinite of 1.2%Ni (350,000tonnes Ni approx.) and 1.2million tonnes of 1.7%Ni (21,000tonnes Ni approx.), all in the inferred category of resource. The Nickel is in serpentine and Cr-hematite. No sulphide or silicate nickel mineral was found in the serpentinite body.

Keywords: serpentinite, Nickel, quartz, feldspathic, gneisses and migmatites

Introduction
Serpentinite occurrences have been reported along the Anka fault as aligned bodies that are traceable intermittently for about 150 km, from Ribah through Tugan Kudaku and Maikwonaga to Sado Serpentinite (Wright and Ogezi, 1977; Onyeagocha, 1979). Another serpentinite body at Mallam Tanko is an 8-km string of small bodies aligned N-S in gneissic rocks. Serpentinite was also reported in the Federal Capital Territory, about 300 km due south of the northwestern occurrences. The serpentinites are typically intrusive bodies up to 15 km in length and 1 km in width, although most are much smaller. Pods and dissemination of chromite have been found in some serpentinites which are also associated with anthophyllite asbestos, talc and magnesite Serpentinite (Onyeagocha, 1979) suggesting a peridotite origin brought to the surface from upper mantle regions through thrust faults. Some derived soils of limited extent over the serpentinites and other ultramafic-mafic rocks are enriched in nickel.

Regional Geology and Structure
The basement complex is one of the three major lithological components that make up the geology of Northwestern Nigeria. The Nigerian basement complex forms a part of the Pan-African mobile belt and lies between the West African and Congo Cratons and south of the Tuareg Shield which was affected by the *c*. 600Ma Pan-African. The Pan-African deformation was accompanied by a regional metamorphism, migmatization and extensive. Late tectonic emplacement of granites and granodiorites and associated contact metamorphism accompanied the end stages of this last deformation. The end of the orogeny was marked by faulting and fracturing which have a consistent NE-SW and NW-SE trends (Figure 1).

Within the basement complex of Nigeria three major rock groups are distinguishable (Fig 1), namely:

i). The Migmatite–Gneiss Complex
ii). The Schist Belts (metasedimentary and metavolcanic rocks)
iii). The Older Granites (Pan African granitoids)

i). The Migmatite–Gneiss Complex This is a polymetamorphic tnigmatite-gneiss complex composed largely of migmatites and gneisses. The migmatite-gneiss complex is considered to be the basement *sensu stricto,* and most radiometric ages lie in the range 600 ± 150 Ma,

dating the imprints of the Pan-African orogeny, but with relict Eburnean (*c*. 2000 Ma) and Liberian (*c.* 2700Ma) ages obtained in many localities. Metamorphism is generally in the amphibolite facies grade. (Holt, et.al 1978).

ii). The Schist Belt (Metasedimentary and Metavolcanic rocks) The supracrustal schist belts consist dominantly of schists, phyllites and quartzites with minor volcanic rocks, banded iron formations and conglomerates. Metamorphic grades are variable from amphibolite facies in the southern belts to predominantly greenschist facies in the northern belts. The dominant tectonic fabric is a steeply dipping N-S phyllitic to slaty cleavage arising from isoclinal folding. Radiometric ages of the schist belts range between *c.*1100 Ma (Kibaran) and *c.* 600 Ma (Pan-African).

iii). The Older Granites (Pan-African Granitoids) These are syntectonic to late tectonic granitic rocks, which cut both the migmatite-gneiss complex and the schist belts. The granitoids include rocks varying in composition from granite to tonalite, with smaller bodies of syenite, charnockite and gabbro. They have generally yielded radiometric ages in the range of 750-500 Ma, corresponding to the Pan-African age

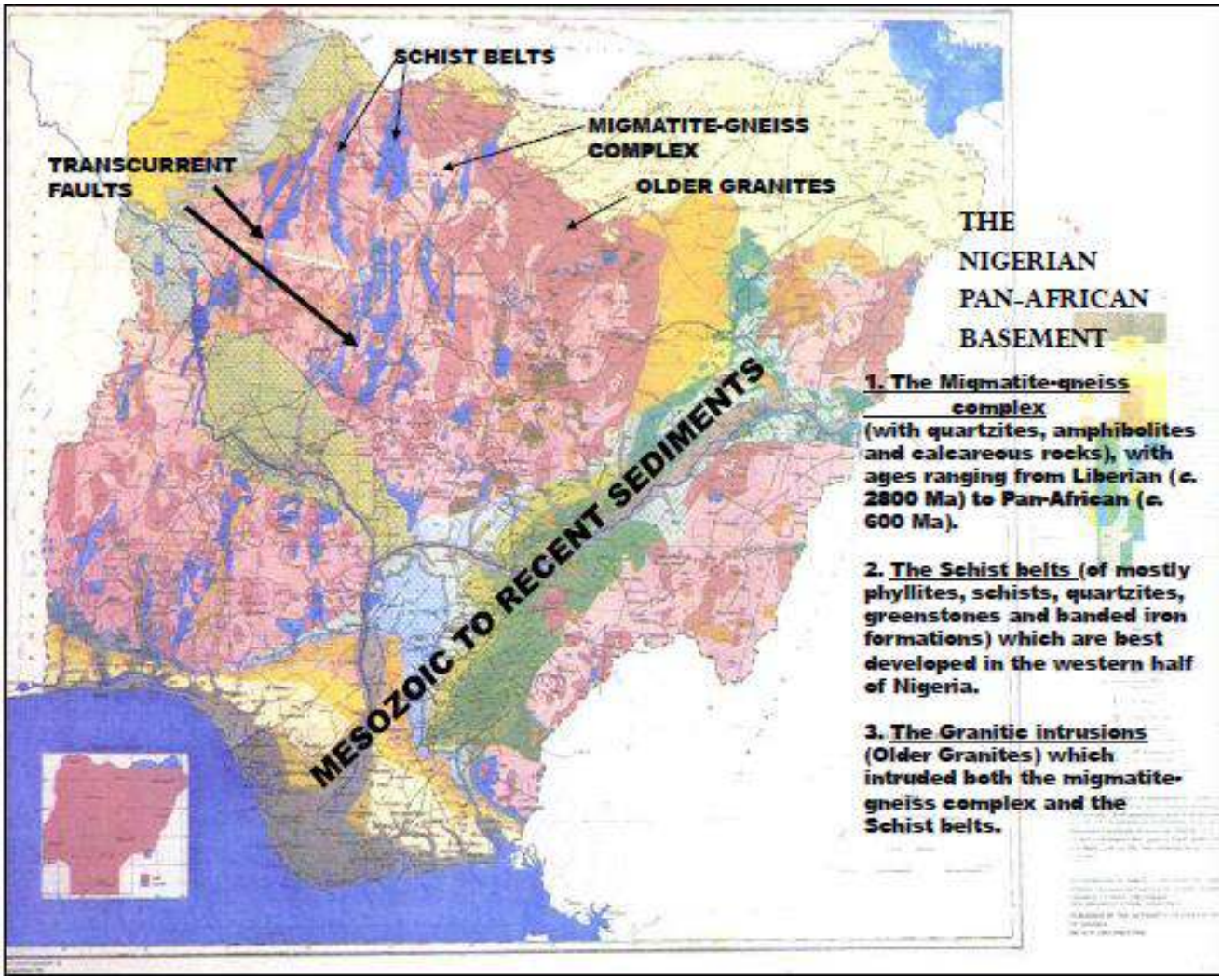

Figure 1. Geological map of Nigeria showing the main rock groups and transcurrent faults, (NGSA 2010)

The Mallam Tanko Serpentinite

The area of interest is made of a pear-shaped body of serpentinite, diorite, amphibolites and greenstone bounded by gneisses to the east and porphyritic granites to the west (Figure 1). The serpentinite and associated rocks are collectively known as the Mallam Tanko Serpentinite (Wright and Ogezi, 1977; Ogezi, 1977; Onyeagocha, 1979). The basic-ultrabasic rocks appear to have been emplaced within a N-S trending fault zone; and the southern part where the serpentinite is more common is cut by some NE-trending faults. The serpentinite shows striated surfaces (slickensides) in many places. (McCurry 1973)

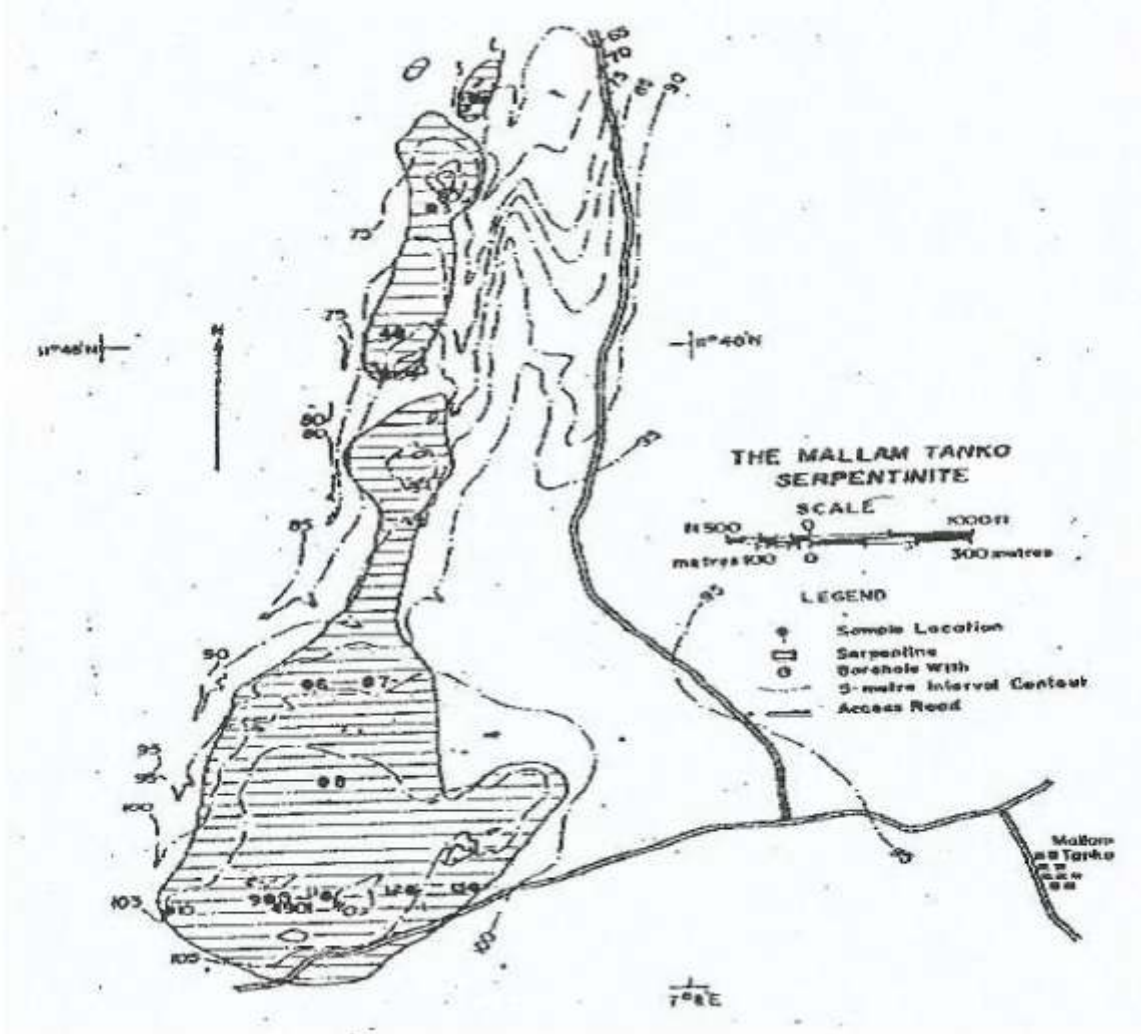

Figure 2. Geological Map of the Mallam Tanko Serpentinite (after Onyeagocha, 1979)

The serpentinite appears to represent tectonic blocks of possibly upper mantle peridotite emplaced along a faulted axial plane of a synclinorial fold and clearly postdates the surrounding Precambrian (Pan-African) country rocks.

Petrology

Rock chip samples were collected in a random manner at locations where outcrops are available. This has resulted in the collection of about 46 rocks samples of serpentinite of varying degree of alteration

and weathering. The serpentinite mass composed of serpentine (84-94 wt.%) and in minor amounts, other silicate minerals as talc, chlorite, tremolite, anthophyllite and tiny remnants of olivine. The original peridotite silicate minerals have been so completely serpentinized and mineralogically reconstituted (Shibayan 1985). Opaque minerals present are mostly Cr-hematite, magnetite-hematite and goethite (3-5 wt.%). Veins of anthophyllite asbestos and zeolites appear as late structures in the serpentinite. Full mineralogical analysis has been done by the Activation Laboratories, Ancaser, Ontario Canada. The data is in Appendix 2 and also presented in Table 1 and Figures 3-4.

The degree of alteration, mostly silicification, varies from mild to intense where there is almost complete replacement of the serpentine and other green minerals by quartz.

Table 1. Modal mineralogical composition of the serpentinite

Measurement Type		BMA		
Sample Name	**S3**	**S239**		**S108**
Mineral Mass (%)				
Sulfides	Chalcopyrite	0.000	0.002	0.000
Pyrite	0.002	0.002		0.000
Oxides/Hydroxides	Magnetite/Hematite	0.83	1.92	0.82
Hematite-Cr	**3.21**	**0.12**		**1.61**
Goethite	0.77	1.34		0.62
Rutile	0.00	0.00		0.00
Chromite	0.00	0.68		0.00
Silicates	Quartz	0.22	4.76	8.90
K-Feldspar	0.00	0.01		0.00
Plagioclase	0.00	0.00		0.00
Mica	0.01	0.00		0.00
Clinochlore	0.18	0.02		0.10
Amphibole	0.00	0.01		0.03
Hornblende	0.00	0.00		0.00
Serpentine (Mg-Serpentine)	**89.21**	**77.33**		**64.64**
Serpentine-Altered	**4.50**	**10.01**		**19.57**
Antigorite (Fe-Mg Serpentine)	0.20	1.27		0.28
Talc	0.07	0.56		1.73
Si-Al Clays	0.00	0.00		0.00
Zircon	0.00	0.00		0.00
Phosphate/Carbonates	Apatite	0.00	0.00	0.00
Dolomite	0.00	0.00		0.00
Calcite	0.00	0.00		0.00
Mixed-Unclassifiable Spectra	Goethite/Clay Mixed	0.00	0.02	0.11
Low Counts	0.02	0.03		0.03
Others	0.78	1.92		1.55
Sum	**100**	**100**		**100**

Mineral Volume (%)			
Chalcopyrite	0.00	0.00	0.00
Pyrite	0.00	0.00	0.00
Magnetite/Hematite	0.41	0.94	0.40
Hematite-Cr	**1.58**	**0.06**	**0.79**
Goethite	0.52	0.91	0.42
Rutile	0.00	0.00	0.00
Chromite	0.00	0.37	0.00
Quartz	0.21	4.69	8.76
K-Feldspar	0.00	0.01	0.00
Plagioclase	0.00	0.00	0.00
Mica	0.01	0.00	0.00
Clinochlore	0.18	0.02	0.10
Amphibole	0.00	0.01	0.03
Hornblende	0.00	0.00	0.00
Serpentine (Mg-Serpentine)	**91.43**	**79.03**	**66.00**
Serpentine-Altered	**4.61**	**10.24**	**19.99**
Antigorite (Fe-Mg Serpentine)	0.20	1.29	0.28
Talc	0.06	0.53	1.62
Si-Al Clays	0.00	0.00	0.00
Zircon	0.00	0.00	0.00
Apatite	0.00	0.00	0.00
Dolomite	0.00	0.00	0.00
Calcite	0.00	0.00	0.00
Goethite/Clay Mixed	0.00	0.01	0.08
Low Counts	0.02	0.03	0.02
Others	0.76	1.87	1.51

There are no sulphide or silicate nickel minerals in the modal composition of the serpentinite. The nickel is therefore within the crystal structure of Serpentine and Hematite-Cr (Figures 3-4). The hematite, and goethite may be alteration products of an original ultrabasic magnetite. There is also no indication whether the nickel values are related to the degree of alteration and or weathering. Since lateritization is not observed over the serpentinite and associated rocks to any reasonable degree, the possibilities of nickel enrichment in the weathered residuum is not considered during this study.

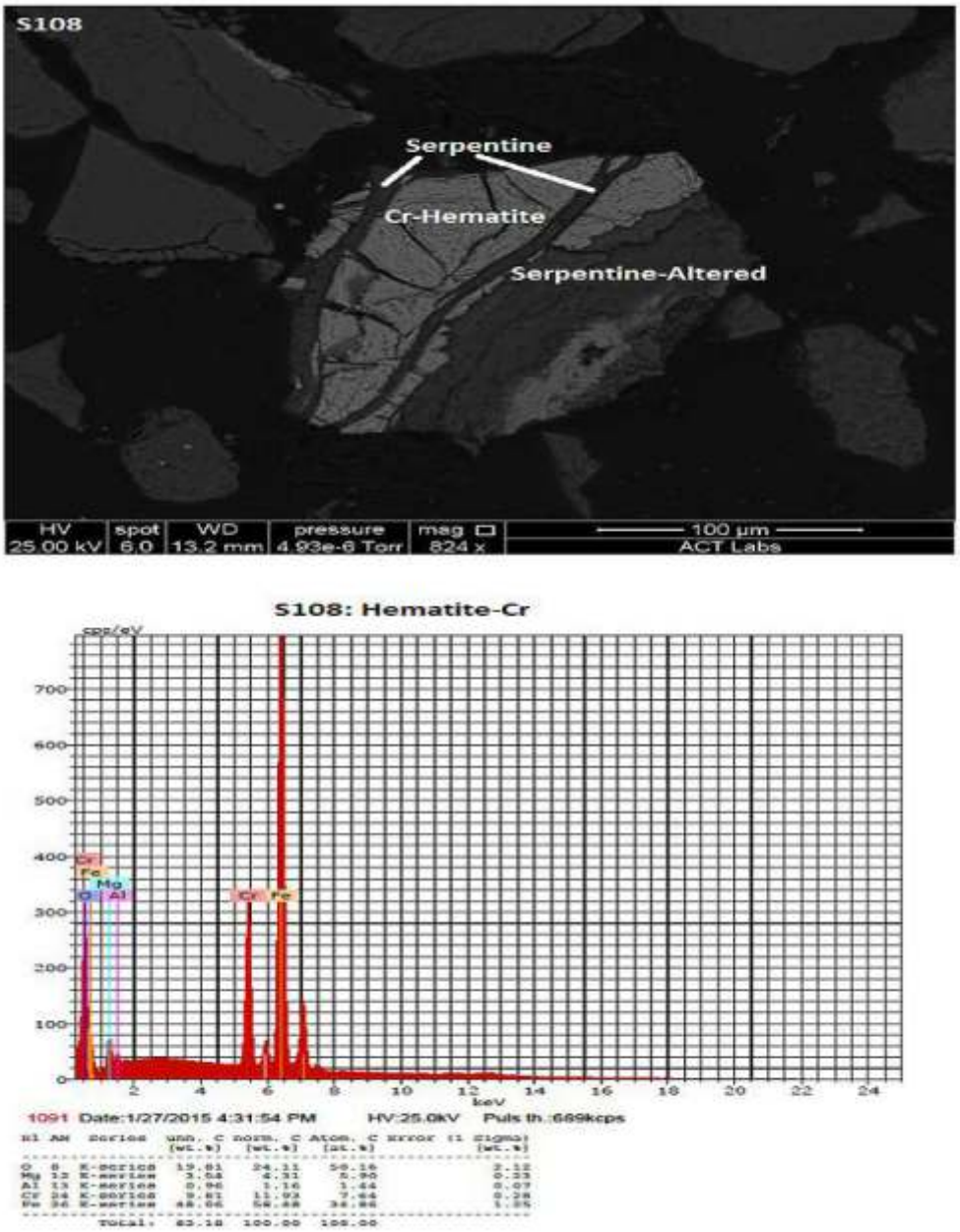

Fig 3. BSE Image and representative EDX Spectrum of Sample in Serpentinite with Pod

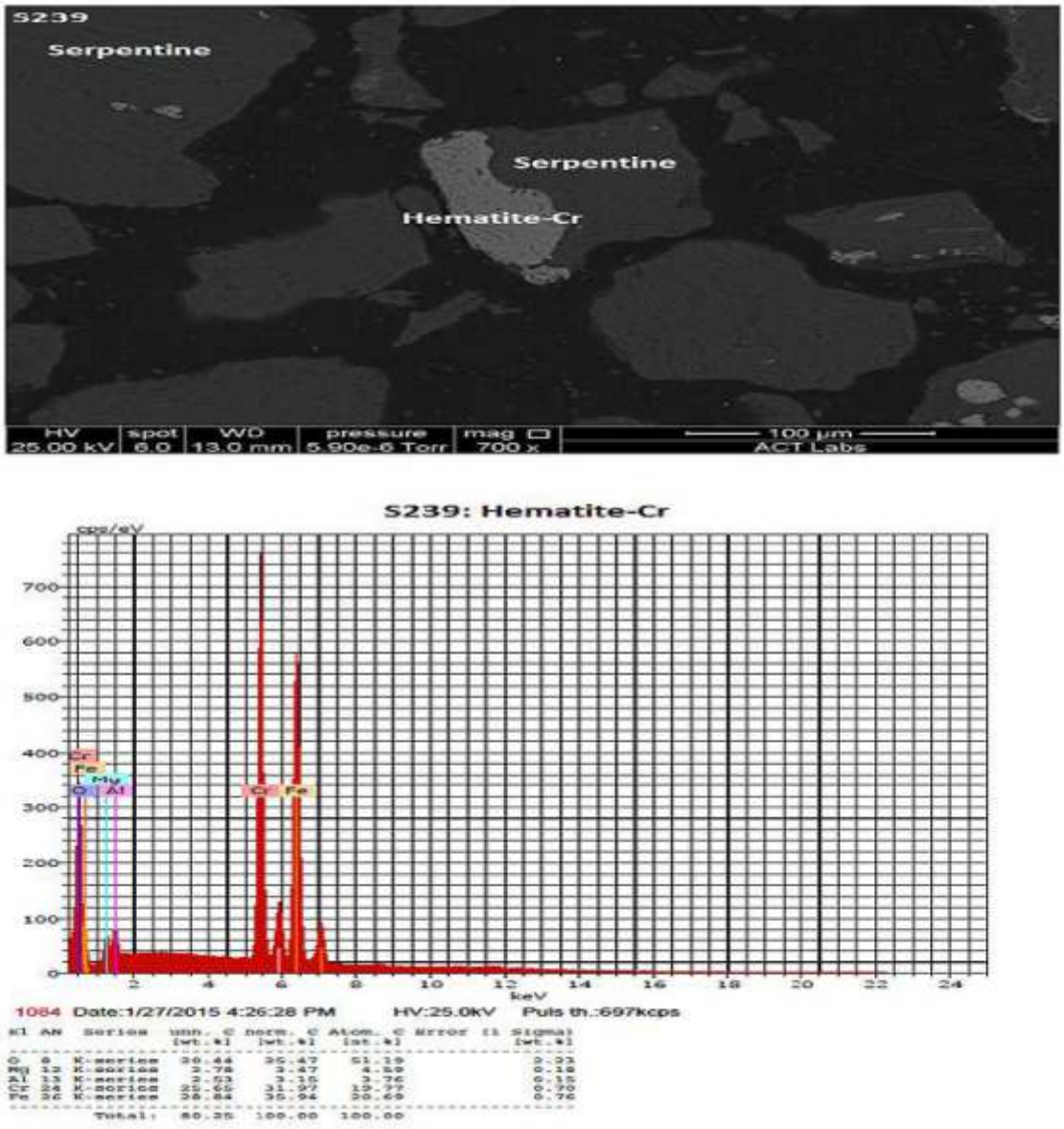

Figure 4. BSE Image and representative EDX Spectrum of sample of massive Serpentinite

NICKELIFEROUS SERPENTINITE OREBODY

Surface Expression

The surface shape and extent of the serpentinite body as revealed from detailed mapping shows blocks of serpentinite and associated rocks (diorite, amphibolites, greenstone) within a major north-south trending fault zone cutting mostly Pan-African (600±!50 Ma) porphyritic granite. Along the fault margins the granite is intensely deformed resulting in the formation of mylonites (phyllonites), best developed in the western margins.

Discussion

i) The highest Ni values are recorded from two blocks where relatively fresh serpentinite is abundant (Block A, Block B). In these blocks the average Ni grade ranges from 1.2% (Block A, 13 samples) to 1.7% (Block B, 2 samples).

ii) The highly altered (silicified, leached, weathered) serpentinite and other basic

rocks (diorite, amphibolite, greenstone) have predominantly the lowest nickel concentration (0.02-0.30%) as shown in Table 1.

iii) The overall average grade of all the samples analyzed (serpentinite, associated rocks and their altered varieties) is about 0.67% Ni.

iv) In addition to Ni few other elements are enriched in the samples (Appendix 1), notably, Cr (up to 0.5%), Fe (up to 8%). However, these relatively high values do not constitute economic grades of the elements.

Conclusion

The serpentinite body is found to have suffered varying degree of alteration and weathering. The alteration consists of intense silicification which has almost completely replaced the serpentine and other mafic minerals with quartz and other forms of silica.

Nickel values in the serpentinite and associated rocks are varied but economic high values tend to cluster in some areas locally within the body, to constitute target blocks with grades about 0.5% to 2.2% (averaging about 1.2%). The intensely silicified serpentine and other basic rocks have nickel values 0.1% or less.

Two blocks of potential orebody have been defined, comprising 29 million tonnes of nickeliferous serpentinite @ 1.2% Ni and 1.2 million tonnes @ 1.7% Ni, all in the *Inferred* category of *Resource*.

There is no clear lateritic profile developed over the serpentinite body and therefore the possibility of laterite nickel occurrence was not investigated.

Acknowledgement

Contributions from colleagues from the Department of Geology A.B.U. Zaria and Department of Mineral Resources Engineering, Kaduna Polytechnic is here acknowledged.

References

Holt R., Egbuniwe, I.G Fitches, W.R and Wright, J.B (1978). The relationship between low-grade metasedimentary belts, calc-alkaline volcanism and the Pan-Africa orogeny in N.W Nigeria. Geol. Rundschau, 67:631-646

McCurry, P. (1973). Geology of Degree sheet 21, Zaria Nigeria. Overseas Geology and Mineral Resources No 45, H.M.O.S London.

Onyeagocha, A.C. (1979). The Mallam Tanko serpentinite: Petrology and economic implications. *Journal of Mining and Geology*, Vol. 16, No. 1, pp37-40.

Ogezi, A.E. (1977). Geochemistry and Geochronology of basement rocks from Northwestern Nigeria. Unpub. PhD dissert. Leeds Univ. England 295p.

Ogezi, A.E. and Wright, J.B (1977). New Occurrences of serpentinites from the basement of northwestern Nigeria. 19th Ann. Rept. Res. Inst. Afr. Geol. (Leeds Univ.) 81.

Shibayan, Y. (1985). Investigation of possible chromite bearing serpentinites and associated rocks of NW Nigeria. Unpub. M.Sc. thesis, Ahmadu Bello University, Zaria, Nigeria.

Tennakone, K., Senevirathna, M.K.I. and Kehelpannala, K.V.W. (2007). Extraction of pure metallic nickel from ores and plants at Ussangoda, Sri Lanka. *Journal of National Science Foundation of Sri Lanka*, Vol. 35, No. 4, pp245-250.

Wright, J.B. and Ogezi, E.A. (1978). Serpentine in the basement of northwestern Nigeria. *Journal of Mining and Geology*, Vol. 14, No. 1, pp34-37.

Usman, et al (2019) Nigerian Mining Journal, (16) 21 - 28
© Nigerian Society of Mining Engineers, ISBN 1117 - 4307

Preliminary Studies of Structures Controlling the Flow of Brine in the Awe Brine Field

***Usman, H.O., *Tanko, I.Y. and **Obaje, N.G.**
*Nasarawa State University, Keffi, Nasarawa State
**Ibrahim Badamasi Babangida University, Lapai, Niger State
Corresponding author: ogelebehu@gmail.com

Abstract
Studies of the Awe brine field in the middle Benue Trough have revealed interesting structural features deserving a considerable attention. Some interesting field evidence points to the probability of the occurrence of dome structures in the brine bearing sediments. This brine field is underlain by Formations of Cretaceous age (Asu River Group, Awe, Keana and Ezeaku Formations). The tectonic set up in this brine field is dominated by the Keana anticlinorium and brine is seen to issue from flanks of the transitional beds of the Awe Formation which have been exposed by erosion.In Old Awe town, structural features mapped revealed dips of up to 14^0 to 30^0 to the north and south. Usually, close conjugate joint systems, infilled by silica revealed the same pattern as the major fold axis, thus contribute to the flow of brine in the field.

Keywords: Awe, Brine field, Cretaceous, anticlinorium, silica

Introduction
The Benue Trough of Nigeria is an intracratonic rift structure,which extends from the Northern limit of the Niger Delta to the Southern margins of Chad Basin.The valley which is occupied by upto 600m of marine and fluviodeltaic sediments, that have been compressionally folded in non orogenic shield environment has been subdivided geographically into the Lower, Middle and UpperBenue Trough for the ease of mapping.The study area is Old Awe town located in Awe Local Government Area of Nasarawa State. The studyarea forms part of the Middle Benue Trough. Six lithostratigraphic formations are found in the Middle Benue Trough which include the Asu River Group, Awe Formation, Keana Formation, Ezeaku Formation, Awgu Formation and finally the youngest which is the Lafia Formation.

Previous Work
The earliest work done in the Middle Benue Trough of Nigeria was reported by Falconer (1911) who reported the Asu River Group to be the oldest marine sedimentary formation which hethen referred to it as the “Lower Shale”, Tattam(1944) described the lithological unit as the“Cross River Series” and the name “Asu River Group” was obtained. The Keana Formation is thought to be equivalent to the “Muri Sandstone”in the north. Cratchley and Jones (1965) subsequently used the “Keana Sandstone” to describe the formation in LafiaAwe area.Simpson (1954) first mentioned the “Ezeaku Formation” in the literature where he described a sequence of hard dark grey to black flaggy calcareous shale, siltstone and sandstone in the stream south of the Okigwe-Afikpo road. The formation wasfirst recognized by Shell-B Pgeologist. The most recent study of the Keana area which was complementary to the work of Offodile (1976) was carried out by Obaje et al.,1994, 1996, 2004, and Sabo 2001 in their studies have revealed and confirmed the different geologicunits similar to those of

previous workers. The mines development of Nigeria also carried out apreliminary survey of Lead-Zinc in 1948 and 1949using student geologist from United Kingdom.

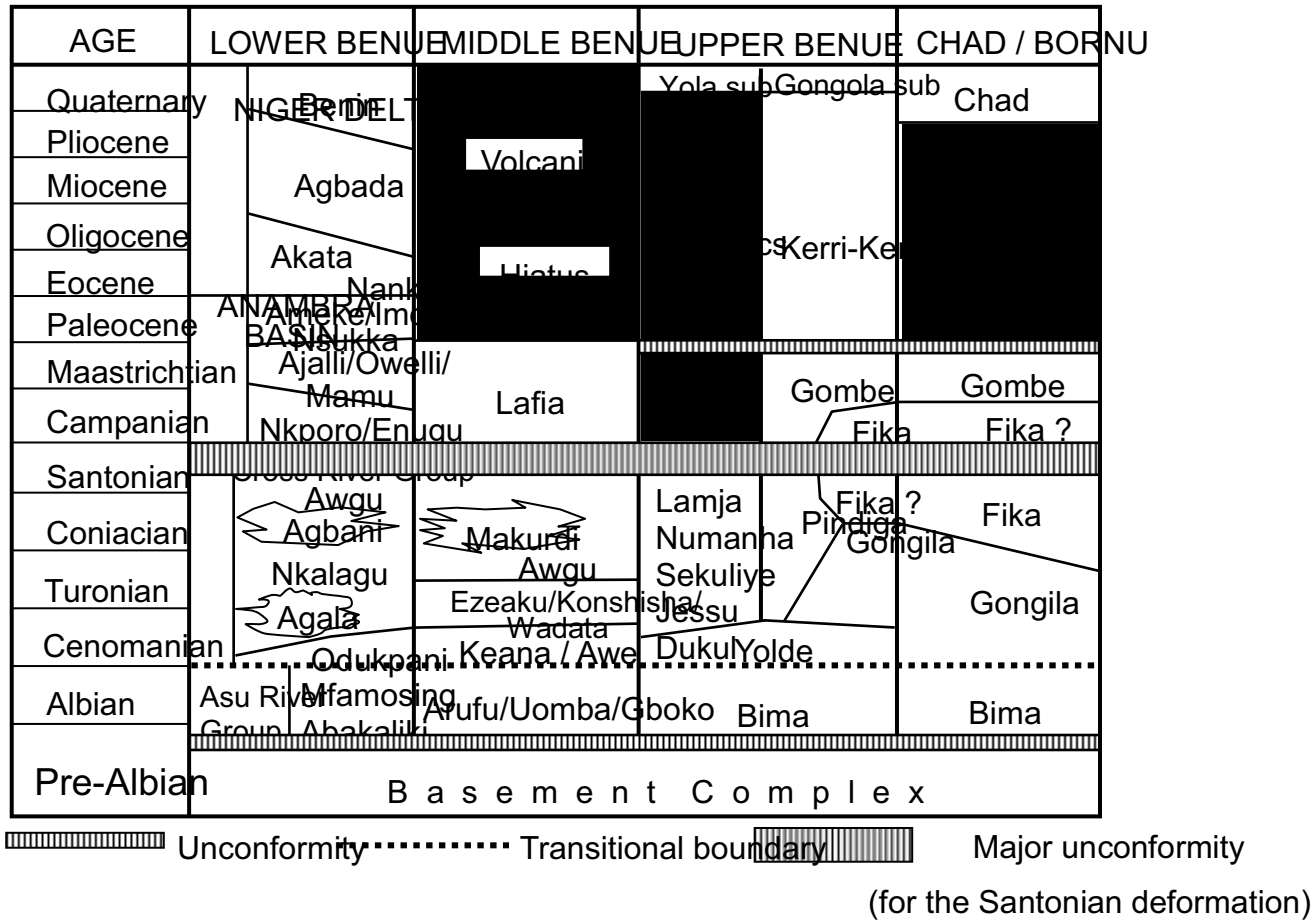

Figure 1: Stratigraphic successions in the Benue Trough and other inland basins (Obaje, 2009)

The study on the structural geology of the area was carried out by Benkhelil (1982,1987, 1989)and suggested that sinistral wrenching that dominated tectonic processes is responsible forthe structural arrangement and geometry of the subbasins in the Lower, Middle and Upper Benue region. Earlier on, he had described the Benue Trough of Nigeria as an intracratonic rift structure which extends from the Northern limit of Niger Delta on the southern margin of the Chad Basin. However, in a bid to investigate theregional structure of the Middle Benue, a detailed gravity survey was carried in 1979 by Ajayi andAjayi et al.,1986 and theirwork discussed in detail folds, faults and intrusions which are the main regional structure of interest. On the economic aspect, worker such as Offodile (1976)carried out a mineral resource survey of the Benue Trough and was able to delineate zones characterized by particular mineral resources.Similarly, Akande et al., (1992) also carried out asystematic study of the formation of Lead-Zinc-Fluorite-Barite deposit

of the Benue Trough. Hydrogeologically, Offodile (1992) delineated water bearing aquifer and discuss the water chemistry and quality of the Middle Benue Trough as good. Although structural works in the middle Benue Trough have been discussed but on a regional scale, no such detail work have been reported on a small scale. Therefore, this paper is a preliminary studies of structures controlling the flow of brine in the Awe brine field.

Geologic Setting of the Benue Trough

The Benue Trough extends from the south where it merges with the Niger-Delta to the north where its sediments are part of the Chad basin. The trough burficates near its northeastern end and the northern branch continues beneath the Chad Formation as an elongate depression that extends well beyond Lake Chad. The Benue Trough is a failed arm of a rift system of the Gulf of Guinea, South Atlantic and Benue Mesozoic triple junction whose center is occupied by the Niger Delta (Grant, 1971). Murat (1972) proposed three major tectonic phases which took place in Albian, Santonian and late Eocene or early Oligocene times. These major tectonic phases resulted in the formation and subsequent remodeling of the Benue Trough. There are folds which consist of series of anticlinorium and synclinorium suggesting that there was a deformational episode in the trough. These folds, coupled with the identification of the igneous rock such as andesites in the Abakaliki area which led some workers to propose a compressional (subduction) rather than an extensional tectonic setting for the Benue trough (Farrington 1972; Burke *et al.,* 1972). The floor of the Basin is irregular and sediments thicknesses vary from place to place. This occurs as a result of extensive block faulting initiated when the trough began to develop.

Geology of the Study Area

In the study area, the Awe Formation is seen to outcrop in several locations. This Formation is deposited as transitional beds which consist of flaggy, whitish, and medium to coarse grained sandstones which are interbedded with carbonaceous shales or clays from which brine springs issue continuously (figures 3c and d). The Awe Formation marks the beginning of the regressive phase of the Albian sea. The sandstone unit of the Awe Formation covers almost all the study area which ranges in colour from whitish to grey and brown with reddish and yellowish spots in some area. The beds of this unit are usually multi-layered,highly micaceous, It ranges in thickness from 20-38m (figures 4a and b).The shale unit of the Awe Formation is found as intercalation within the sandstone. Strike and dip were measured to establish the dominant trend in the area. Structures observed in the study area include fold, lamination, bedding, bedding, fold, joints, and mudcrack (figures 4 a,b,c,and d).

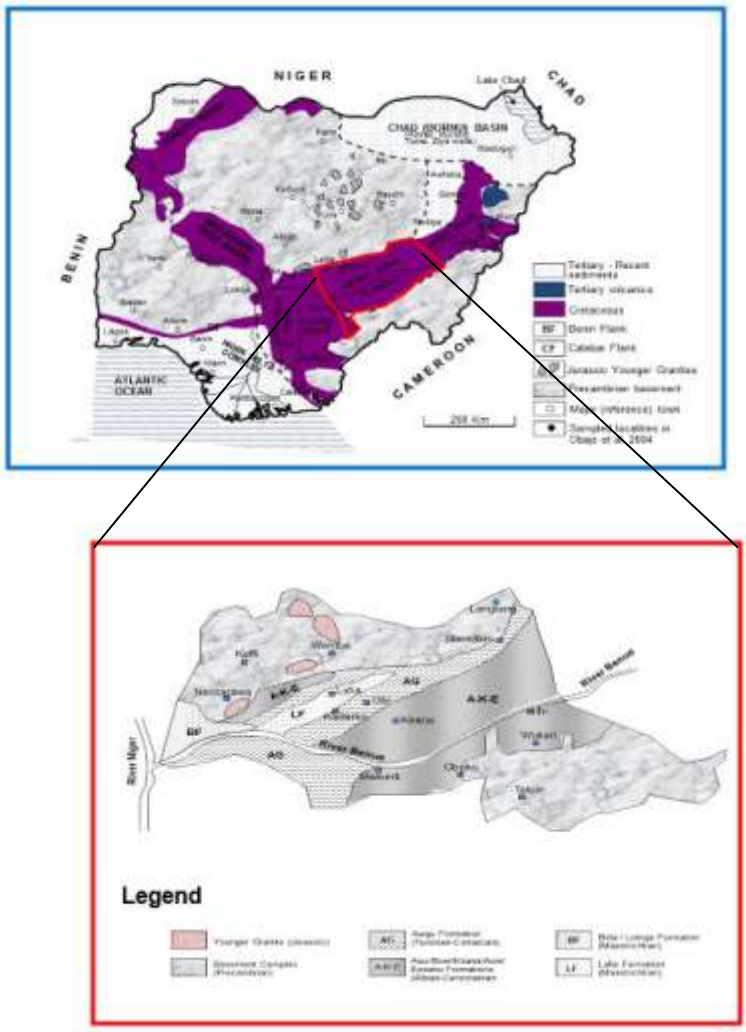

Figure 2 : Generalized Geological Map of Nigeria and Middle Benue Trough (Redrawn from Offodile, 2002)

(a) **(b)**

(c) **(d)**

Figure 3a, b, c, and d:(a) Left fold limb, (b) Right fold limb, (c) and (d) brine issuing out from the limbs of the fold

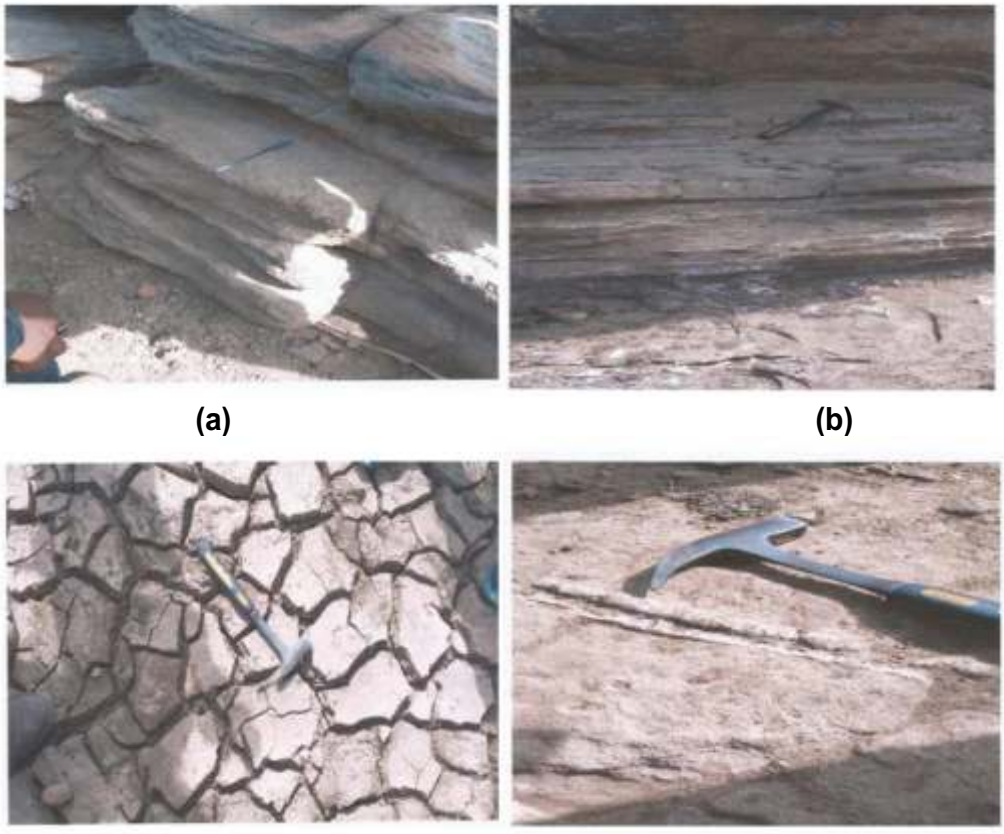

(a) **(b)**

(c) **(d)**

Figure 4 a, b, c & d: (a) Sandstone unit of the Awe Formation (b) a typical section of the Awe Formation (c) mudcrack observed along river Bakin Abu and (d) Joints infilled by silica

METHODS AND MATERIALS

The geologic mapping fold Awe town was carried out and structures, textures and mineralogy were studied and observed. Strike readings on joints and quartz veins were also taken. Materials used include compass, camera, field notebook, Global Positioning System (GPS).

Results and Discussion

It was observed in several places that brines are associated with depression created by anticline.Some interesting field evidence points to the probability of the occurrence of dome structures in the brine bearing sediments. These brine-fields are underlain by Formations of Cretaceous age.The tectonic set up in this brine field is dominated by the Keana–Awe anticlinorium. In the study area brines are closely associated with these structures and are commonly seen to issue from the transitional beds at the flanks of the folds in Awe Formation irrespective of their mode of occurrence. It is quite clear that these page movements or inflow of the brines are mostly controlled by the fracture systems within the trough. However, the variation in the local lithology at the outcrop sites from predominantly shales in lower region to sandstones and intercalation of shale/limestone units in the middle region suggests that the brines are not lithologic controlled.

Table 1: Strike reading for set of joints

Number	Strike (^{0})
1	160
2	138
3	078
4	156
5	160
6	162
7	166
8	070
9	174
10	164
11	158
12	098
13	158
14	160
15	088
16	150
17	156
18	156
19	150
20	168

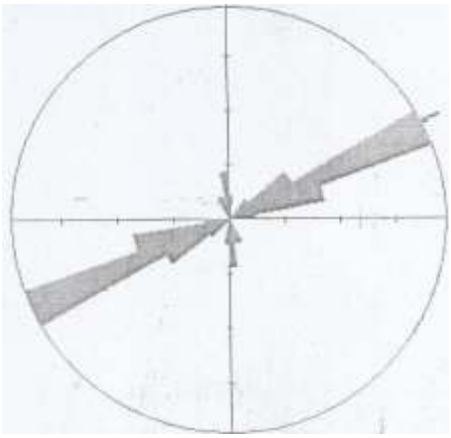

Figure 5: Rose diagram plot for joints readings

Table 2: Strike reading for set of quartz vein

Number	Strike (^{0})
1	168
2	174
3	162
4	130
5	132
6	160
7	118
8	130
9	010
10	018
11	152
12	144
13	174
14	172
15	140

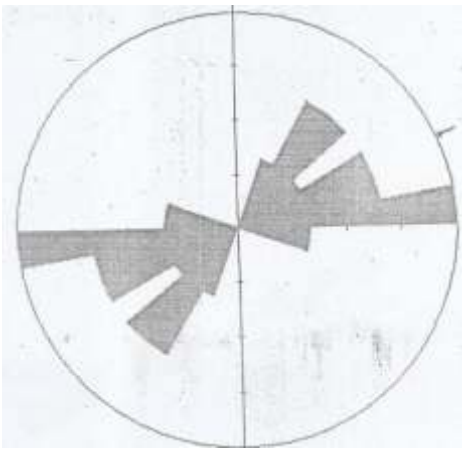

Figure 6: Rose diagram plot for quartz vein

Again, from the above strike measurement of both the joints and quartz veins, it can be observed that the dominant trend is NE-SW which coincides with the major fold trend of Offodile (1976). The variability in the strike trend reflects the sinousity of the fold axis. Apart from these a counter minor flexure runs approximately NW-SE almost at right angle to the former. The sinousidal feature of the main fold axis is thought to be due to the later fold which appear to have affected all the geological formations, this effect is obvious on the Awe Formation at Awe town. In general, the disposition of the folds is similar to what has been recorded in the Upper Benue Trough, where also two main fold trends have been observed, a major NE-SW fold and a minor NW-SE fold (Carter et al.,1963).

Conclusion

The study area covered Old Awe town in Awe Local Government area of Nasarawa State. The area is part of the Middle Benue Trough of Nigeria and the area is composed of the Late Albian-Cenomanian Awe Formation (consisting essentially of sandstones with intercalations of bands of shales and clays). Structures observed on the field include bedding, lamination, mudcracks, fold, joints. The major structural trend is oriented in the NE-SW and NW-SE direction which coincides with the major fold axis in the study area. This work concluded that brines are closely associated with these structures and are commonly seen to issue from the transitional beds at the flanks of the folds in Awe Formation irrespective of their mode of occurrence. It is quite clear that the seepage movements or inflow of the brines are mostly controlled by the fracture systems within the trough.

References

Ajayi, C.O. (1979). “A Detail Gravity Survey of the Middle Benue”. Ph.D. Thesis. Ahmadu Bello University: Zaria, Nigeria.

Ajayi, C.O. and Ajakaiye, D.E. (1986). “Structures Deduced from Gravity data in the Middle Benue, Nigeria”. Journal of African Earth Sciences. 5:359-369.

Akande, S.O., Hoffknecht, A. and Erdtman, B.D. (1992). “Environment of Ore Formation Archi Zonal Metamorphism in Pb-Zn-Fluorite-Barite Deposits of the Benue Trough, Nigeria”. Geologie Mijinbouw. 71:131-144.

Akande, S.O., Horn, E.E, and Reutel, C. (1988). “Mineralogy, Fluid Inclusion and Genesis of the Arufu and Akwana Pb-Zn Mineralization, Middle Benue Trough, Nigeria”. Journal African Earth Sciences. 7:167-180.

Avbovbo, A.A. (1980). “Basement Geology in the Sedimentary Basins of Nigeria”. Geology. 8:323- 327.

Benkhelil, J. (1982). “Benue Trough and Benue Chain”. Geological Magazine. 119:155-168.

Benkhelil, J. (1987). “Cretaceous Deformation, Magmatism and Metamorphism in the Lower Benue Trough, Nigeria”. Geological Journal. 22:467-493.

Benkhelil, J. (1988). “Structure et E’volution Ge’odynamique du Basin Intracontinental de la Be’nue (Nigeria)”. Bulletin Centres Recherches Exploration Production Elf-Aquintaine. 12:29-128.

Benkhelil, J. (1989). “The Origin and Evolution of the Cretaceous Benue Trough (Nigeria)”. Journal of African Earth Sciences. 8:251-282.

Carter, J.D., Barber W., Tait, E.A., and Jones, G.P., (1963). “The Geology of Parts of Adamawa, Bauchi and Bornu Provinces in the North-eastern Nigeria”. Bulletin Geological Survey, Nigeria. 30:1-99.

Cratchley, C.R. and Jones, G.P. (1965). “An

Interpretation of the Geology and Gravity Anomalies of the Benue Valley, Nigeria". Overseas Geol. Surv. Geophys. 1:1-26

Obaje, N.G. (2009). Geology and Mining Resources of Nigeria. Springer. Pp. 221.

Offodile, M.E. (1976). The Geology of theMid dle Benue, Nigeria.
Ph.D. Thesis. University of Uppsala, Sweden. 166p.

Offodile, M.E. (1984). "The Geology and Tectonics of Awe Brine Field". Journal of Earth Sciences. 2:191-202.

Offodile, M.E. and Reyment, R.A. (1977). "Stratigraphy of the Keana-Awe area of the Middle Benue Region of Nigeria". Bulletin Geological Institutions University Uppsala (N. S.) 7:37-66.

Sabo, A. (2001). "The Geology and Geochemistry of Keana Brine Pit". Unpublished M.Sc Thesis Department of Geology and Mining. University of Jos: Jos Nigeria. 11-40.

Simpson, A. (1954). "The Nigerian Coal Field. Th eGeology of Parts of Owerri and Benue Provinces". *Bull. Geol. Surv. Nigeria*. 24, 85.

Tattam, C.M. 1944. "A Review of NigeriaStratigra phy". *Rep. Geol. Surv., Nigeria* (1943). 27-46.

Muhktar, et al (2019) Nigerian Mining Journal, (16) 29 - 40
© Nigerian Society of Mining Engineers, ISBN 1117 - 4307

Optimizing Petroleum Reservoir Modeling based on the Extended Elastic Impedance Approach

Muhktar Habib, L.K. Salati and I.S. Amoka
Department of Mineral and Petroleum Resources Engineering, Kaduna Polytechnic, Nigeria
Corresponding author: mukhtarhabib102@gmail.com; +2347034913167

Abstract
Deterministic seismic inversion and extended elastic impedance (EEI) were applied to obtain quantitative estimates of reservoir properties over a West African Congo Basin Field. The optimum EEI angles corresponding to the reservoir properties were analyzed using the well logs data, together with a lithology indicator. Pre-stack seismic data were simultaneously inverted into density, acoustic and gradient impedances cubes, through model-based inversion algorithm. The last two broadband inverted volumes were projected to the Chi angles corresponding to petrophysical indicators, resulting to two broadband EEI volumes. At Well location, the EEI versus petrophysical parameters linear trends were then used to transform EEI volumes into quantitative porosity and shale volumes based on a specific lithology. In order to obtain the reservoir facies distribution, a background EEI was established based on an identified minimum energy angle, thereby enabling the mapping of reservoir facies.
Keywords: elastic impedance, hydrocarbon reservoir, lithology, seismic inversion, well log

Introduction

A reliable quantitative measurement of petrophysical parameters and distribution of reservoir facies in 3D space are key objectives for Plutonio field development. A proper understanding of sand body distribution is vital for well planning and production enhancement. As a result, measurement of important petrophysical parameters such as shale volume (V_{sh}), effective water saturation (S_w) and porosity are of great importance for static modeling and reserve estimation. These reservoir properties are usually derived from Seismic impedances (P and S-impedance) data through either statistical relationship between rock properties and elastic properties derived from well logs (Dubucq, 2001; Vernik, 2002), or geo-statistical approach (Doyen, 2009).

In this work, the concept of extended elastic impedance (EEI) was applied on the Plutonio field. The approach was selected considering the thickness of targeted reservoirs, largely above the tuning thickness. The concept was applied to derive three petrophysical properties targeted at different reservoir units and to map the distribution of reservoir facies in 3D space. After a careful comparison with results derived from conventional geostatistics, it was realized that EEI corresponding to minimum energy 翩 is a robust way to extract the spatial distribution of geo-bodies.

Elastic Impedance

The basic idea behind conventional acoustic impedance (AI) inversion method is an assumption of a P-wave from subsurface interface at normal incidence angle (Latimer, 2000). In some cases like small offset range in a CDP gather, this theory is almost fulfilled and the inversion produces reliable results. However in many hydrocarbon reservoirs, similar acoustic impedance value has been observed between hydrocarbon saturated reservoir and the surrounding shale, which makes it difficult, or in some cases even impossible to analyze and discriminate between reservoir sand and surrounding area on zero offset seismic data (Connolly, 1999). With recent progress on amplitude versus offset (AVO) technique which makes it easier to differentiate hydrocarbon reservoir from the surrounding shale and cap rock, there is a rise in demand on analyzing non-zero offset seismic data. Elastic parameters from non-zero offset data achieved by elastic impedance technique were introduced by Connolly (1999). This method is suitable for fluid discrimination and lithology prediction for various reservoirs, since it includes more information on lithology and fluid than acoustic impedance.

Hence, elastic impedance (EI) is a generalization of acoustic impedance for variable incidence angle. It provides a consistent and absolute framework to calibrate and invert non-zero offset seismic data. Preliminary work on elastic impedance undertaken by Connolly demonstrated that the elastic impedance approach provides inversion results compared to traditional quantitative use of AVO information (e.g intercept and gradient method). The EI approximation is derived from linearization of zoeppritz equation, usually aki and Richards two term approximation where (q) is the angle of incidence at reflector interface. The most popular definition of elastic impedance is illustrated by Equations 1 to 4.

$$El(\theta) = V_p^a \times V_s^b \times \rho^c \qquad \ldots 1$$

$$Where\ a = 1 + \sin^2\theta\,; b = -8k\sin^2\theta\,;$$

$$c = 1 - 4k\sin^2\theta\,; and\ k = \left[\frac{V_s}{V_p}\right]^2$$

As shown in Equation 1. the elastic impedance is a function of P-wave velocity (V_p), S-wave velocity (V_s), density (r) and incident angle (q) The factor K is assumed constant and is usually set to the average of V_p and V_s across the inter-phase or over the zone of interest (ZOI) (Connolly, 1999).

Connolly (1999) showed that EI decreases with increasing incident angle compared to EI at normal incidence (q). While Connolly's work provides good result and useful guide for enhanced reservoir characterization, restriction of incident angle of Eqn. 1 was a serious challenge. The key problem is that EI has strange unit and dimensions and the values do not scale correctly for different angles (Whitcombe, 2002). The EI limitation was overcome by Whitecombe (2002) who modified Equation 1 by introducing reference or normalizing constant a_o, b_o, r_o which represent average value of velocities and density over the zone of interest or value at the top of the target zone.

Extended Elastic Impedance

Impedance inversion is usually applied to zero offset data. Whitecombe (2002) redefined elastic impedance in which he broadened the definition of elastic impedance by removing the dependence of its dimensionality on the angle (q). He realized that some properties of rocks cannot be predicted from the existing seismic gathering due to limitations on incidence angle range $(0 \quad 30^o)$ in the elastic impedance. Thus, $\sin^2 q$ needs to exceed unity in order to estimate some petrophysical properties; however, it is impossible that the reflectivity values exceed unity without negative impedance contrast, making it unrealizable (Francis, 2006).

Whitecombe et al (2002) recognized that outside of the $0 \quad 30^o$ angle range, although EI is not valid for predicting pre-stack seismic data it may correspond with rock physics or petrophysical properties of interest. They therefore extended EI so that it is defined for all values of $Sin^2 q$ between positive and negative infinity. This is achieved by replacing $Sin^2 q$ with $\tan x$ and introducing the notion of scaled reflectivity (normal reflectivity multiplied by $Cosx$). This further results in bounds of the angle x with 90 to $+90^0$. Whitecombe et al. therefore extended the concept of elastic impedance (Connolly, 1999) so that it is applied for the purpose of fluid and lithology discrimination. The variable q is now a function called x (Chi angle) which varies between 90^o and 90^o (Figures 1 and2). The EEI equation is expressed as:

$$EEI = \alpha_0\rho_0\left[\left(\frac{\alpha}{\alpha_0}\right)^p\left(\frac{\beta}{\beta_0}\right)^q\left(\frac{\rho}{\rho_0}\right)^r\right] \qquad \ldots 2$$

Obtaining valuable reflectivity at χ=0° and χ=90° so that it can be converted into acoustic and gradient impedances was one of the reasons leading to development of the EEI technique. Therefore Eqn. 5 can also be written as:

$$EEI(x) = Al_0\left[\left(\frac{AI}{AI_0}\right)^{\cos x}\left(\frac{GI}{GI_0}\right)^{\sin x}\right] \qquad \ldots 3$$

The coordinate rotation can also be expressed in log scale as,

$$\log EEI(x) = \log Al_0 + \cos x \log\left(\frac{AI}{AI_0}\right) + \sin x \log\left(\frac{GI}{GI_0}\right)$$

Where $\alpha = \mathrm{P} - \text{wave velocity}; = \mathrm{S} - \text{wave velocity};$ $\mathrm{AI} = \mathrm{P} - \text{impedance}; \mathrm{GI} = \text{gradent impedance};$ $\rho = \text{Density}; \mathrm{p} = \cos x + \sin x\,; q = -8k \sin x$ $and\ r = \cos x - 4\mathrm{ksin}\, x.$ $\mathrm{AI}_0, \alpha_o, \beta_o and \rho_o$ are average of respective properties used as normalization factors for P – impedance, P velocity, S velocity and density, respectively. K is the average of $\left(\frac{V_s}{V_p}\right)^2$ in the time depth interval. x is considered as the rotational angle in the intercept gradient (AB) plane derived from AVO which is related to the angle of incidence θ.

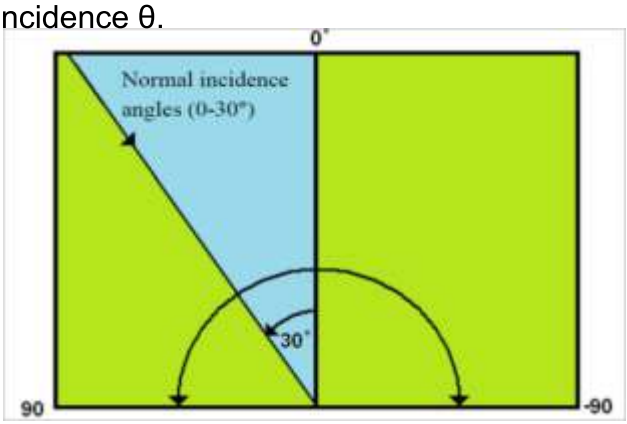

Figure 1: Extended elastic impedance angles ranginge from 90 to (Hampson-Russell knowledge base, 2005)

The distinct difference between the extended elastic impedance and the normalized version of elastic impedance is the change of variable. EEI is a function of chi angle (an angle in an abstract construction) and EI is a function of q (an angle in a physical experiment) (Francis and Hicks, 2006). This can lead to EEI much more efficient than EI and should give different outcomes than standard EI inversion method. The new variable (x) allows calculation of impedance value beyond physically observable range of angle q(including imaginary angles not necessarily recorded in the gathers). A clear example of this situation happens when shear impedance corresponds to $\sin^2 q$=1.25. It is obvious, negative angle is not physically recordable but can be projected from angle gathers by linear extrapolation (Iske, 2006; Alebouyeh and Chehrazi, 2018).

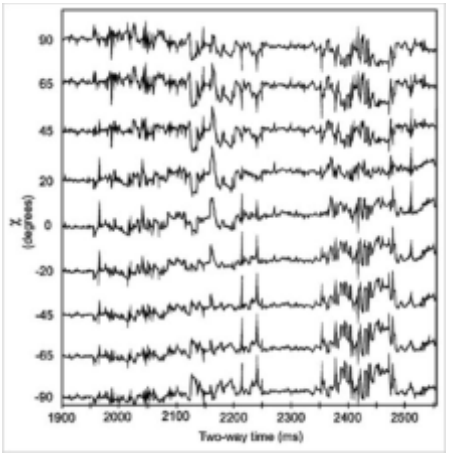

Figure 2: EEI function for various (x) values for a particular well (Whitecombe, 2002)

The EEI log at x=0 is similar to EEI log at q= 0, which is simply the acoustic impedance EI. Whitecombe et al (2002) provided a simple robust application for deriving lithology and fluid sensitive seismic impedance volumes. According to his perspective, under certain approximation the EEI log at various chi angles are proportional to different rock elastic parameters (Figure 3). In other words, the chi angle can be selected to optimize the correlation of the EEI logs with petrophysical reservoir parameters, such as V_{shale}, S_w and porosity, or with elastic parameters such as bulk modulus, shear modulus, lame constant (Whitecombe, 2002). Therefore, EEI logs for specified angles from these parameters can be produced using EEI equation which is suited for tying well data directly to seismic data (Figure 3). Directness of EEI method is the main advantage which provides an EEI volume attributes that corresponds to petrophysical parameters of interest. Eqn 8 is two term linearization zoeppritz equation for reflectivity (Aki and Richards, 1980). The comparison between elastic parameters and equivalent EEI curve for particular well, represents the high degree of correlation. The EEI function is defined as a function of the angle x, not the reflection angle q. (Whitecombe, 2002)

This angle is referred to as "**Minimum Energy angle"** (Hicks, 2006). It is the angle at which reflectivity defined by the two terms AVO equation is zero. The equivalent θ angle is commonly beyond the range of recorded seismic, but if it happens to be within the recorded angle of seismic gather, one might expect to see a phase reversal of seismic reflection. Since the Impedance contrast at the shale-shale interface is usually negligible at minimum energy, synthetic seismic obtained for this angle is referred to as background trend. This will definitely help to identify bodies highly contrasting within the background volume.

Figure 4 shows the general concept on EEI inversion approach. The flow chart shows that EEI inversion method involves building (x) model and inverting an EEI (x) volume using an inversion algorithm to create an EEI output. This study focuses on the extended elastic impedance (EEI) based on the simultaneous model-based inversion method, which is carried out to generate several seismic attributes ($V_p/V_s, LMR$, Poisson ratio, Bulk modulus, Water saturation, etc.). Comparisons of these properties with rock properties help to determine the sensitivity of elastic parameters to seismic anomaly, improve reservoir characterization and enhance fluid and lithology imaging.

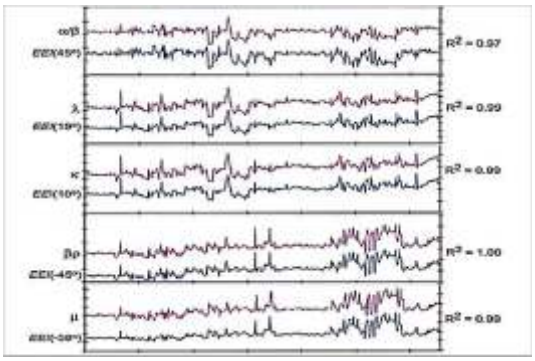

Figure 3: Comparison between elastic parameters and equivalent EEI curve for particular well

$$R_p(\theta) = A + B\sin^2\theta \qquad \ldots 4$$

With respect to Whitecombe's method, $\sin^2 q$ is replaced by $\tan x$, so that Equation 4 becomes Equation 5, thereby allowing the angle to vary from 90^0 to 90^0.

$$R_p(\theta) = A + B\sin^2\theta \Rightarrow R(x) = A + B\tan x \qquad \ldots 5$$

If we assume $x = x_o$ so that $R(\theta)$ is zero in (Equation 5), then it becomes

$$\tan x = \frac{A}{B} \qquad \ldots 6$$

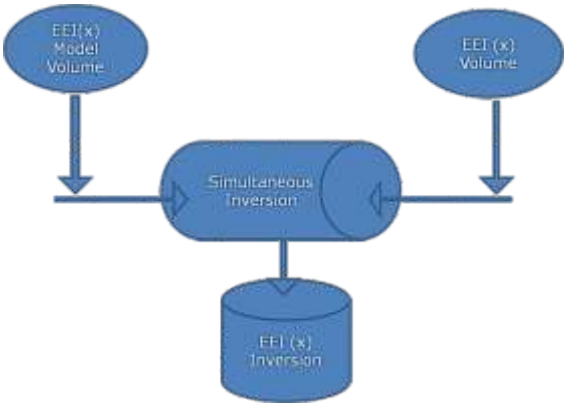

Figure 4: General concept on extended elastic impedance (EEI) inversion approach (Hampson and Russell knowledge base, 2005)

Materials and methods

The main steps followed in this research are:

1. Well log data quality control (QC) and conditioning; this was first conducted in order to ensure that the required data (measured P and S Sonic, density, and petrophysical logs) are available and physically reasonable in support of further rock physics activities.
2. Computation of EEI logs for different χ angles by applying Eqn. 5 and determination of the optimum angle that gives the best correlation (positive or negative) of EEI with petrophysical target log (Porosity, shale volume and Water saturation). This is the key step to successful application of the proposed technique.
3. QC, conditioning and simultaneous inversion of pre-stack time migrated angle partial stacks, such as near (5°-18°), mid

(18°-31°) and far (31° 45°) into acoustic and gradient impedances

4. Based on the optimal angles generated, computation of equivalent EEI volume through Eqn. 9 was achieved.
5. Transformation of EEI volume into quantitative petrophysical property.
6. Finally, Reservoir facies distribution was captured through the concept of minimum energy angle (Eqn. 10). The easiest approach for determining this angle is to compute the EEI log spectrum with 翿 ranging from -90° to +90° (with the angle increment equals to 1). The determination of minimum energy angle χ_0 is a visual process by analyzing the entire log spectrum in order to pinpoint zones where anomalies are better characterized. Once the angle χ_0 is determined, step 4 was then applied to generate equivalent EEI volume based on minimum energy angle.

Results and Discussion

Optimum EEI angles

Well log Data Gathering and Quality Check: This step ensures that the required data is available in support of petrophysics and rock physics activities; it deals with improving well data which involves gaps correction and other unavoidable problems with gathered data. It also accounts for up scaling when the need arises. The stage is an intensely visual process, requiring visualization tools and interactive manipulation widgets to make the process smooth, easy, and accurate. All succeeding steps in the workflow depend on the quality and veracity of this step in the process. In this research, the measured P and S velocities as well as density logs were of good quality, as shown in Figure 5. On Figure 5a, the lines representing constant $\frac{V_p}{V_s}$ ratio show that the values of both P and S velocities are in physically reasonable range while the evaluation of multi-well trend plots (Figure 5b) reveals that there are no spurious data for the sonic and density.

EEI angles computation and correlation: Determining optimum angle for a particular target reservoir property log is the primary base to a successful implementation of the proposed technique. Hence, high-quality wire line log was applied for the calculation of EEI logs based on Equation 3 for ranges of $X = 90$ to $X = +90$. A correlation between the target log and the EEI logs for every X angle is obtained. Maximum/minimum angles are identified and considered optimal. This indicates how well a given petrophysical property can be predicted

.

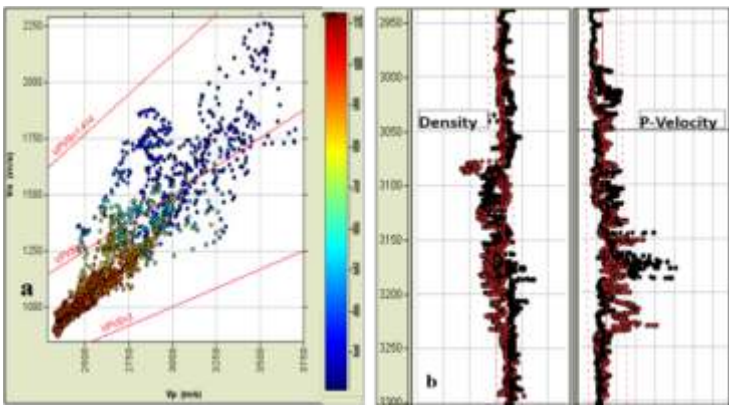

Figure 5: (a) Cross plot of measured P and S velocity with the overlain lines of constant Vp/Vs ratio. (b) the evaluation of multi-well trend plots

In this study, an EEI analysis was carried out, where three reservoir properties; Porosity (f), Water saturation $(S_{w_{eff}})$ and Shale Volume (V_{sh}) correlate well with EEI logs at $\chi = 22^{o}, 30°$ and $69°$, respectively. This is depicted in Figure 6). Even though some wells are not closely spaced, it has been observed that at each well, EEI corresponding to $\chi = 69^{o}$ or close to it gave a maximum correlation with the shale volume $(V_{sh}\log)$ at a correlation of 86% while EEI corresponding to $\chi = 22^{o}$ or close to it gave a maximum correlation with the porosity log (f) at a correlation of 85%, and EEI corresponding to $\chi = 30^{o}$ or close to it gave a maximum correlation with the effective Water saturation log $(S_{w_{eff}})$ at a correlation of 78%.

Pseudo-petrophysical property logs derived from EEI were then generated at the angles of maximum correlation which gave room for comparison with the corresponding petrophysical well logs as shown in Figure 7. A good match can be observed between petrophysical parameters and the computed extended elastic impedances. To ease the comparison, both petrophysical and EEI logs were normalized. The matched curves therefore validate any interpretation that is based on the petrophysical volume derived from the EEI based seismic data.

Seismic inversion

Seismic data QC and Conditioning:

For the well log data, preparation consists of editing and conditioning log curves when needed, an inordinate amount of time can be spent when it comes to seismic data (offset gather). In recent times, seismic partial stacks have become the “evergreen” Pre-stack data as inputs for detailed AVO studies. As argued out by many scholars, despite its superior resolution, the overall quality of seismic partial stacks may suffer from time misalignment, side lobe wavelets, scaling of relative amplitude between near and far sections, especially for deep targets reservoirs. The idea of conditioning seismic partial stacks consists of detecting and fixing potential problems and thus preparing the seismic data for quantitative AVO studies. The different steps of conditioning the seismic partial stacks depend upon the results of the quality control (QC) and the knowledge of AVO end members gained through modeling.

In this research, several types of seismic data are available among which are three partial stacks corresponding to the incidence angle ranges of 5-18 for near, 18-31 for mid, and 31-45 for far. Synthetic seismogram for near and far sections is shown in Figures 7 and 8. Data were subjected to strict quality control which did not reveal any severe problems. All the steps used during the QC process are outlined in Table 1.

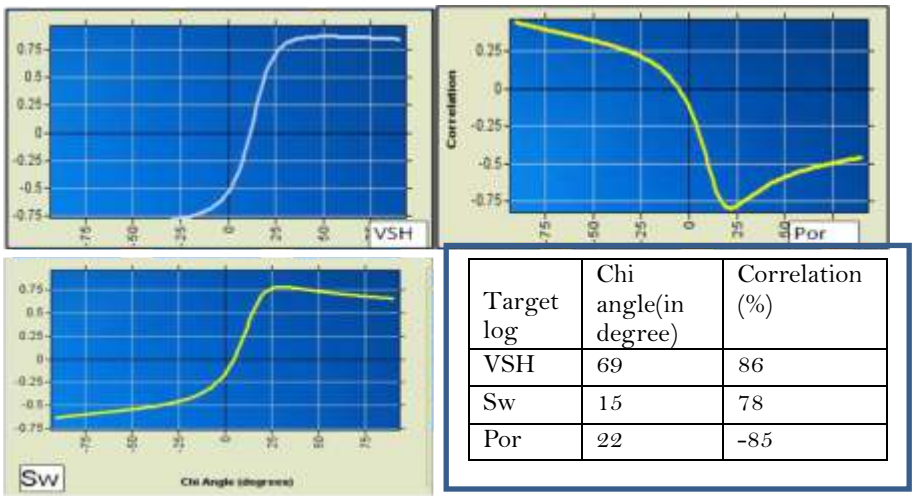

Target log	Chi angle(in degree)	Correlation (%)
VSH	69	86
Sw	15	78
Por	22	-85

Figure 6: Chi angle Correlation for Volume of Shale (V_{sh}), Water Saturation (S_{wt}) and Porosity

Table 1: Seismic data QC and Conditioning

Step	Checked/not checked	Qc Results
Zero phase QC	Checked	All three seismic cubes are zero phase (Figs. 4.3 and 4.4)
Time Shift QC	checked	Far section is time shifted to about -6ms (correction was apply)
Frequency and phase balancing	checked	Well balanced

Figure 7: *Comparison of petrophysical logs with logs derived from EEI using the optimum angle after normalization (Plutonio– 2B)*

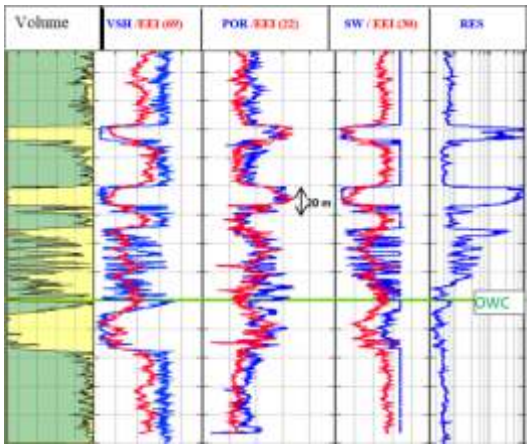

Figure 8: Near Seismic well tie showing the extracted wavelet is zero phase. (Plutonio – 2B)

Low frequency modeling:
In order to make a low frequency model, this work filtered the available well logs in the 0-10 HZ low frequency range and then interpolated them along the mapped horizons with accurate stratigraphic control (Figure 9). The inverse distance-based algorithm was applied and hence obtained the detail model. Only low frequency trend un-accountable in seismic data is contained in the model. A total of six wells have been included in the model in which three background models (AI, GI, and Vp) were generated and then used as the starting models for the inversion.

Statistical / quantitative wavelet extraction and synthetic seismogram:
Prior to the inversion, near, mid and far partial stacks were used to conduct seismic well tie. This is achieved by comparing the real and synthetic seismic data in the time window of interest (500ms was used). The time depth relationship at each well was available, which permits an extraction of statistical wavelet in the target interval. The extracted statistical wavelet was then used to build a synthetic data (Nascimento, 2013; Salleh, 1999). The correlation coefficient between the latter data and the real near seismic was improved from 0.4 to 0.5 by applying a wavelet phase rotation, and therefore the time depth relationship was updated. Finally, the correlation coefficient was improved again up to 0.6 after using well data (P-wave, S-wave velocities and density logs). The process consists of creating a reflectivity from P-wave, S-wave velocities and density logs using Zoeppritz equation or its approximations, convolving it with the extracted near angle wavelet and rotated to generate the synthetic seismic traces, then the wavelet (especially the phase) and time depth relationship are iteratively updated so that the synthetic seismic traces fits the real seismic data as described by Figures 7 and 8. QC on wavelet showed that it is stable up to the frequency of 55Hz. Once the edited time depth relationship is produced for each well, it becomes straightforward to carryout to the inversion of based on Equation 10.

Seismic inversion result and QC:
Deterministic inversion is at its best when reservoir layering is relatively thick with high reflectivity. The data applied for this study was found to be suitable for deterministic inversion. The deterministic model applied herein is called simultaneous model-based inversion. Figure 10 illustrates sections passing through wells showing the inverted acoustic impedance (top) and gradient impedance (bottom).

In this type of inversion, an initial impedance model is modified iteratively so as to make better the fit with seismic trace. With a good initial model, model-based inversion can be able to remove wavelet as well as turning effects. The initial model comprises the interpolated impedance data from the wells guided by a stratigraphic framework defined by the pick seismic horizons. Hence, by convolving the AVO approximation equation of Wiggins et al. (1985) with wavelet W (θ), the synthetic seismic trace applied here is written as;

$$S_{pp}(\theta) = \frac{\alpha}{2W(\theta)\Delta Ln(AI)} + \frac{b}{2W(\theta)\Delta\delta n(GI)} + \frac{c}{2W(\theta)\Delta\delta n(vp)} \quad \ldots 8$$

$$\text{Where } a = 1 + \alpha_{GI}b + \alpha_{Vp}c;\ b = sin^2\theta \text{ and } c = sin^2\theta tan^2\theta$$

α_{GI} is the gradient coefficient of the linear equation GI (in y axis) versus AI (in x axis); α_{Vp} is the gradient coefficient of the linear equation V_p (in y axis) versus AI (in x axis); $\delta Ln(V_P)$ ois the deviation away from the linear equation V_p (in y axis) versus AI (in x axis); $\delta Ln(GI)$ is the deviation away from the linear equation GI (in y axis) versus AI(in x axis)

In the matrix form, Equation 8 is reduced t

$$S = J.Ln(Z) \quad \ldots 9$$

J is the system matrix of the product of W and D.

The diagonal matrix D is composed of the difference operation Δ, applied to each Ln (AI), $\delta Ln(V_P)$ and $\delta Ln(GI)$. Column vector Ln (Z) is composed of Ln (AI), $\delta Ln(V_P)$ and $\delta Ln(GI)$. W is a banded matrix composed of extracted wavelets per partial angle stack. S is a column vector of the near, mid and far seismic traces.

To solve Equation 9 for $Ln(Z)$, the following total objective function is minimized;

$$\|S_{real} - X \cdot Ln(Z)\|^2 + \mu \ \|Ln(Z) - Ln(Z_0)\|^2 \quad ..10$$

Where μ is the model weight, it has to be small to guarantee the inversion is driven by real seismic data.Z_0 is the initial model with which the inversion starts.

The conjugate gradient method is used to iteratively modify Ln(Z*)* until the difference between the synthetic seismic data $S_{pp}(\theta)$ and real seismic data $S_{real}(\theta)$ is minimized for near, mid and far stack angles. It is then straightforward to derive Z by exponentiation of Ln(Z*)*.

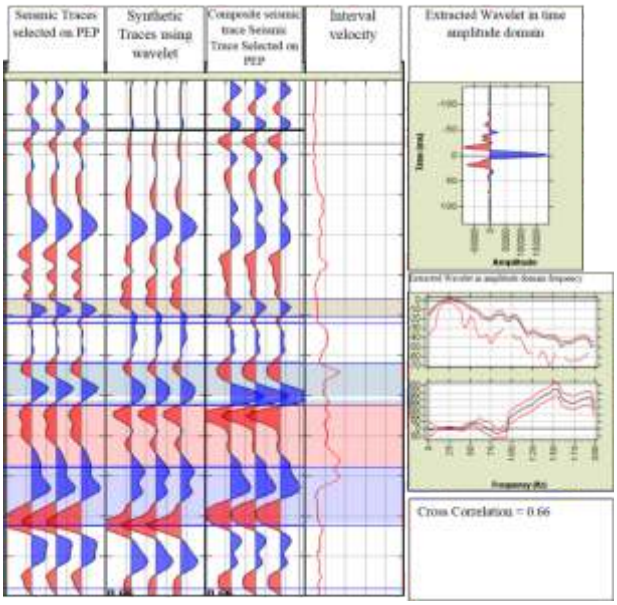

Figure 9: Far Seismic well tie for the extracted wavelet of zero phase. (Pu – 2B)

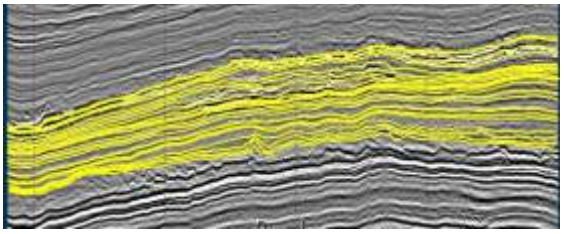

Figure 10a: Numerous auto tracked horizons used together with interpreted horizon to build the low frequency model

In this area, the stratigraphic framework comprises of the 072 and 073 horizon picks. A total of 6 wells have been included in the model in which three models were generated based on the developed optimal angles. Figure 10 shows the acoustic and gradient impedance inversion results in a section passing through 3 wells depicted by gamma ray logs. Pu 1A well was omitted in the inversion process to serve as a blind test well, and the rest wells were used to generate the low frequency background model. Considering the wells used in this study,

including the blind test well, the correlation coefficients between the inverted and the initial logs were 0.90 for acoustic impedance, and 0.82 for gradient impedance. Figure 11 shows the inverted impedances (acoustic and gradient in red color) with the initial well log measurements (in black color). The high correlation factors seen in the figure and the acceptable inversion results at the blind well test demonstrates the high quality of inversion results to be used for further studies.

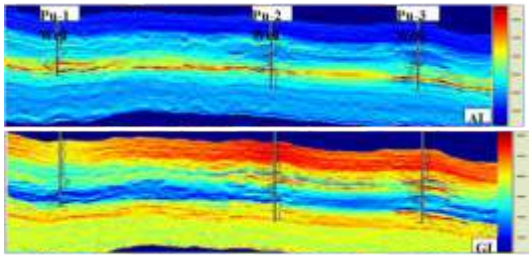

Figure 10b: Sections passing through wells for inverted acoustic impedance (top) and gradient impedance (bottom).

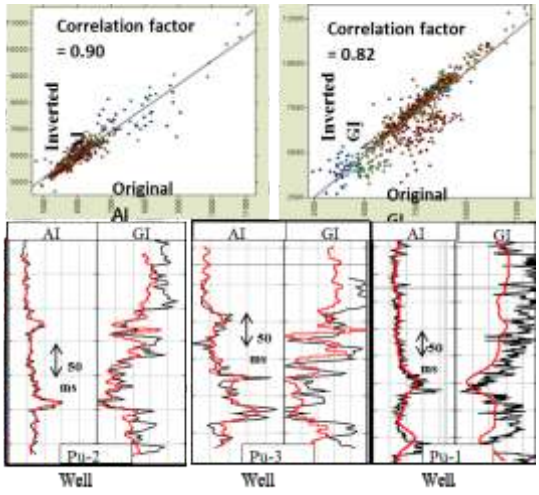

Figure 11: *QC of results: (Top) Inverted seismic impedances versus well log impedances; (bottom)*

Computation of equivalent EEI volume through Equation. 10

The fact that the inverted seismic data match with the initial log measurements gave confidence that both inverted impedances can be transformed into EEI volumes using Equation 7 and the optimal angles estimated. The target time interval bounding with two horizons was used for computing the normalization factor AI_0.

Figure 6 shows the EEI volumes corresponding to the optimal angles of $\chi = 22^{o}$, and $69°$, computed from (Eqn. 7). The two sections passing through wells are extended elastic impedance at $\chi = 22^{o}$ (top of Figure 12), corresponding to porosity volume and extended elastic impedance at $\chi = 69^{o}$ (bottom of Figure 12), corresponding to shale content volume. For comparison reasons, the corresponding properties initially derived from EEI (22^{o}) and EEI (69^{o}) well logs were overlain on each section, and it can be clearly seen that the inverted volumes honor the original data. Figure 12 shows sections passing though wells showing extended elastic impedance at $\chi = 22^{o}$ (top), corresponding to porosity volume. While extended elastic impedance at $\chi = 69^{o}$ (bottom), corresponds to shale volume. Corresponding properties derived from well logs are overlain on the two sections for comparison.

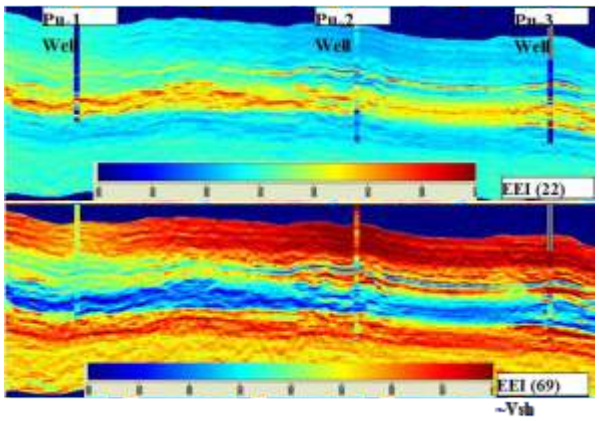

Figure 12: *Sections passing through wells showing extended elastic impedance at 翻= $22^{翻}$ (top), corresponding to porosity volume. While extended elastic impedance at 翻= $69^{翻}$ (bottom), corresponds to shale volume. Corresponding properties derived from well logs are overlain on the two sections for comparison*

The corresponding EEI curve for water saturation $(\mathrm{Sw}_{\mathrm{eff}})$ was not applied due to its in ability to provide a good match with the well log.

From Figure 12, it is easy to map the sand reservoirs which show high impedance for EEI at (22^o) and low impedance for EEI at (69^o). It therefore becomes easier to map the reservoir sands from those EEI derived petrophysical properties.

Transformation of EEI volume into quantitative petrophysical property

The linear trends shown by different lithologies after cross plotting EEI log data in 3D space color coded by porosity and shale volume, were used to convert the EEI volumes into shale content and porosity volumes. (Fig. 13) shows the RMS of top and bottom o73 unit through porosity (right) and shale content (left) volumes. Zones where contour lines are inferior to 3640 ms with high porosity and lower shale content are favorable zones. A close observation of Figure 13 reveals that the reservoir is clearly defined by shale volume. In addition, high values of porosity map which should be related to the presence of reservoir are also observable. In the East of the porosity map, there is a quite big zone with very high values which geologically does not make sense to be a potential zone if the zone is in the low relief, thus is declared a non-hydrocarbon potential zone. *Zones where contour lines are inferior to 3640 with high porosity and lower shale content are favorable zones.*

Facies distribution based on the Minimum Energy Angle

In order to obtain the reservoir facies distribution, this study applied the concept of minimum energy 翻 (as described by Eqn. 10) on the entire formation; this is because one of our targets in this study is to isolate the oil reservoir sand from the non-reservoir facies. The minimum energy was identified by creating an EEI log spectrum for the angle range of χ = -90° to χ= +90° based on good quality logs analysis. An analysis of the spectrum was as well carried out and a minimum energy region was located at exactly 22° as shown in Figure 14. This corresponds to EEI log at the minimum energy angle which was applied together with the interpreted horizons to build a low frequency model and then subsequently to a model based deterministic inversion that was converted to absolute rock property. This suggests that at χ = 22°, the variation in the log property in the top non-reservoir facies is at minimum, hence consider it as the minimum energy angle.

Therefore, considering the EEI log corresponding to a value of χ = 22° as the background EEI. It is important to mention that the same angle was found to give the minimum high correlation for porosity log. In this case, the results of EEI have to be negated in order to be able to make proper comparison with initial porosity log. A comparison between the background EEI with resistivity log and P-Impedance log is shown in Figure 15, which revealed that a huge difference exists between the background EEI log and P-impedance log especially at the base and top of the formation under study. It can be seen that the reservoir facies are more prominent at EEI (22) log.

To capture the oil sand reservoir facies, the distribution in background EEI (Figure 16) at well locations were analyzed and values for cut off criteria were then obtained that can be applied for volume calculation. A voxel search methodology was applied in determining the distribution of sand oil reservoir facies as shown in (Figures 17 and 18).

Figure 16 shows a potential extension of oil water contact as interpreted from wells. In the reservoir unit, the background EEI capture accurately the high EEI sand corresponding to water sand, while the oil sand reservoirs are characterized by low background EEI.

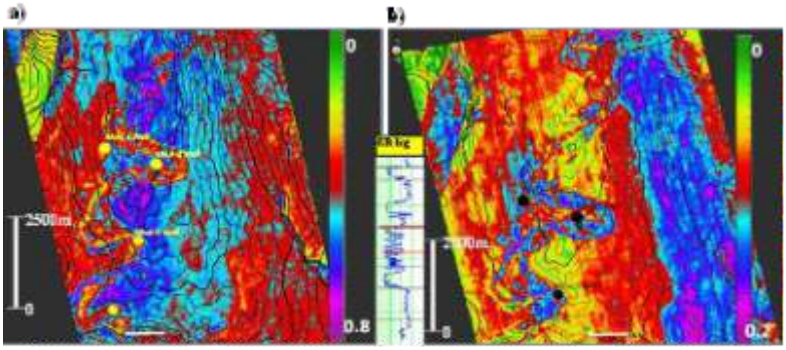

Figure 13: RMS of the top and bottom section of the o73 with the shale volume (left) and porosity content (right).

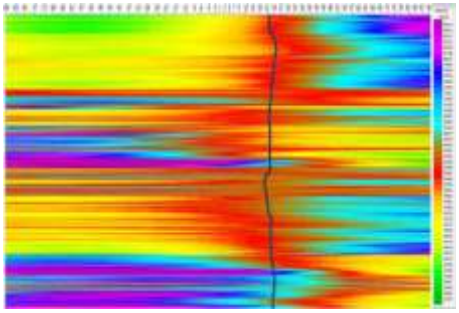

Figure 14: EEI log spectrum for the minimum energy x at 22 deg.

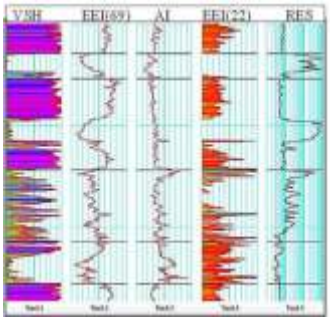

Figure 15: *Comparison of EEI log at minimum energy (x) with P-Impedance.*

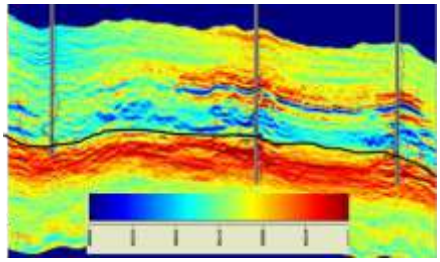

Figure 16: A section passing though wells showing extended elastic impedance at $\chi = 22^{o}$ corresponding to the background EEI

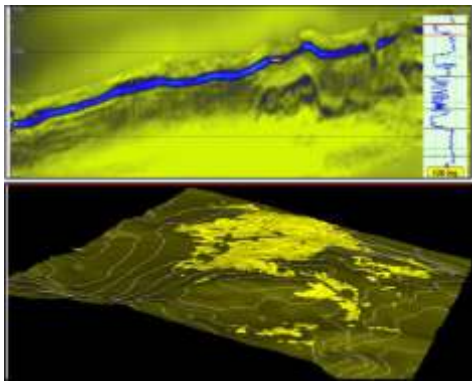

Figure 17: *072 sheet Sand body distribution clearly reproduced. While the Gr log on the top figure shows the top and bottom of the sheet sand*

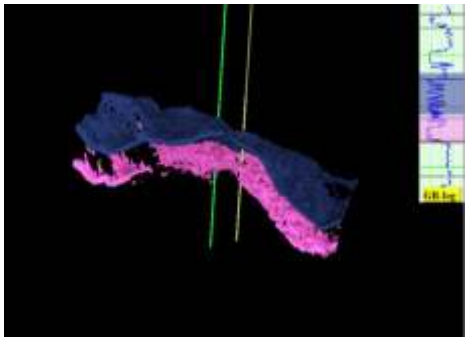

Figure 18: *O73pcf (blue) and 073ucc channel and sheet Sand body distribution clearly reproduced*

Conclusion

This case study from derived from the West African Congo basin revealed that reservoir sands can be mapped away from wells using petrophysical property volumes derived from extended elastic impedances especially when computed at minimum energy angles. It has also revealed that porosity, EEI background and

shale content volumes can be used to pinpoint favorable hydrocarbon zones. Thereby delineating and identifying reservoir boundaries more accurately than using only acoustic impedance. A validation was conducted based on comparison with conventional Geo-statistical approach.

References

Doyen, P.M., 2009. Porosity from Seismic data: A geostatistical approach. *Geophysics*, 53: 3963-3975.

Dubucq, D.B., & van Riel, S. 2001. Turbidite reservoir characterization: Multi-offset stack inversion for reservoir delineation and porosity estimation; a Gulf of Guinea example. 71st Annual International Meeting, Society of Exploration Geophysics, pp. 609-639.

Connolly, P. 1999. Elastic Impedance: *The Leading Edge*, [J] 18, 438-452.

Contreras, O., Hareland, G. & Aguilera, R. 2013. Pore Pressure Modelling and Stress-Faulting-Regime Determination of the Montney Shale in the Western Canada Sedimentary Basin: *Journal of Canadian Petroleum Technology*[J]. 52, 349-359..

Francis, A.M. 2002. Deterministic inversion: Overdue for retirement, PETEX: London.

Francis, A.M. 2006. Understanding stochastic inversion: *First Break*.24, 69-77.

Hicks, 2006. Extended Elastic Impedance and its relation to AVO crossploting and Vp/Vs: EAGE（Extended Abstract）

Iske, T. &Randen, T. 2006. Atlas of 3D Seismic Attributes, Mathematics in Industry, Mathematical Methods and Modelling in Hydrocarbon Exploration and Production:[J].Berlin, Springer

Kemper, M. 2010. Rock Physics driven inversionThe importance of workflow: *First Break*,28, 69-81.

Latimer, R.B., 2000. Davidson, R. & van Riel, P. 2000. An interpreter's guide to understanding and working with seismic derived acoustic impedance data: *The Leading Edge*, 19(3),242-256..

Alebouyeh, M. & Chehrazi, A. 2018. Application of extended elastic impedance (EEI) inversion to reservoir from non-reservoir discrimination of Ghar reservoir in one Iranian oil field within Persian Gulf. *Journal of Geophysics and Engineering*, 15(4),1204–1213, https://doi.org/10.1088/1742-2140/aaac50

Whitecombe, D.A., Connolly, P.A. & Reagan, R.L. 2002. Extended Elastic Impedance for Fluid and Lithology Prediction: *Geophysics*, 67, 63-67.

Tanko, et al (2019) Nigerian Mining Journal, (16) 41 - 53
© Nigerian Society of Mining Engineers, ISBN 1117 - 4307

Heavy Metal Distribution in Soil and Stream Sediment in Villages around Udegi Mbeki Mining District.

Tanko, I. Y. Jatau, B. S., Oleka A.B., and Kidze K. L.
Department of Geology and Mining, Nasarawa State University Keffi, Nigeria
*E-mail of the corresponding author**:** iyantanko 2014@gmail.com

Abstract

The Udegi Mbeki mining district a typical environment characterized by unorganized small-scale mining is a rugged terrain due to the Afu Ring complex intrusion and characterized by indiscriminate disposal of the mining waste which are likely to constitute environmental problems. This study is aimed at determining the extent of distribution and concentration of some heavy metals (Pb, Zn Cu, Cd, As, Cr, Sn, Nb), pH and Electrical conductivity (EC) in soil and stream sediments of some surrounding villages (Garin Shehu, Agasa and Jenta). Fifteen samples (10 soil and 5 stream sediments) were collected, digested and analyzed using atomic absorption spectrophotometer (AAS). The physico-chemical results show that pH is generally acidic which range (4.5-6.7) for both soil and stream sediment and Electical conductivity are also low for the two-sample media and ranged between (40.24-70.55) µs/cm. The results of heavy metal analysis for soil samples shows that the trend of mean concentration as: Nb (14.8693) >Sn (10.4619)>Cd (0.1873)>As (0.08019) > Cu (0.0493) >Zn (0.03284) >Pb (0.0224) >Cr (0.00559) in (mg/l). Also, Nb, Sn, Cd and As have mean concentrations higher than the local background values. Whilst for stream sediments mean trend of heavy metals indicates that: Nb (8.99970) >Sn (0.8854)> Cd (0.2656) > Zn (0.1928) > Cu (0.1518)> Cr (0.03758) > Pb (0.0224) > As (0.01566) in (mg/l). Similarly, Nb, Sn, Cd and As in stream sediment were higher than the local background concentration from upstream sediments free of mining activities in the area. These results suggest that the soil and stream sediments around Garin Shehu, Agasa and Jenta villages in Udegi Mbeki mining district are contaminated with Nb, Sn, Cd and As due to many years of random dumping of waste from the mining and processing activities in the area. Furthermore, anthropogenic sources may as well have contributed to the high concentrations.

Keywords: Distribution, soil, stream sediments, heavy metals, mining,

Introduction

The study area cut across Agasa, Garin Shehu and Jenta in Kokona local government area of Nasarawa State, North Central Nigeria. The study area lies between latitudes N8^0 31' 00" and N8^0 35' 00" and longitude E8^0 00' 00" and E8^0 03' 00" (Figure 1). The study area covers an area of 22.8km x 21.7km. Soil and stream sediment are the preeminent sources of most biologically active trace elements such as Lead, Zinc, Cadmium, Arsenic, Nickel and Copper that reach man through plants and animals (Mitchell and Burridge, 1979; Tanko, 2014). The trace element content of these two media (soil and stream sediment) depends on the nature of its parent rocks and also the amount of sewage effluents, industrial wastes and agricultural chemicals entering the soil sediments (Williams and David, 1976). Although fewer than 20 trace elements are required for the healthy growth of plants and animals (Mitchell and Burridge 1979), the excess concentration of these metals might be hazardous with negative health effects (Dickshroom et. al, 1979, Malini et. al; 1995, Underwood, 1971).

The area is accessible by major road, minor roads, and footpaths. The Basement Complex underlies the study area; the area is partly intruded by the Younger granites. The main study streams are in Agasa and Garin Shehu (this run through Agwada).

Although, Researchers like Jacobson and Webb (1946), have done a great work on the Basement Complex, yet more research works are needed to ascertain the environmental implication of the distribution of these heavy metals in soil and stream sediments in the area. This work therefore, attempts to review the geology and geochemistry of the area.

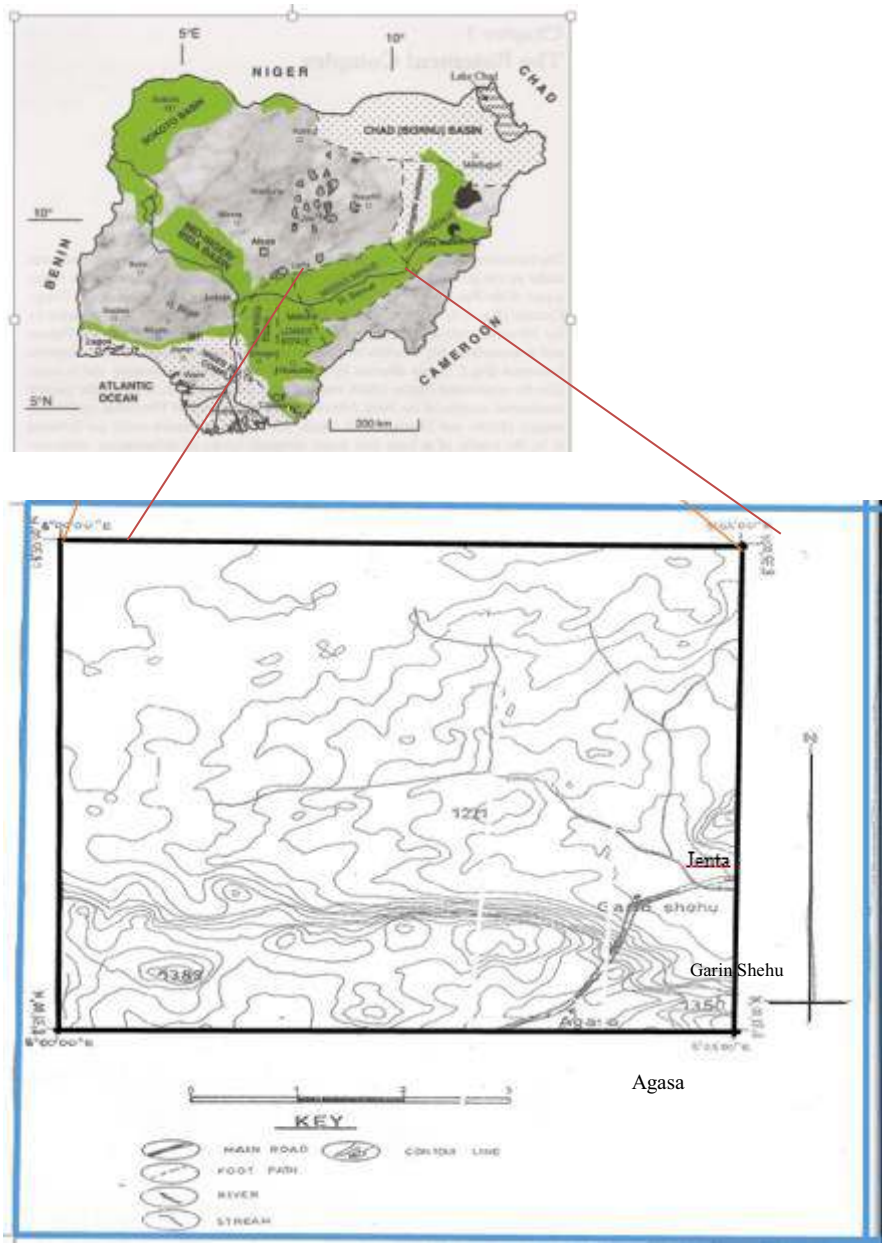

Figure: 1. Geological map of Nigeria and location of the study area (Modified after Obaje *et al.*, 2006)

Plate 1: Mining site at Jenta Village

Geology of the Study Area

The study area falls under a rugged terrain formed by the intrusion of Younger Granites with steep escarpment to the surrounding. The Younger Granite from Afu complex composes of perthitic alkaline feldspar, quartz is usually less than 10% of various mafic minerals. Generally, the granite containing perthitic orthoclase or microcline are minerals like monazite, zircon, cassiterite, and occasionally wolframite, commonly associated with iron oxides often characterized the area younger granites (Kinnaird, 1985). Migmatites occur at contact point of the area of contact of the basement and Younger Granites.

Rock Types

The two main rock types identified in the study area are the migmatite-gneisses and Younger granites.

Migmatite-gneiss

The migmatite-Gneiss was observed at the contacts between the Younger Grantie and the basement. The rock shows alternating bands of dark and light coloured minerals. They are strongly foliated fine to medium. They contained more of feldspar (Orthoclase) than quartz, mica and biotite. Features such as micro folds, fractures and joints were observed.

The Younger granite

Plutonic suit found in the area is the brownish coloured medium to coarse grained biotite granite, commonly referred to as Younger granite of the Afu ring complex. Also present is the felsic and fine to medium grained biotite granite. Generally, contains microcline and plagioclase feldspars, quartz, hornblende, biotite, and other accessory mineral such as zircon, sphene, cassiterite, columbite from field observation, the rock is leucocratic.

The quartz veins identified in the area are narrow to wide, mostly horizontal opening filled with quartz. A lot of such veins were observed in the study area. The structural trends of the veins are mainly in the NE-SW. Groups of parallel joints and fracture which may have resulted from the response of the rocks to too much stress was observed on the rocks. The dominant trends of the lineaments is in the NW-SE, NE-SW and N-S (Plates 2a & b).

(a) (b)

Plates 2 a & b: (a) Photographs of joint and (b) quartz veins on biotite granite.

Materials and Method

Geochemical Analysis

This section describes the methods involved in the study. The stages involved are sample collection, sample preparation and analysis.

Sampling Method

Stream sediments samples were collected from down to upstream at a depth of about 10 to 20 cm. whilst the soil samples were collected at about 30 cm depth. This is in order to get the actual representative samples and to avoid debris and other unwanted materials. Samples were collected from different location, stored in a labelled bags and containers and GPS reading were taken. Fifteen (15) samples were collected altogether along Garin Shehu –Agasa through to Jenta on the southern limb of the Afu Complex.

Sample preparation

The samples collected were air-dried and ground using the agate mortar and pestle then subsequently sieved to obtain the minus 75μm fraction for hot extraction treatment. The extraction process is done with 10gm portion of the minus 75μm fraction which were weighed by electronic weigh balance into a beaker and about 10ml of HNO_3 was added. This was heated until all the organic content of the samples was burnt off. After the sample preparation, the contents were filtered and made up to 120ml with distilled water ready for analysis. The analytical technique used is the Atomic Absorption Spectrophotometry (AAS) at the Chemistry and Geological laboratory of the Nasarawa State University, Keffi.

Results and Discussion

Results

The tables below represent the correlation coefficient (r) in stream sediment and soil samples of Udegi and its Envir

Table 1: Correlation Coefficient (r) in Stream Sediment Sample of Udegi and its Environs

	Pb	Zn	Cu	Cd	As	Cr	Sn	Nb
Pb	1	0.093165	0.97312	0.240885	0.080593	-0.31536	-0.23773	0.295878
Zn		1	0.191557	0.724838	-0.65354	0.418485	0.496836	0.271119
Cu			1	0.209753	0.009043	-0.27518	-0.28886	0.449987
Cd				1	-0.30233	-0.05851	0.444976	-0.32161
As					1	-0.16825	-0.69164	-0.10567
Cr						1	0.094732	0.598584
Sn							1	-0.13682
Nb								1

Table 2: Correlation Coefficient (r) in Soil Sample of Udegi and its Environs

	Pb	Zn	Cu	Cd	As	Cr	Sn	Nb
Pb	1	-0.23707	0.828239	-0.39782	-0.14111	0.837994	0.953843	-0.44636
Zn		1	0.12422	-0.1138	0.9659	-0.0589	-0.6918	0.02923
Cu			1	-0.36788	0.159697	0.970881	-0.77421	-0.7619
Cd				1	0.045022	-0.45592	-0.40201	0.470517
As					1	-0.05747	-0.74604	0.143728
Cr						1	-0.63524	-0.84874
Sn							1	0.942482
Nb								1

Physico-Chemical Characteristics of the Sediment and Soil

Soil pH varies between 4.5and 6.7. The majority of the soils have pH values between 6.0 and 6.7. Generally, the pH variations are high and all acidic, which is indicative of high quantity of sulphides and limited neutralizing capacity to the metals in soil and sediments.

Electrical conductivity (EC) of the soils in the study area is relatively high and ranges from 40.24-70.55**(µs/cm)**. This could be due to the lack of saline nature of the soil and sediment in the area.

Distribution of Heavy Metals

Pb (Lead)

The range of lead in the soil sample is from 0.006 - 0.091 Mg/L and 0.001- 0.068Mg/L in the stream sediments. The mean value for lead in soil sample is 0.0252 Mg/L which was higher than that of the soil background value of 0.0522Mg/L and the mean value of 0.0224 Mg/L in sediment is lower than the background value of 0.0522 Mg/L (Figures 2a & b). Thus, Pb is generally low in the two media compare to the background values outside the miming area of Udegi. These values therefore show the lack of prevalence of Pb in the mine wastes from mining activities. However, Pb correlates well with Cu (r = 0.97) for soil and Cu (r = 0.82), Cu (r = 0.82) and Cr (r = 0.84) and Sn (r = 0.95) reflecting the common association of lead minerals with the Sn-Nb ores. Lead and Zinc have been reported to occur as secondary minerals (Farrington, 1952). Lead is very important, used for the coating of steels, other details about the element lead (Pb) is shown below; the graphs plotted with concentration of the elements against the locations.

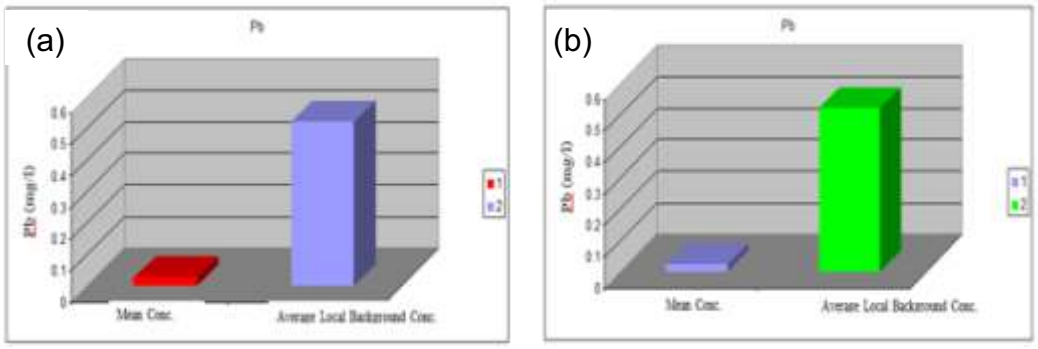

Figures 2 (a & b): The mean concentration and local background concentration of Pb in soil and stream sediments in Udegi and its Environs.

Zn (Zinc)

Zinc concentration ranges from 0.002-0.072 mg/l in soil sample with a mean concentration 0.03284 mg/l, while Zn concentration in stream sediment ranges from 0.017-0.692mg/l with a mean concentration of 0.1928 mg/l and local background value of 0.2450 mg/l (Figures 3a & b). Generally, Zn concentration in both soil and sediment is also low similar to that in Pb above.

Zn forms useful dispersion pattern in soil and stream sediments. The concentration of Zn depends on the presence of source and limited by tendency to be absorbed by MnO_2 and by insoluble organic matters. Zinc sulphate is a weathering product of Zinc as well as hydrate,silicate, carbonates (Rose et al., 1979).

The high correlation of Zn with Cd (r = 0.72) for soil and As (r = 0.97) for sediment suggests geochemical and probable mineralogical association with these elements. Zn and Cd are pairs of elements geochemically associated with one another. Cadmium most likely occurs as a solid solution in sphalerite represented by CdS. However, Cd is more volatile than most heavy metals and significant amount is released to the atmosphere during the mining of Sn-Nb ores (Levinson, 1980).

Concentrations of Pb, Zn, Cd and As increase from background levels to the soils and sediments in the region of the Sn-Nb mines, indicating that there is contamination from the mine waste; through weathering of the sulphides.

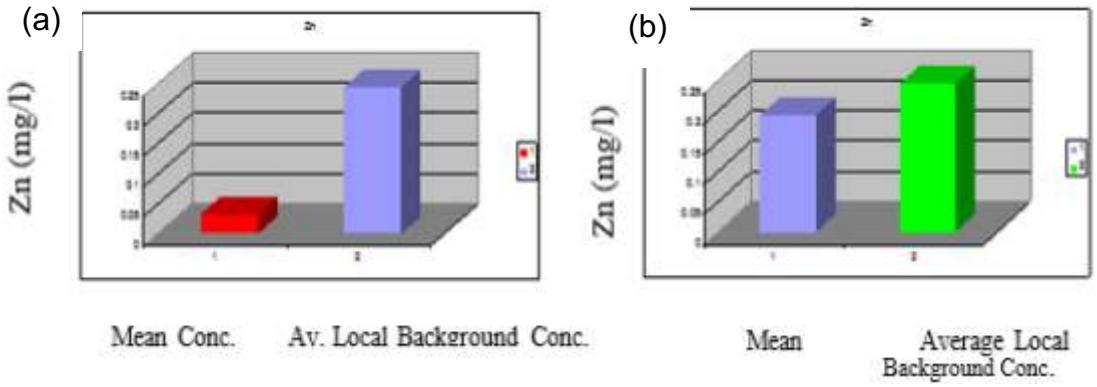

Figures 3(a & b): The mean concentration and local background concentration of Zn in soil and stream sediments in Udegi and its Environs

Copper (Cu)

The range of mean concentration of Cu in soil is 0.028- 0.091, while it is 0.042 – 0.380 in sediment. The mean concentration for copper in soil of the study area is 0.0493mg/l and 0.1518mg/l in sediment. The local background concentrated value in both soil and sediments is 4.650 mg/l (Figures 4a & b). Cu has low concentration in the two media. This low concentration can be linked to anthropogenic source (Wuyep and Tanko 2012). Cu is a transition metal, reddish/orange in colour. Due to similarities of ionic size between Cu^{2+} (0.96), Fe^{2+} (0.78) and Na^{2+} (0.95) there is always ion change between them (Rose et al., 1979).

Mobility of Cu in primary environments is high as in the case of porphyry copper deposit it is also high in secondary environment in oxidizing acidic water but low in alkaline and reducing waters (Rose et al., 1979). Also, Cu correlates weakly with Nb (r = 0.5) for soil and Cr (r = 0.97) for sediment reflecting the common association of copper minerals with the Sn – Nb ores in the mining areas.

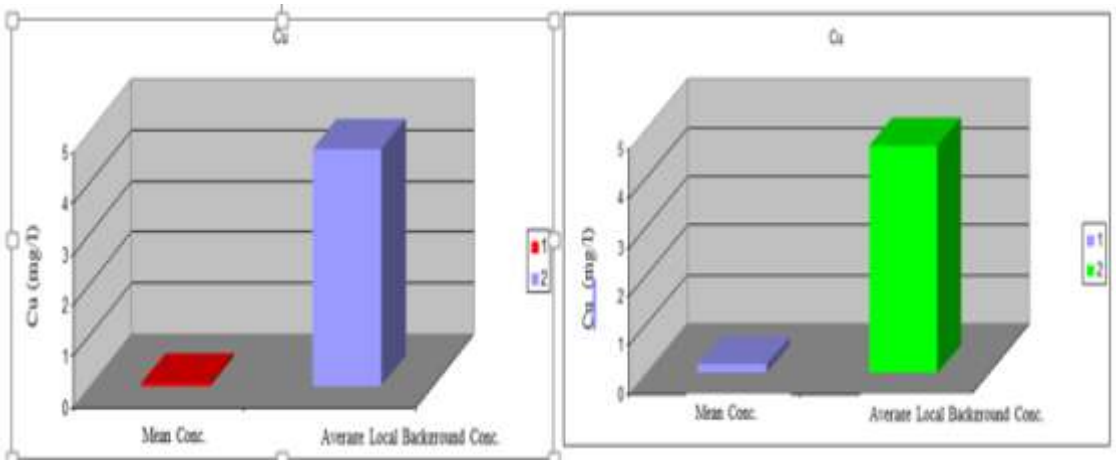

(a) (b)

Figures 4(a & b): The mean concentration and local background concentration of Cu in soil and stream sediments in Udegi and its Environs

Cadmium (Cd)

The concentration range of Cd in soil sediment is between 0.115 – 0.307mg/l while in stream sediment is between 0.0038 – 0.0950 mg/l. The mean concentration of Cd in soil sediment is 0.1873 mg/l and is 0.2656 mg/l in stream sediment (Figures.5a & b). The local background concentration of (Cd) in soil and sediment is 0.0120mg/l.

Cd by classification is a chalcophile metal. It shows high affinity to zinc, though in ore environment. Because of its relative immobility Cd became controllable by cadmium sulphide (CdS) in ore environment. The mobility of the same cadmium reflected in its high average

concentration in fresh water compared to rock (Rose et al., 1979).

The high concentration probably could have resulted from mobidity of element and, the lower concentration probably because of the erosion and later deposition of non-Cadmium mineralized materials. In addition, the concentration of cadmium in the analysis of sample is higher than the WHO (World Health Organization) (0.05mg/l). The higher concentration of cadmium in the study area is probably due to weathering and subsequent deposition from the Afu ring Complex.

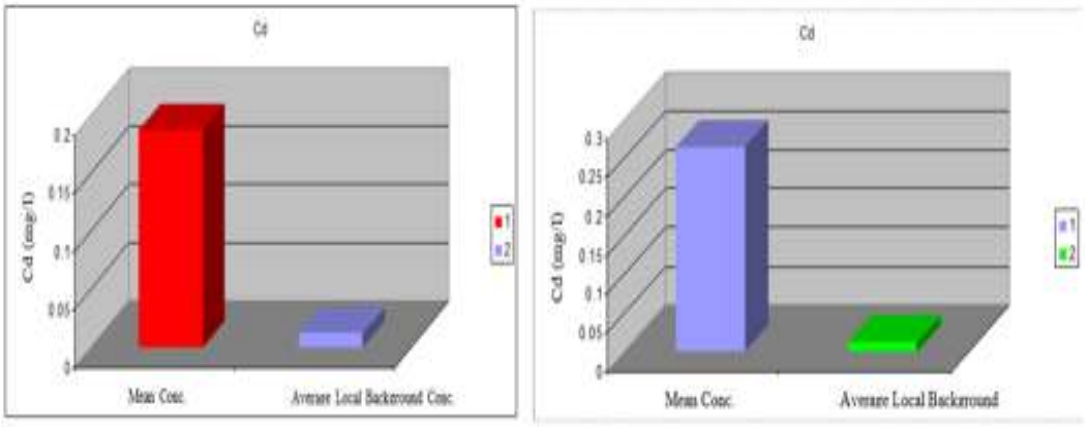

Figures 5(a & b): The mean concentration and local background concentration of Cd in soil and stream sediments in Udegi and its Environs

Arsenic (As)

The concentration of (As) in the study area ranges between 0.0105-0.3040mg/l in soil sediment and 0.0098 – 0.272mg/l in a stream sediment. The mean concentration in the soil is 0.08019mg/l,whilst in sediment is 0.0157 mg/l (Figures.6 a & b). These values are higher than the local background in the soil and sediment (0.004mg/l).The mean of As is closely the same to that of WHO admissible limit (0.10mg/l).

Arsenic (As) a chalcophilic metal is found in association with Cu, Ni, Co, Fe, Ag etc. it could be found as hydrothermal veins in primary environment and as arsenopyrite (Fe AsS) real gal poisoning used in making rat poison.

The high concentration could probably be as a result of weathering and also because the sediment is high and it concentrates in late differentiation and veins and also the mobility of secondary environment is fair (Levinson, 1980). The lower concentration might be attributed to Arsenic high mobility.

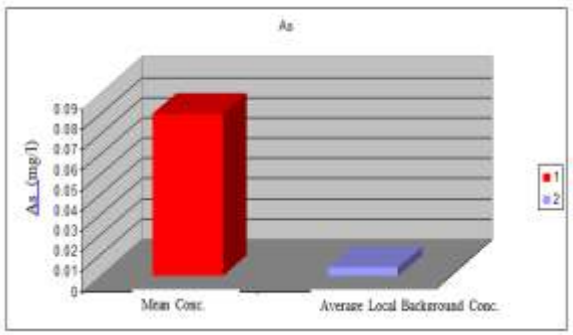

(a)

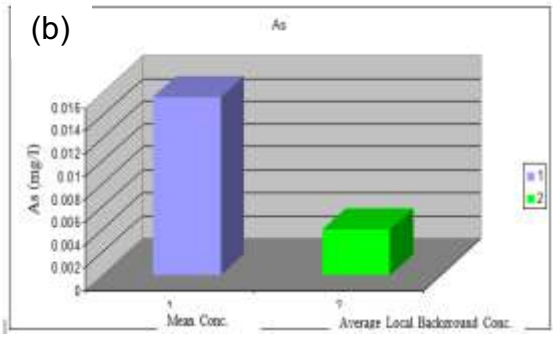

Figures 6 (a & b): The mean concentration and local background concentration of As in soil and stream sediments in Udegi and its Environs

Chromium (Cr)

The concentration of chromium ranged between 0.0037 – 0.0326 mg/l in soil and mean value is0.00559mg/l, but in sediment Cr ranged between0.0206 – 0.0811mg/l and the mean concentration is 0.03758 mg/l (Figures.7 a & b), and the local background concentration for both soil and sediment is 0.042mg/l.

The result obtained from the analysis indicates that the mean for both soil and sediment are normal compare to the local background concentration 0.043mg/l in soil and sediments. But the mean value 0.0811 for sediment sample at location. ST1 has higher concentration; this high concentration could probably be as a result of weathering and also because of chromium concentrates in late differentiates (Rose, 1979).

Chromium Cr is a steel grey lustrous hard metal, blue white metal and very resistant to corrosion. It is mostly used to make Armour plates, ball bearing and cutting tools.

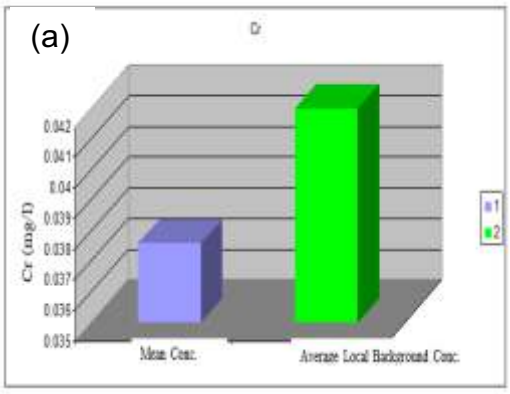

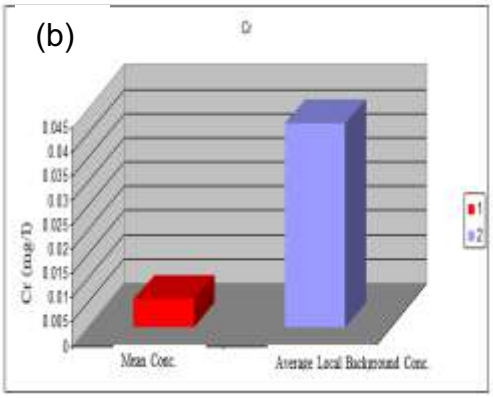

Figures 7 (a & b): The mean concentration and local background concentration of Cr in soil and stream sediments in Udegi and its Environs

Tin (Sn)

The concentration of tin is the study area ranged between 6.511 – 15.010mg/l, mean value is 10.4619 mg/l. But in the stream sediment the range is between 1.027-2.188 mg/l, the mean value is 0.8854mg/l and their local background concentration is 5.0260 mg/l (Figures 8a & b).

The results obtained from the analysis of Sn indicate that the mean value in soil is about 2 times, it is even 3 times (15.010mg/l) the local background concentration. But generally low in sediment samples of the study area. In addition, the correlation of Sn with Nb (r = 0.94) for sediment reflects the common association of Sn minerals with Nb and the mining activities in the area.

Tin is a siderophile metal, grey and white in colour and geochemically associated with chromium and columbite occurs as cassiterite (SnO_2). Tin is commonly used as protective coating on metal.

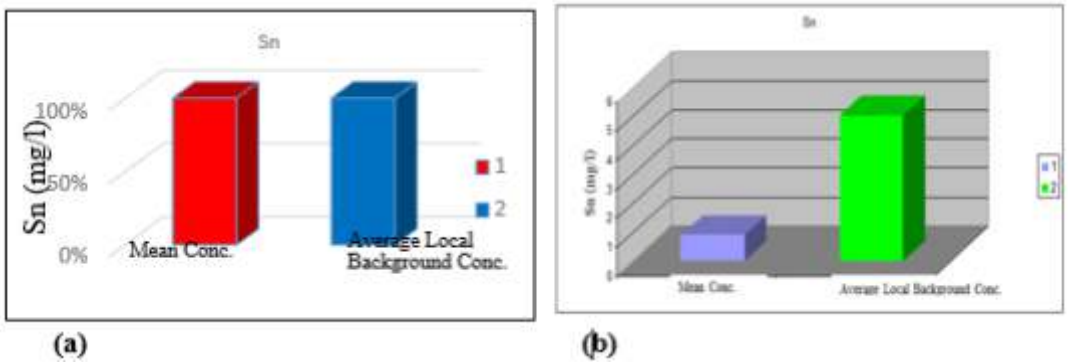

Figures.8 (a & b): The mean concentration and local background concentration of Sn in soil and stream sediments in Udegi and Environs.

Niobium (Nb)

Niobium is geochemically associated with columbite. The metal has a shining surface, white soft and ductile, mostly found in niobite and columbite. Niobium has atomic number of 41 with atomic masses of 92.9063g. It's used for arc welding and stabilized grades of stainless steel.

The concentration of Nb in the study area ranged between 6.006 – 20.623 mg/l, mean value is 14.8693 mg/l. On the other hand, in the stream sediments the concentration range between 0.682-2.060 mg/l and mean value of 1.4054 mg/l. Background value for both soil and sediment is 8.9870 mg/l.

The result obtained from the analysis of Nb as shown in Figures 9a & b, indicate that soil sample has the highest concentration above the background value, at location SS10 (20.623mg/l) is twice the background value of (8.9970). But the mean value is generally low in stream sediment samples. Furthermore, the correlation of Nb with Cr (r = 0.60) and Sn (0.94) for soil and sediment respectively indicate the common association of Nb minerals with Cr and Sn and also suggest that there is contamination from the mine wastes; through weathering of the sulphides in Jenta

.

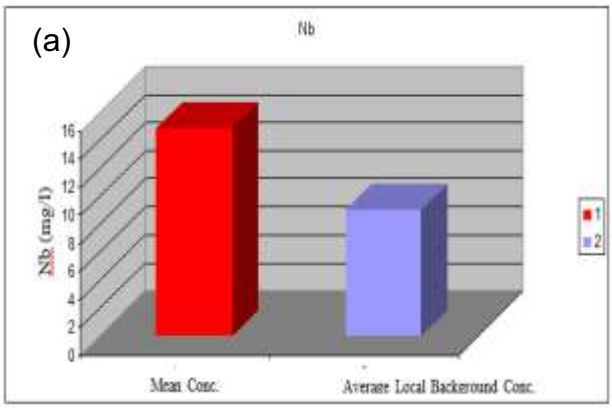

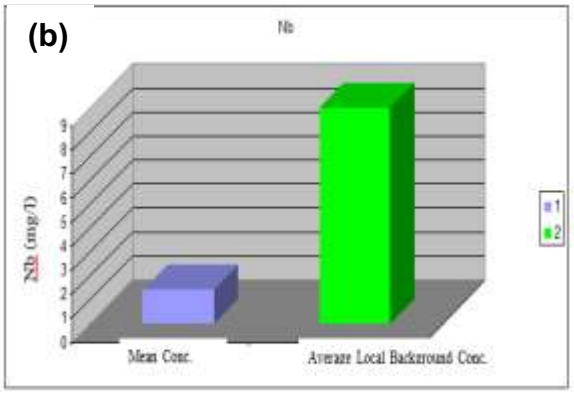

Figures.9 (a & b): The mean concentration and local background concentration of Sn in soil and stream sediments in Udegi and its Environs.

Contamination Factor (CF)

The assessment of contamination of the stream sediment and soils of Udegi and its Environs was also carried out using the contamination factor. This calculation was used to evaluate the potential risk of the heavy metals to the environment using the formula below (Kumar and Edward, 2009): Cif =Ci0 - 1/Cif

Where Cif is the contamination factor from the soil or stream sediment, Ci0 - 1 is the mean concentration of metals from the soil and stream sediment sampling sites of the Udegi and its Environs (at least five) and Cin was taken as the average concentration of elements from the background as a reference value.

Tables 3,4 and 5 indicate that in soil Pb, Zn, Cu and Cr show low contamination, Sn and Nb have moderate contamination while As and Cd have very high contamination respectively. In stream sediment Cd and As have very high contamination, while Pb, Zn, Cu, Cr, Sn and Nb all show low contamination (Tables 3, 4 and 5). The very high contamination factor of Cd and As in both the soil and sediments is probably as a result of their high mobility in the media, while the moderate contamination of Sn and Nb in soil could be a result of the close proximity to the mines in Jenta. Also, the general low contamination factors in stream sediment could be attributed to their being far away from the mines.

Table 3: Contamination factors of heavy metals in soils from Udegi and its Environs

Metal	Average Heavy Metal Concentration (mg/l)	Contamination Factor (CF)
Pb	0.0252	0.0483
Zn	0.03284	0.1340
Cu	0.0493	0.0106
Cd	0.1873	15.6083
As	0.08019	20.0475
Cr	0.00559	0.1331
Sn	10.4619	2.0816
Nb	14.8693	1.6527

Table 4: Contamination factors of heavy metals in stream sediment from Udegi and its Environs

Metal	Average Heavy Metal Concentration (mg/l)	Contamination Factor (CF)
Pb	0.0224	0.0429
Zn	0.1928	0.7869
Cu	0.1518	0.0326
Cd	0.2656	22.1333
As	0.01566	3.9150
Cr	0.03758	0.8948
Sn	0.8854	0.1762
Nb	1.4054	0.1562

Table 5: Categories of contamination factor distinguished by (Kumar and Edward, 2009)

Contamination factor	Categories of contamination
$C^i_f < 1$	Low contamination factor indicating low contamination
$C^i_f = 1 – 3$	Moderate contamination factor
$C^i_f = 3 – 6$	Considerable contamination factor
$C^i_f > 6$	Very high contamination factor

Conclusion

The physico-chemical results show that pH is generally acidic which range (4.5-6.7) for both soil and stream sediment and Electical conductivity are also low for the two-sample media and ranged between (40.24-70.55) µs/cm.

The trend of mean concentration of heavy metal is: Nb (14.8693) > Sn (10.4619) > Cd (0.1873) > As (0.08019) > Cu (0.0493) > Zn (0.03284) > Pb (0.0224) > Cr (0.00559) in (mg/l). The high concentration of metal like Cd and As and Sn and Nb above the local background values in both soil and stream sediments suggest natural source from the weathering of the surrounding waste dumps from the mines in Agasa, Garin Shehu and Jenta in the study area.

The very high contamination factor of Cd and As in both the soil and sediments is probably as results of their high mobility in the media, while the moderate contamination of Sn and Nb in soil could be a result of the close proximity to the mines in Jenta. Also, the low contamination factors in stream sediment could be attributed to their being far away from the mines.

References

Dickshroon W. Van Broekhoven L.W., Lampe J.E.M (1979). Photo toxicity of Zn, Ni, Cd, Cu and Cr in three pasture plant species supplied with graduated amount from the soil Nz Agric. Sci. 27 241-253.

Farrinton J.L (1952). A Preliminary Description of the Nigerian Pb – Zn Field. Econ. Geol. Vol. 47, 583-608 Garcia – Miragaya 1984. Levels, Chemical Fractionation

Jacobson, R. and Webb, J. S. (1946), "The Pegmatite of Central Nigeria",*Geological Survey of NigeriaBulletin,* Vol. *17*, 61pp.

Kinnard, J.A (1985). Hydrothermal alternation and Mineralization of the Alkaline Anorogenic Ring complex of Nigeria Journal of African earth science vol. 3Pp 229 – 253.

Krauskopt, K.B. (1979) Introduction to Geochemistry 2nd edition. McGraw Hill, New York Pp. 617.

Kumar, S. P. and Edward, J. K. P. (2009). Assessment of metal concentration in the sediment cores of Manakudy estuary, south west coast of India. *Indian Journal of Marine Science* 38 (2), 235-248.

Levinson A. A. (1980). Introduction to Exploration Geochemistry, U.S.A Wilmette, Illinoiss: Applied Publishing Ltd.

Malini, S., Nagaiah, N., and Paramesh, L., Venkataramaian P. (1995). Study

of the distribution of Trace elements in soils in and around Mysore City, Karnataka. Environmental Geol. 26; 107-110.

Mitchell, R.L. Burridge, S.C. 1979. Trace Element in soils and crops. Phil. Trans. Royal Soc. London B 288, 15-24.

Obaje, NG. Nzegbuna, A.I., Moumouni, A, Goki, N.G Channda M.S. (2006): Geology and Mineral Resources of Nasarawa State, Aninvestor Guide Published by Nasara Scientifique Vol. 1 Pp 7 - 20.

Rose, W., Hawkes E., Webb S., (1979). Geochemistry in Mineral Exploration. 2nd Edition, Academic Press Inc. (London) Ltd. 549-563.

Tanko I.Y. (2014). Petrogenesis and Mineralisation Potential of the Pegmatites of Keffiarea, North cental Nigeria. An unpublished PhD Thesis, Univerity of Mines and Technology Tarkwa, Western Region, Ghana.

Underwood, E.J. 1971. Trace Elements in human and animal nutrition, New York. Academic Press 461 – 477.

Williams, C. H. David J. 1976. The accumulation of Cadmium from Phosphorus

Fertilisers and their effect on the Cadmium Content of Plants. Soil Sci. 121, 86-93

Wuyep E.O., Tanko I.Y., (2012). Physicochemical Analysis and Distribution of Heavy Metals around Keffi and its Environs, Journal of Earth Science and Engineering 2,271-276.

Determination of Chemical and Mineralogical Composition of Gurum Cassiterite Deposit, Jos Plateau State, Nigeria.

***Asuke F., *Thomas D. G. and **Dogara E. M.**

*Department of Metallurgical and Materials Engineering, Ahmadu Bello University Zaria, Nigeria.

*National Metallurgical Development Center, Jos, Plateau State Nigeria.

Email: asukef@gmail.com, dungkathomas@gmail.com, muguh86@yahoo.com

Abstract

The determination of chemical and mineralogical composition of Gurum cassiterite deposit was carried out. The ore sample was sourced from Gurum village near Jos in Plateau State. The samples from different pits were homogenized, the homogenized sample was pulverized and analyzed for their chemical and mineralogical composition using XRF, XRD and petrological microscope respectively. The chemical analysis (XRF) of the head sample revealed that the ore contained 8.90% SnO_2, 12.6% TiO_2, 6.20% ZrO_2, 47.3% SiO_2, and15.7% Fe_2O_3 as the major minerals, with 1% P_2O_5, 1.2% SO_3, 0.52% CaO, 0.48% V_2O_5, and 0.40% MnO as the minor minerals and 0.01% Yb_2O_3, 0.03% OsO_4, 0.06% PtO_2 and 0.04% Au as traces. The XRD analysis of the ore revealed the mineral phases of the ore are cassiterite (SnO_2), Rutile (TiO_2), Silicon oxide (SiO_2) and Hematite (Fe_2O_3). The petrological analysis revealed that cassiterite, silica, rutile and hematite are the major minerals separated by grain boundaries which agrees with the XRD results.

Keywords: Gurum Cassiterite, Characterization, Mineralogy, Petrology.

Introduction

Exploitation of mineral has assumed prime importance in several developing countries including Nigeria. Nigeria is endowed with abundant natural resources, which has contributed immensely to the national wealth with associated socio-economic benefits (Ogwuegbu and Muhanga 2011). Tin is one of the earliest known metal in the history of metallurgy (Grijalba *et al.*, 2013). With advanced technological development, tin becomes more and more important in production and human life (Sreenivas and Padmanabhan, 2002). Tin has found application in circuit-board for television, computer and for metal coating. Presently for health reasons it is recommended to use solder with 95.5%Sn instead of solder with 40% lead and 60%Sn. This single policy change increased global tin demand by over 20% (Cowie, 2010).

There are over twenty (20) known minerals of tin (Sn), the only economically important mineral of tin is cassiterie SnO_2 (78.6%Sn), other sources are Stannite or tin pyrites Cu_2FeSnS_4 (27.7%Sn), Tealite $Pb_3Sn3SbS_4$ (17%Sn) and Cylinderite $Pb_3Sn_4Sb_2S_{14}$ (26.0%Sn). Cassiterite is the sole economic tin mineral in Nigeria: stannite has been recorded but never in economic quantities (Akanbi e*t al.*, 2012).

Cassiterite is associated with impurities especially those that occur in pegmatite. They are found to contain iron oxide, manganese oxide, zirconium oxide, titanium oxide, silica, columbite, mozanite, topaz etc. which sometimes are impediments in the extraction of tin from cassiterite (Thomas and Yaro, 2016). Hence, the need to beneficiate the ore in order to remove or reduce the impurities associated with it before smelting. Table 1: Show some Nigeria Cassiterite Resources, their location and estimated reserves.

Research has shown that every mineral deposit is unique in its nature. Therefore; the process flow sheet for the beneficiation of an ore must be designed to suit the particular ore deposit.

Table1: Some Nigeria Cassiterite Resources (in million tonnes)

S/N	Location	State	Metal type	Estimated Reserved (Million Tonnes)
1	Tare Nandu	Kaduna	Sn, Ta, Nb	Partially investigated
2	Akwanga	Nasarawa	Sn, Ta, Nb	Partially investigated
3	Gurum	Plateau	Sn, Ta, Nb	Partially investigated
4	Jos-Bukuru	Plateau	Sn, Ti, Nb	Partially investigated
5	Haita-Vom	Plateau	Sn, Ti, Nb	Partially investigated
6	Barkin Ladi	Plateau	Sn, Ti, Nb	Partially investigated
7	Kuru	Plateau	Sn, Ti, Nb	>200 inferred resources
8	Akata	Kogi	Sn, Ta, Nb	>20 Tonnes have been shipped in the 1940s
9	Isanlu	Kogi	Sn, Ta, Nb	Partially investigated

Ministry of Mines and Solid Minerals Development, (2012).

Gurum Cassiterite Deposit

The Gurum cassiterite deposit is one of the new deposits in Jos Plateau State Nigeria. The cassiterite deposit is of alluvial origin from the biotite granite within the jurassic alkaline ring complex (the younger granite), (Pastor and Ogezi, 1986). Mallo (2007) reported that mineralized rock with disseminated cassiterite mineralization may have invaded the basement structure that leads to the concentration of the tin mineral in its basement structure. Denudations of the basement exposed the roof zone of the younger granite early alluvial deposit intrusion rise to primary deposits of high grade enriched silicified deposits. Further denudation erodes and robes the roof zone giving rise to alluvial deposits associated sand and gravels that have been transported by water. With the roof zone eroded further, denudation attracts poorly mineralized main body of the granite giving rise to the deposition or comparatively barren over burden sediments covering the area (Mallo, 2007); (Pam, 2015); (Thomas and Yaro, 2016).

The Gurum cassiterite has not been fully characterized, the absence of the data on the characterization of the ore makes it difficult to predict the process route parameters of the mineral deposit. It is based on this that this research work was carried out to establish the chemical and mineralogical composition of the ore, with the hope of building toward developing a process route for the beneficiation of the ore.

Materials and Methods

Materials

The ore used in this research work was sourced from Gurum village in Jos North Local Government Area of Plateau State Nigeria. The samples were collected from four different pits at interval of 10m apart at 5m depth in order to have a representative sample of the ore deposit. Five kilograms (5kg) of the ore sample was collected from each pit and thoroughly mixed to obtain homogenous sample which was used for further analyses.

Equipment

The equipment used for this research work are: Denver pulverizer, digital weighing machine, X-ray fluorescence machine (XRF),

X-ray Diffraction (XRD) machine and Petrological microscope.

Methods

Determination of the Chemical Composition of the Ore Sample using X-ray Fluorescence (XRF)

The chemical composition of the ore sample was determined using Mini pal 4 X-ray fluorescence machine. The required parameters of the machine were set to standard. The parameters are pressure values, set at 16Pa (Pascal), chamber for the opening and lifting of the cassette (a holder that houses the pellets sample), the current recommended value was 40A and the voltage recommended level was 45V. The equipment was allowed to run for at least one (1) hour to enable the standards and other mechanical part responsible for the analysis to initialize and stabilize. The sample was loaded onto the cassette with the help of spring balance, the cassette was then locked manually by turning it clockwise, this is to keep the pellets safe from falling off or being scattered on the goniometer when analysis is going on. The loading point and the cassette point were positioned to face the goniometer for ease of analysis, the opening valve was then closed. The analysis was then carried out on the machine (Dogara 2018).

Mineralogical Analysis of the Ore Sample

(i) X-ray Diffraction (XRD)

The equipment used for analysis is the X-ray diffractometer (ARL X'TRA) the homogenous pulverized sample was examined using X-ray diffractometer (XRD), the mineralogy was determined by collecting a series of peaks showing the distribution of the minerals, this shows the major phases.

(ii) **Petrological Analysis**

Petrological analysis of the ore was carried out using Petrological Microscope. The samples for the thin section was mounted on glass slide using adhesive (glue), the sample was then ground and polished until a thin transparent surface was obtained on the glass slide. It is then viewed and observed under plane polarized light and cross polarized light of a petrological microscope with an in-built camera and a point-counter machine attached to it. The distribution of mineral in the sample was determined using the point-counting.

Results and Discussions.

Chemical Composition of the Head sample.

Table 2: Chemical analysis of the head sample (XRF).

Compound	Assay (%)
SiO_2	47.30
P_2O_5	1.00
SO_3	1.20
CaO	0.52
TiO_2	12.60
V_2O_5	0.48
MnO	0.40
Fe_2O_3	15.70
NiO	0.02
CuO	0.39
ZnO	0.02
Y_2O_3	1.38
ZrO_2	6.20
Nb_2O_3	1.29
Ag_2O	0.35
SnO_2	8.90
Nd_2O_3	0.81
Yb_2O_3	0.01
WO_3	0.06
OsO_4	0.03
PtO_2	0.06
Au	0.03
PbO	0.20
Bi_2O_3	0.05
ThO_2	0.65
U_3O_8	0.08

Table 2 reveal that the head sample of the ore contain 8.90% SnO_2, 12.6% TiO_2, 6.20% ZrO_2, 47.3% SiO_2, and15.7% Fe_2O_3 as the major minerals, with 1% P_2O_5, 1.2% SO_3, 0.52% CaO, 0.48% V_2O_5, and 0.40% MnO as the minor minerals and 0.01% Yb_2O_3, 0.03% OsO_4, 0.06% PtO_2 and 0.04% Au as traces. From the results obtained, it is observed that SnO_2 is one of the major minerals present in the matrix of the ore though in low grade. This phenomenon could be attributed to the mineralization of the deposit during mineral formation processes of the younger granites of the Gurum area of Plateau State (Pastor and Ogezi, 1986).

Mineralogical Analysis of the Ore Sample Using XRD

Figure 1 and Table 3 present the mineralogical analysis of the Head sample using XRD.

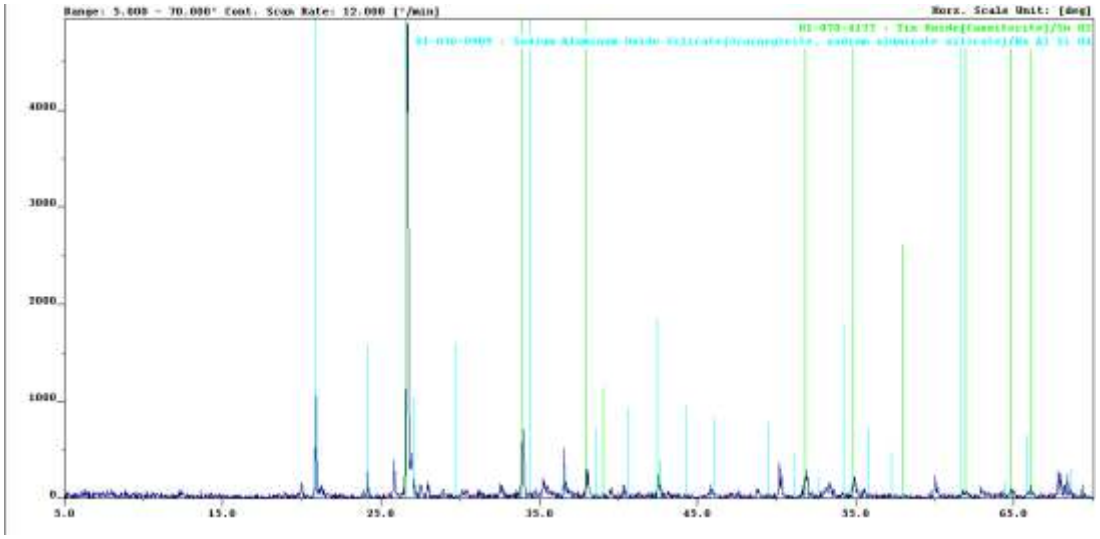

Figure 1: Spectrum of the major element for head sample

Table 3: XRD Mineral Analysis of the Head Sample

Card no	Mineral name	Chemical name	Chemical formula
26-6014	Rutile	Titanium oxide	TiO_2
33-9015	Cassiterite	Tin oxide	SnO_2
37-9743	Hematite	Iron oxide	Fe_2O3
39-0071	Zircontate	Zirconium oxide	ZrO_2
42-6624	Silica	Silicon oxide	SiO_2
51-8090	Manganesite	Manganese oxide	MnO_2
54-7899	Zirconia	Zirconium Oxide	ZrO_2
61-6449	Zincite	Zinc oxide	ZnO

The peaks of the various minerals present in the ore and the result of major and minor mineral phases in the head sample of Gurum cassiterite are depicted in Figure 1 and Table 3 respectively. The minerals phases are cassiterite (SnO_2), Rutile (TiO_2), Silicon oxide (SiO_2) and Hematite (Fe_2O_3), Zincite (ZnO), Zirconium Oxide (ZrO_2), Manganese oxide (MnO_2) as mineral

phases. This confirms the result of the XRF of the head sample and in line with initial reports by MMSD, Thomas and Yaro (2016).

Petrological Analysis of the Ore Sample using Plane and Cross Polarized Light

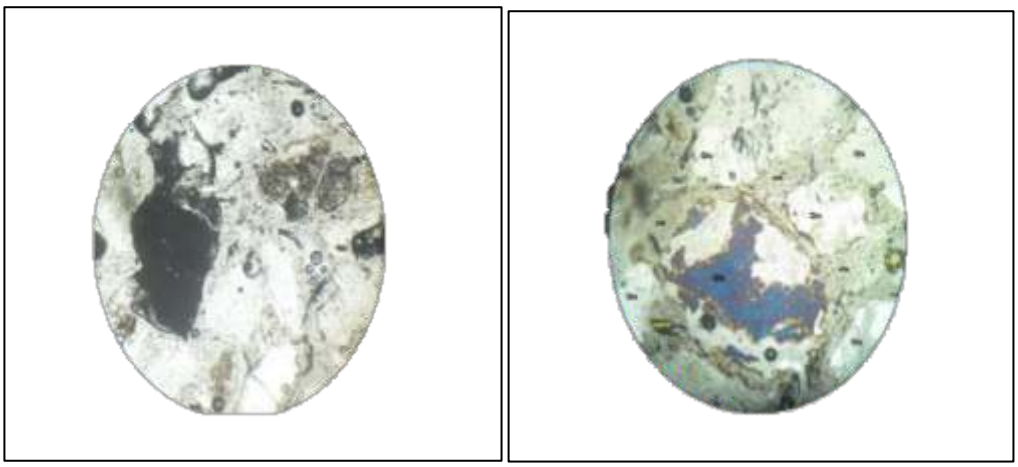

Plate 1: Plain Polarized Light (PPL)X50Plate 2: Crossed Polarized light (XPL) X50

Plate 1 is the photomicrographs of the head sample under plane polarized light (PPL) and plate 2 is the photomicrograph of the head sample under crossed polarized light (XPL) respectively. It is observed from plates 1 and 2 that the white to grey areas are quartz (Quartz/SiO_2) while the dark to reddish areas show (TiO_2, FeO_3) and the blue areas are SnO_2. It is observed that the ore has smooth boundaries which create segregation between the cassiterite and other minerals contained in the ore. This phenomenon may enhance easily liberation of the valuable mineral during grinding. This is in line with the XRD results presented earlier.

Conclusion

From the research carried out on the determination of chemical and mineralogical composition of Gurum Cassiterite. The following conclusions were drawn:

(i) The chemical analysis of the head sample using XRF revealed that the ore contained 8.90% SnO_2, 12.6% TiO_2, 6.20% ZrO_2, 47.3% SiO_2, and15.7% Fe_2O_3 as the major minerals, with 1% P_2O_5, 1.2% SO_3, 0.52% CaO, 0.48% V_2O_5, and 0.40% MnO as the minor minerals and 0.01% Yb_2O_3, 0.03% OsO_4, 0.06% PtO_2 and 0.04% Au as traces. This has confirmed that Gurum in Plateau State Nigeria as another potential source of cassiterite of low grade which can be concentrated and smelted.

(ii) The mineralogical analysis of the ore sample using XRD revealed cassiterite (SnO_2), Rutile (TiO_2), Silicon oxide (SiO_2) and Hematite (Fe_2O_3) as the major phases while others are minor and traces.

(iii) The petrological analysis revealed the presence of cassiterite as the blue areas and the dark to reddish areas as (TiO_2, FeO_3) coloured grains under plane and cross polarized light. It also

revealed that the ore has smooth boundaries which create segregation between the cassiterite and other minerals contained in the ore.

References

Akanbi, E. S., Ugudulunwa, F.X.O. and Gyan, B.N. (2012). Mapping Potential Cassiterite Deposits of Naraguta Area, North Central, Nigeria Using Geophysics and Geographic Information, *Journal of natural science research*, vol2 pp 132-143.

Cowie, A (2010): Tin an overlooked commodity. The market oracle, Aug. 19, 2010. Retrieved from http://MarketOracle.co.uk

Dogara, E. M. (2018). *Characterization and Beneficiation of Gurum Cassiterite Ore Deposit Jos, Plateau State Nigeria.* Department of Metallurgical and Materials Engineering, Ahmadu Bello University, Zaria. Ongoing.

Grijalba, A. C., Urresa, J., Ramirez, A. and Barrault, J. (2013). *Preparation and Characterization of Cassiterite and its Application in the hydrogenation of Methyl-Esters*. Revista De Ciencias, vol. 17 pp. 81-93.

Mallo, S.J (2007). Mineral and mining on the Jos plateau, 1st edition, ACON Publishers.

Ministry of Mines and Steel Development (MMSD) (2012). *Road Map for the Development of Solid Minerals and Metals Sector*, Stake-Holders forum Abuja, pp 4-9.

Ogwuegbu, M.O.C. and Muhanga, W. (2011). The effect of unplanned exploitation of environmental resources: the Nigeria's experience. *Journal of environmental pollution and human health*, 3(2) pp 39-45.

Pam, T.S. (2015). *Characterization and Upgrading of Haita Cassiterite Ore Deposit, Plateau State, Nigeria*. Department of Metallurgical and Materials Engineering, Ahmadu Bello University, Zaria. Unpublished.

Pastor J. and Ogezi A. E. (1986). New evidence of cassiterite –bearing Precambrian basement rocks of the Jos plateau, Nigeria- the Gurum Case study, *Springer link,* vol. 21 pp 81-83.

Sreenivas, T. and Padmanabhan, N.P.H. (2002). Surface chemistry and flotation of cassiterite with alkyl hydroxamates [J], *Colloids and surfaces*. A physical and engineering aspects, 205:47-59.

Thomas, D.G. and Yaro, S. A. (2016). Characterization of Haita-Vom Cassiterite Ore usin X-ray fluorescence (XRF) Spectrometry and Scanning Electron Microscope (SEM). *Nigeria Mining Journal.* 14(1) 27-31.

Oyeladun, et al (2019) Nigerian Mining Journal, (16) 61 - 71
© Nigerian Society of Mining Engineers, ISBN 1117 - 4307

Enrichment of Itakpe Iron Concentrate using Multi – Gravity Separator

Oyeladun, O. A. W. Damisa, E. O. A. and Tolu S.
Department of Mineral and Petroleum Resources Engineering, Kaduna Polytechnic, Kaduna
Corresponding Author E-mail: oawoyeladun@gmail.com

Abstract
The desire to reduce alumina and silica contents of Itakpe iron concentrate led to further concentration of the ore. The productivity of blast furnace increases and energy consumption reduces with the input of superior quality of raw material especially iron concentrate. The ore sample had a feed grade of 65% total Fe, 15.1% Si and 4.1% Al. In order to reduce the alumina and silica contents, Multi Gravity Separator (MGS) was used and was found to be effective in reducing loss of fine iron ore particle and increasing the grade of the concentrate. The MGS process improved the Fe from 65.2% to 68.81% along with decreasing the silica from 15.05% to 10.5% and alumina from 4.1% to 2.3. This will make blast furnace to consume less coke and reduce the use of flux and slag produced.
Keywords: Multi Gravity Separator, concentrate, feed, fines.

Introduction

Itakpe Iron ore concentrate to Ajaokuta steel Company for blast furnace process requires 64% Fe, concentrate while Aladja steel complex requires 68% Fe, for direct reduction process. Therefore, there is need to further upgrade the concentrate from 64% Fe, of the gravity separation method using Humphrey Spiral whose process designed is to use flotation (Gupta and Yan, 2003).

This research is to study how to replace flotation with Multi-Gravity Separator (MGS) which is more environmental friendly and less expensive than flotation to further upgrade the 64% Fe, concentrate of Itakpe Iron ore to 68% Fe, for direct reduction process at Aladja steel complex.

Modern high capacity mining equipment and the fine grinding required liberating highly disseminated ore are generating much higher levels of fines than before. A considerable amount of these fine short circuit the mineral beneficiation equipment and report to the wastes. It has been estimated that one third of the potash “and tin mined in Florida, and one fifth of word’s Tungsten are lost in the slimes (Ozbayoglu et al,2002).

Research into the methods of recovering this fine has been at the forefront of mineral engineering studies for long. Gravity separation, the work horse of mineral dressing plants in the early twentieth century yielded place to flotation because of its better selectivity and effective in the – 44 micron particle size range and most of the fine handling now are in this range. (Uwadiale, and Nwoke 1985)

Moreover, the increasing interest that environment is attracting and rightly so, is exposing the limitation of the flotation technology. Even though its superiority is still undisputed particularly in base metal ore beneficiation, Over the years a number of gravity separation equipment have been developed to handle the fine particles, these could be used as stand-alone equipment, Multi-gravity Separator (MGS) is one such equipment (Yaro, 1998).

Nigeria Iron Ore Deposits

Nigeria is endowed with abundant iron ore deposit of which some of them have been investigated and some are still under investigation as shown in Table 1 Iron ore is the major raw material in Iron and steel industry. It occurs as iron oxide [magnetite

(Fe_3O_4) and Haematite (Fe_2O_3)], hydro oxide [goethite ($HFeO_2$) and Limonite ($2Fe_2O_3.xH_2O$)], and carbonates [siderite ($FeCO_3$)]. The Nigeria iron ore deposit fall into two (2) categories depending on their mode of occurrence: the sedimentary Oolitic/Pisolitic type in which the mineral occurs as an aggregate of rounded pellets either small or large. The second group are deposits of cretaceous recent years age and of meta sedimentary banded iron ore formation of the Precambrian (early years) age (Famuboni, 1990).

Table 1: Iron ore deposits of Nigeria with their iron content

Locality	Type	State of Occurrence	Grade(%Fe)
Ajabanoko	Haematite, Magnetite	Kogi	40
Agbaja	Haematite	Kogi	47.6
Itakpe	Haematite	Kogi	36.8
Kotonkarfe	Siderite	Kogi	48.18
Muro Hills	Haematite, Magnetite	Nasarawa	31.6
Chokochoko	Haematite	Kogi	33.5
Dakin gari	Haematite	Kebbi	37.0
Egeneja	Siderite	Benue	45.7
Nguje	Siderite	Anambra	40.0
Tajimi	Haematite	Kogi	39.05
Birnin Gwari	Haematite Magnetite	Kaduna	N.A

Types of Iron Ore

The most widely available iron-bearing minerals are oxides and consist mainly of hematite (Fe_2O_3), which is red; magnetite (Fe_3O_4), which is black; limonite or bog-iron ore ($2Fe_2O_3 \cdot 3H_2O$), which is brown; and siderite ($FeCO_3$), which is pale brown. Hematite and magnetite are by far the most common types of ore. Pure magnetite contains 72.4 % Fe, hematite 69.9% Fe, limonite 59.8% Fe and siderite 48.2% Fe but, since these minerals never occur alone, the metal contents of real ores are lower. Deposits with less than 30 % Fe are commercially unattractive, although some ores contain as much as 66% Fe, there are many in the 50–60% range. The quality of iron ore is also influenced by the presence of another constituent which are collectively known as gangue. Silica (SiO_2) and phosphorus-bearing compounds (usually reported as P_2O_5) which caused cold embrittlement in steel and cannot be removed during the iron making except in steel making process which make the production of steel more expensive. The quality of iron ore is mainly judged based on the Fe content. More specifically, ores with Fe contents above 65% are regarded as high-grade ores; 62–64% as medium- (or average) grade ores and those below 58% Fe are considered as low-grade ores (Thomas and Yaro, 2007).

Study of some Nigeria Iron Ores Characteristics

Research on the up-grading of locally available iron ores in Nigeria has recently received interest after earlier efforts dating back to the last two decades when the defunct Nigeria Steel Development Authority (NSDA) was established. A metallurgical research laboratory was also set up as an appendage of the NSDA with a mandate to characterize and process

locally available iron ores and other raw materials for the then springing Iron and Steel industries (Uwadiale, 1985). The first recorded indigenous reports on the beneficiation of a locally available iron ore are those of Adigwe, (1973) and Edah, (1974) who worked on the Itakpe iron ore deposit, which at that time was the only geologically characterized iron ore reserve that was focused on. However, between 1973 upwards, many other iron ore deposit has been located and their beneficiation characteristics ascertained, Table 2 and 3 give the summaries of the findings of the studies carried out on the characterization of the locally available iron ore deposits.

Table 2: Chemical Compositions of Some Nigerian Iron Ore in Percentages.

Deposits	K_2O	CaO	TiO_2	MnO	Fe_r	MgO	Al_2O_3	SiO_2	P_2O_5	S
Itakpe	**0.42**	**0.3**	**0.10**	**0.05**	**36.88**	**0.20**	**1.00**	**44.80**	**0.18**	**Trace**
Chokochoko	**0.53**	**0.15**	**0.61**	**0.08**	**34.45**	**0.18**	**9.67**	**51.07**	**0.02**	**Trace**
Ajabanoko	**0.26**	**0.21**	**Trace**	**0.01**	**37.22**	**0.15**	**3.39**	**46.50**	**0.01**	**0.33**
Agbaja	**0.04**	**0.75**	**0.37**	**0.14**	**47.80**	**0.38**	**9.60**	**10.89**	**2.08**	**0.12**
Koton-Karfi	**0.02**	**0.45**	**0.25**	**0.56**	**48.18**	**0.07**	**6.70**	**5.13**	**2.14**	**0.04**
Bassa-Nge	**0.02**	**0.17**	**0.17**	**0.13**	**46.90**	**0.46**	**10.87**	**8.28**	**1.45**	**0.05**
Toto-Muro	**0.10**	**2.39**	**0.10**	**0.10**	**33.06**	**0.00**	**0.12**	**54.14**	**0.13**	**0.20**

Source: (Raw Material Research and Development Council, 2010)

Table 3: Characteristics of Some Nigeria Iron Ore

ORE	MINERALOGY	BENEFICIATION TECHNOLOGY
Agbaja	Principal constituent mineral is goethite with minor Haematite, magnetite, siderite, quartz, kaolinite and pyrite, Fe content 46-50% 1.5% P_2O_5. Liberation size less than 5μm	Most conventional beneficiation techniques may not be suitable due to its fine grain size. Selective oil agglomeration and magnetizing reduction may be applicable
Itakpe	Coarse grain with magnetite, Haematite and quartz. Liberation is achieved at about 600-800μm	Gravity concentration on shaking table produces a concentrate assaying f 65% Fe with 80% recovery
Toto-Muro	Coarse grain with magnetite, Haematite and quartz. Liberation is about -80-60μm	Gravity concentration on shaking table produces a concentrate assaying f 54.10% Fe with 77.3% recovery

Source: (Dungka, 2000).

Mineral Processing Conceptual Parameters

Ores are usually subjected to some concentration processes in order to separate the various minerals in the ore into two or more products. This is done for the purpose of beneficiating the ore for its desired mineral or metallic value (Sirajo 2008). Beneficiation of minerals is a physical, chemical and physico-chemical process of using the inherent properties of the minerals in order to maximize its quality (Olokesusi, 2010). Separation is achieved by utilizing some specific difference in physical or chemical properties between the valuable and the gangue minerals in the ore. After the geological survey has been carried out, the standard procedure usually followed in the development of the conceptual flow sheet for the beneficiation of a newly discovered ore deposit and is as follows (Thomas and Yaro, 2007).

Concentration Processes

There are a number of ways of increasing the concentration of the valuable minerals: in any particular case the method chosen will depend on the relative physical and surface chemical properties of the mineral and the gangue. Concentration means the increase of the percentage of the valuable mineral in the concentrate in relation to the feed.

A. Gravity Concentration Technique

Gravity concentration is the process for the separation of minerals of different specific gravity by inducing variable movement in response to gravitational force and one or more natural or applied force with the aid of a flowing film. It is used, sometime along with other processes in particle flotation, magnetic separation and chemical treatment (Gupta, 2003). Gravity separation process is effective, practical and efficient in the treatment of many ores. But their applicability to the treatment of any specific ore or in combination with other processes must be determined through the mineralogical composition and characteristic of representative samples of the ore and from careful and comprehensive testing (Yaro, 1997). The major demerit of gravity separation process is the recovery of fines and it is inherent in the process itself, even with advance slime gravity concentrators, the practical lower limit of particle size which can be handle is still about 100μm (Yaro, 1997).

The following are gravity separation methods:

Jigs – conventional, in line pressure and centrifugal

Pinched sluices – trays and cones

Spirals – wash water and wash waterless

Shaking tables – wet and air

Fine particle separators – Falcon and MGS

Gravity /sizing – hydrosizers and cyclones

Sources (Gupta and Yan, 2003).

B. Multi-Gravity Separator

The multi gravity separator is a unique enhanced gravity separator for the separation of fine and ultra-fine minerals. The principle of the multi gravity separator may be the combination of principle of conventional shaking table and spiral concentration. Feed slurry is introduced continuously midway into the internal surface of the drum via an accelerator launder, which is to reduce turbulence caused by the introduction of the feed. Wash water is introduced via a similar accelerator launder close to the outer end of the drum. Studies indicate that the slurry follows a spiralling pattern on the revolving drum surface. Heavier particles or particles of higher specific gravity penetrate the slurry and are pinned to the surface of the drum as a result of the centrifugal forces to form a semi-solid base layer. An intermediate layer consisting of a relatively dilute suspension of lower specific gravity particles, and slime particles forms above this. The top layer consists of relatively clear water. The shake provides an additional shearing force on the particles in the flowing film, resulting in improved separation; whilst the specially designed scrapers moving across the drum surface continually re- grade the settled particles, thus minimizing entrainment of gangue. Thus, the high-density particles pinned to the surface of the drum are continuously swept up the slope by the scrapers, during which time they are subjected to counter current washing before discharging at the open, front end as concentrate. The lower density minerals along with the majority of the wash water flow down-stream to discharge as tailings via slots at the inner end of each drum.

Multi-Gravity or Enhanced Gravity Separation gives unrivalled efficiency in the continuous recovery and upgrading of mineral values contained in fine and ultra-fine particles. It is unique in enabling the production of high grade concentrates at high recovery from low-grade tailings and middling streams.

The operating principle may be likened to powerful, compact shaking tables. However, in the MGS the normally horizontal separating surface of a shaking table is wrapped into a conical drum which, when rapidly rotated, develops an enhanced gravitational field ideal for the recovery of ultra-fine heavy particles.

Slurry is fed into the MGS towards the centre of each drum.

The Multi -gravity separator is a continuous thin film separation device used mainly for beneficiating ores with fine particle distribution using an enhanced gravitational field. A schematic diagram of a drum section is given in Figure 2 to indicate the important features of the design.

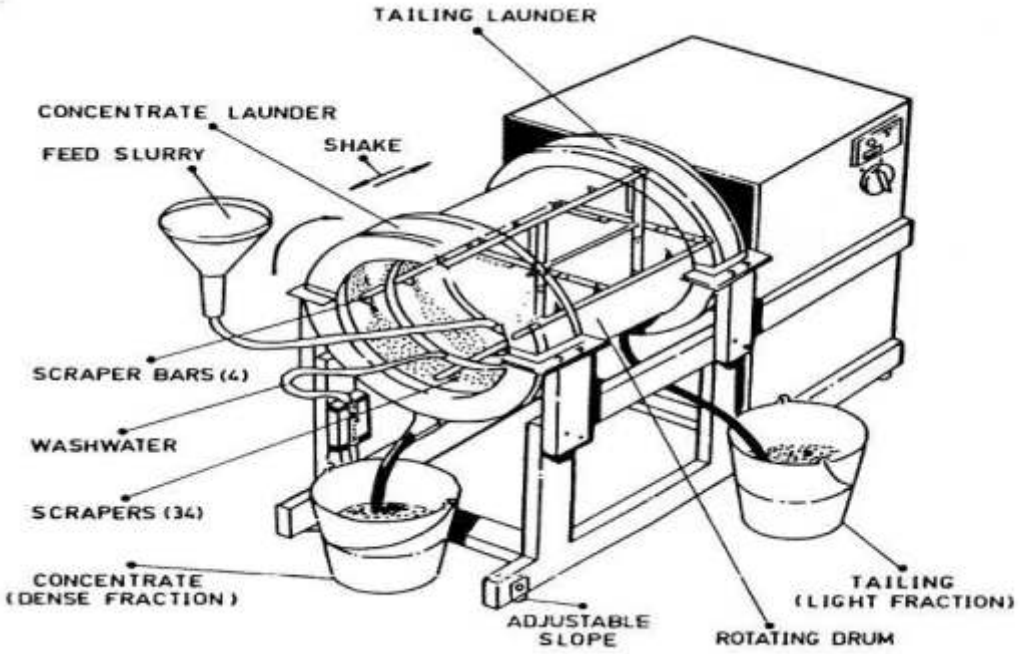

Figure 1: Multi-Gravity Separator Schematic diagram

The operation of the MGS is controlled by the following design and operating parameters:

(a) Speed of rotation of drum
(b) Inclination of the drum
(c) Frequency and amplitude of shake
(d) Flow of wash water
(e) Pulp density of feed and feed rate

Other factor like scrapper width, scrapper speed and angle of lining also affect the performance of the MGS to some extent.

While all the parameters mentioned above affect the performance to some extent, the principal variables that affect most and which can he easily/quickly controlled are

* Drum speed
* Wash water flow rate
* Shake intensity/amplitude
* Pulp density in feed (% solids)

C. Applications of Multi-Gravity Separator (MGS)

There is scope of application of MGS in various locations in mineral processing plants e.g.

(a) Recovering precious metals from fine alluvial ground ores

(b) Pre-concentration of heavy minerals from fine ground ores.

(c) Up grading concentrate

(d) Scavenging valuable minerals from tailing/effluents.

Iron Ore Beneficiation Process

For purpose of beneficiating any type of ore for its minerals or metal values and for design of accompanying flow-sheet(s) after chemical and mineralogical investigation, the ore is subjected to some concentration processes that can separate the minerals into two or more products. Separation is usually achieved by utilizing some specific differences in physical and chemical properties between the valuable and gangue minerals in the ore. However, mineral processing operations are mainly concerned with utilizing the physiochemical methods of separation. Some of these methods are: gravity, magnetic, froth flotation and the combination of these methods.

Beneficiation Route for the Itakpe Iron Ore

The Itakpe iron ore beneficiation flow sheet consists of the comminution section, gravity and magnetic sections. The comminution section consists of crushing and semi-autogenous machines. The ground and screened product from the autogenous grinding plant is classified at a mesh of 150μm in a double stage primary cyclone. The underflow of the first stage is recycloned in the second stage so as to eliminate the residual fine products. Then, the proportion of fine product. The overflow of the two-stage primary cyclone contains fine magnetite (Fe_3O_4) particles, which cannot be recovered using gravity method. The fine magnetite particles are recovered using low intensity magnetic separation (separator) with parallel single drum (primary Low Intensity Magnetic LIM separators). Magnetic products treated in gravity section are recovered in two one-stage low intensity magnetic (LIM) separators with single parallel drum installed on the tailing circuit. The primary LIMS concentrates as well as the concentrate in the tailings is screened using screening panels partitioned so as to retain eventual middling coarse particles, which may be misplaced. The undersize concentrate from screening panel is purified in a secondary LIM separator with two drums in series. This purified concentrate is the final concentrate.

Overflow fine particles that cannot be upgraded by gravity separation are sent to the tailing thickener and the underflow coarse particles (-150 +40μm) are properly deslimed and mixed with –1600+150μm particles from the primary cycloning. This overall product constitutes the feed to the gravity concentration circuit. The gravity concentration circuit consists of three stages (1) spirals, roughing stage, which produces a pre-concentrate and a final tailing. (2) Cleaning stage – which produces an intermediate concentrate and middling recycled to the feed of the roughing stage, and (3) re-cleaning stage – which produces a final concentrate and middling recycled to the feed of the cleaning stage. The control being used in the gravity concentration circuit is to maintain constant feed at each stage via pump rotation with a speed variation to keep the density constant and to maintain a unit feed rate per spiral in a definite range by measuring the pulp feed and by splitting up this capacity among a variable number of spirals.

The concentrates coming from the gravity concentrations circuits as well as from the magnetic circuits are mixed and sent to the

filtration, where the pulp is thickened to (more than 40% of solids). In the event of the pulp being dilute (when starting the circuit for instance), it is recycled to the feed of the re-cleaning circuit. The tailings from the gravity concentration circuit are highly diluted and required a thickening prior to filtration. This thickening is made in a bank of cyclones. The thickened underflows as well as the fine tailings coming from the thickener underflow are directed to the tailings filter the overflow pulp of cyclones, almost free of solids, is used as dilution water in the grinding circuit (Hoffmann, 1992)

Methods and Materials

Materials and Equipment

Iron ore concentrate sample, Ball mill, set of sieves, Laboratory sieve shaking machine, Weighing machine, X-ray florescence (XRF) Machine and Laboratory Indigenous Multi-Gravity Separator (MGS).

Methods

Sample Collection

4000g Samples of iron ore concentrate were collected from The Nigerian Iron-Ore Mining Company (NIOMCO), Kogi State. The samples were collected from their concentrate storage yard.

Sample Preparation

Sample preparation involves comminution which consists of further grinding process. The concentrate from Itakpe Iron Ore was subjected to further grinding to liberate the valuable mineral and also to make it fine for Multi-Gravity Separator (MGS).

and dirty on it. The moving parts and wires of the machine were properly checked and the machine was switched ON for operations.

Separation Test

2,500g sample on sieve size 355μm was weighed out and used to prepare slurry. Slurry was used as feed to the Multi-gravity separator.

From these feeds concentrates and tailings were obtained after the Multi-gravity separation. The concentrates and tailings obtained after Multi-gravity separator were then dried and weighed. They were assayed for iron and silica using XRF technique.

Results and Discussion

Sieve Analysis

Sample collected were coned and quartered to yield a representative sample, then sieved to pass through 355μm after a successful sieving, 2500g was obtained readily for further analysis.

Recovery Permutations

The recovery in a mineral concentrating operation is the percentage of the total metal content in the ore that is recovered in the concentrate. The purpose of calculating recovery is to determine the distribution of the metal in the feed or heads among the various products of the mineral concentrating operation. Below is the permutation for the recovery of the minerals of interest (Iron Fe) of the MGS process.

$$\text{Recovery, R} = \frac{\text{Cc}}{\text{Ff}} \text{ x } 100\%$$

$$\text{Recovery, R} = \frac{1918.7 \times 68.81}{2500 \times 65.22} \times 100$$

$$= 80.97\%$$

Ratio of Concentration Permutations

The ratio of concentration is the weight of the feed (heads) to the weight of the concentrate.

$$\text{Ratio of Concentration, K} = \frac{\text{F}}{\text{C}}$$

$$\text{Ratio of Concentration K} = \frac{2500}{1918.7}$$

$$= 1.30\%$$

The ratio of concentration is sometimes referred to as the grade of the concentrate and it is a measure of the efficiency of the Multi-Gravity Separation process.

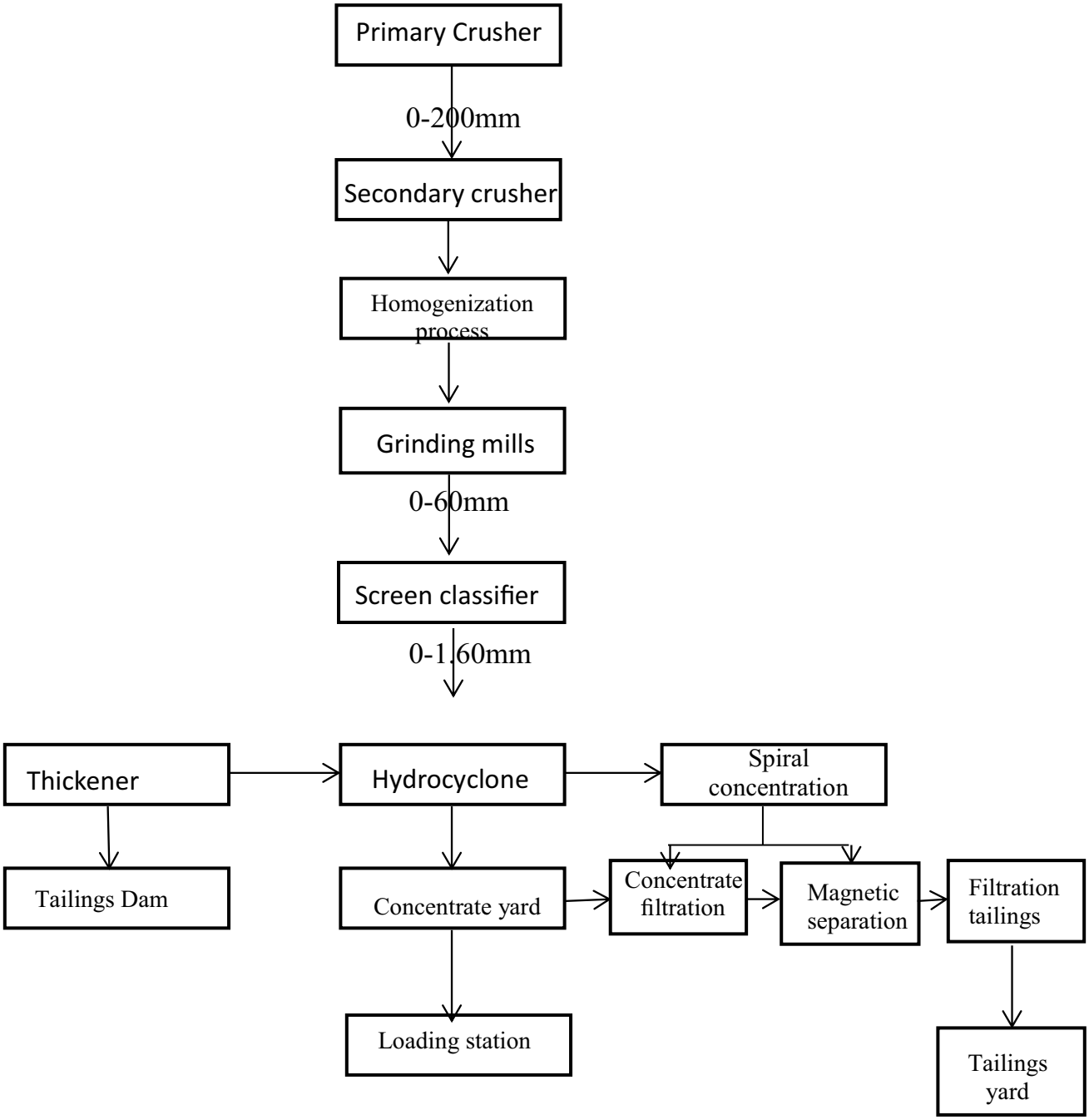

Figure 2. Block diagram of Itakpe Beneficiation process

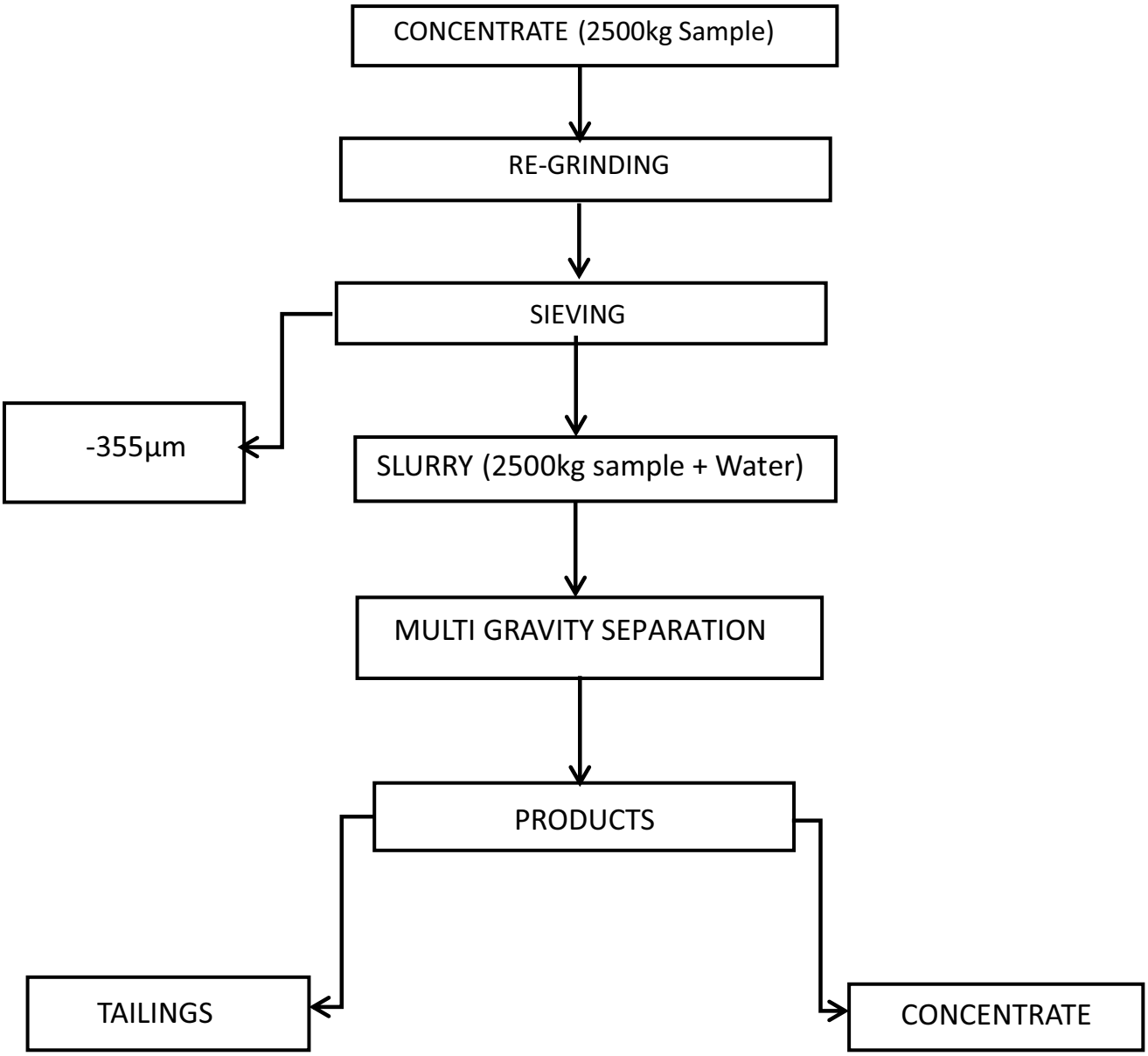

Figure 3: Processing Flowsheet for Multi-Gravity Separation

Table 3: XRF analysis of the Head Sample (Itakpe Iron Ore Concentrate)

Element	Mg	Al	Si	Ti	Mn	Fe	Zn	Cr	Ca
%	1.315	4.104	15.052	0.193	0.073	65.225	0.017	0.063	0.141

Multi-Gravity Separation Process

The results obtained during the course of the concentration tests are presented in the Tables 3 and 4.

Table 4: Results of Multi-Gravity Separation Technique

Sieve Size (μm)	Product	Weight (g)	Recovery (%)
-355	Feed	2500	100
	Concentrate	1918.7	76.7
	Tailing	220.7	8.83

Table 5: XRF analysis of the Multi-Gravity Separation products

Element	Mg	Al	Si	Ti	Mn	**Fe**	Zn	Cr	Ca
Concentrate	1.592	2.292	10.525	0.217	0.055	**68.81**	0.029	0.06	0.27
Tailing	1.016	3.212	14.949	0.076	0.067	**64.69**	0.027	0.06	0.155

Conclusion and Recommendation

Conclusion

Based on the results of this study the following can be concluded that Itakpe Iron Ore concentrate can be beneficiated using MGS for recovering fine particles and the concentrate produce has a grade of 68 % Fe can be obtained using MGS.

At present, MGS seems to be the most promising equipment for the beneficiation of fine material particles thank to the simplicity of the process and the low overall costs.

Recommendation

I recommend further investigation to determine the list of variables studies of the MGS which include:

Shake Amplitude in cm. (SA)
Drum Speed in rpm (DS)
Tilt Angle in degree (TA)
Wash Water Flow Rate in lpm (WW)
Shake Frequency in cps (SF)
Solid Feed Rate in tph (SFR)
Feed Pulp Density in %solids by wt.(FPD)

This will help in the effective operations of the MGS.

References

Akande, J.M. and Olaleye, B.M, (2005): Recovery of Galena Concentrate from lead Zinc, Journal of Minerals & Materials Characterization & Engineering, Vol.4, No.1 pp 21-30.

Dungka, G.T. (2002): Beneficiation of Toto Muro Iron Ore Deposit. M.Sc Thesis. Dept. of Metallurgical Engineering, A.B.U. Zaria. (unpublished)

Dwight, F.K., (1976): Experimental Technique with general applicability for the study of magnetic phenomena, Journal of applied physics, Vol.5 No.1, pp 24-29.

Famuboni A.D, (1990): Sourcing of Mineral Raw Materials. The Nigerian Iron and Steel Industries. A paper delivered at

the distinguished lectureship programme. Department of Mineral Resources Engineering, Kaduna Polytechnic, Unpublished.

Gilchrist, J. D. (1989): Extraction metallurgy (3rd Ed). Oxford Pergamon press Ltd.

Gupta A. and Yan D. S. (2003). Mineral Processing Design and Operation; 2nd edition Elsevier Ltd.

Hoffman C. (1992): Cannon initiation course Nigeria, Iron ore mining project industrial plant. Unpublished

Jain S.K. (2001): Mineral processing, 2nd edition, CBS publishers: New Delhi.

RMRDC. (2000) and GNS (1987): Journal of the Raw Material Research and Development Council and the Report of the Geological Survey of Nigeria.

Thomas, D.G. and Yero, S.A. (2007): The effects of calcination on the beneficiation of KotonKarfe Iron ore. Nigeria Mining Journal, A publication of Nigerian Society of Mining Engineers, Vol.5, No.1, pp 49-59.

Uwadiale, G.G.O.O., and Nwoke M.A.U (1985): Journal of Mineral and Metallurgical processing, Vol.2 No.3 pp 38-43

Wills B.A (2006): Wills Mineral processing technology; an introduction to the practical aspect of ore treatment and mineral recovery; 7th edition, Elsevier Ltd Oxford, UK

Usaini, et al (2019) Nigerian Mining Journal, (16) 73 - 77
© Nigerian Society of Mining Engineers, ISBN 1117 - 4307

Concentration of Bodinga Phosphate Rock using Flotation and Thermal Treatment Techniques

***Usaini M.N.S, *Akindele U.M, and **Ndanusa I. A**
*Department of Mineral and Petroleum Resources Engineering, Kaduna Polytechnic, Kaduna
**Department of Chemical Engineering, Kaduna Polytechnic, Kaduna

Abstract

In nature, minerals of interest exist physically and chemically combined with the host rock and removal of the unwanted gangue to increase the concentration of mineral in an economically viable manner is the basic goal of mineral processing operations. Phosphate rocks are used for phosphoric acid, fertilizers and animal feed production: a key factor for successful agricultural sector. The phosphate sample obtained from Bodinga, Sokoto State was pulverized, sieved to fraction of 75µm and then upgraded by using both froth flotation technique as well as thermal treatment (calcinations) processes. Significant parameters like scrubbing, desliming, collector, depressant, pH and lime slaking process were taken care, to achieve the best recovery. The results of this study revealed phosphate concentrate of about 26% by flotation and 30% by thermal treatment obtained from a feed sample containing 17.9%P_2O_5. Thermal treatment route of upgrading proved to be better however; the minimum requirement for fertilizer production of 34%P_2O_5 has not been met. The study, therefore recommended calcining the concentrates from flotation technique.

Keywords: Pulverized, phosphate rock, flotation, calcinations, Bodinga.

Introduction

With the urgent need for intensive farming due to diversification of the economy and increasing population, the fertility of the soil needs to be maintained by its external additions (Anon, 2002). Nigeria has been importing fertilizers and other phosphorus related products for farming as well as to sustain her agricultural programme. This has led to the importation of millions of metric tons of fertilizer amounting to millions of USdollars from the United States of America and other countries within the African continent like Tunisia, Senegal, Morocco and Togo despite the large deposits of phosphate minerals available in the country (Umar et al, 2016).

Phosphate ores are in high demand all over the world because they are the raw materials for the production of phosphate fertilizers and other chemicals (Fang and Jun, 2011). About 191Mt of phosphate were produced in 2011and the USGS predicts that worldwide phosphate production will be increased to 228Mt by 2015. High percentage of phosphate rock (~ 95%) is consumed in manufacturing of fertilizers and animal feed supplements. The rest of the production is used to produce elemental phosphorus and de-fluorinated phosphate rock, which is used for direct application to the soil (Jasinski, 2012). The world phosphates are distributed according to their type, approximately as follows: 75% from sedimentary deposits, 15-20% from igneous, metamorphic and weathered deposits, and 2-3% from biogenic sources (Abouzeid, 2008).

Because of the increasing world demand for phosphate, P_2O_5 content of the rock is gradually falling, and it is becoming economical to mine and beneficiate many

lower-grade deposits (El-Jalead et al., 1980). The majority of the process is dependent on methods of separation of phosphate minerals from their associated gangue minerals (Elgillani and Abouzeid, 1993 and ÖZER, 2003). These phosphate rocks are classified into siliceous, clayey, calcareous, igneous and metamorphic ores (Abouzeid, 2008). Flotation process is the most applicable technique to upgrade phosphate rock. Flotation method has been carried out successfully to separate oxides and silicate minerals from sparingly soluble minerals such as apatite, fluorite, magnesite and sheelite, which have hydrophilic character, giving hydrophobic nature to the desired minerals by various reagents (Sis and Chander, 2003). In this paper, the amenability of upgrading Bodinga phosphate rock by flotation and thermal process has been studied, since developing process route to concentrate phosphate rock is a serious challenge for the fertilizer industry.

Materials and Methods

Materials

A phosphate rock sample was obtained from Bodinga, Sokoto State. Oleic acid was used as a collector and sodium silicate as a silica depressant. Sodium Carbonate (Na_2CO_3) was used as pH modifier.

Methods

Sample Preparation

The obtained sample was subjected to primary, secondary crushing and grinding. The ground product was coned and quartered in order to have representative and desired quantity (head sample) and deslimed at 75µm.

Experiments

The flotation tests were performed in a conventional Denver D-12 sub-aeration flotation machine with 2 liter capacity cell with 200g feed. The floated fraction was collected until the froth was barren. The reagents utilized were depressant (sodium silicate, dose of 3ml); collector (oleic acid, dose of 2.5ml) and pH modifier (sodium carbonate). Conditioning of the pulp with reagents was performed for 2 min, and the system agitated for 8 min at 2000 rpm. The flotation products (froth and sink) were collected, dried, weighed and analyzed. The same quantity of sample (200g) after desliming was taken into the furnace heated to about 1000^oC, then lime slaked to effect the changes of CaO to Calcium Hydroxide Ca(OH)2 and thoroughly washed with plenty water. The product was dried, weighed and analyzed.

Results and Discussions

Table 1: XRF result of Head sample

Oxide	Al_2O_3	SiO_2	P_2O_5	SO_3	CaO	ZnO	TiO_2	V_2O_5	MnO	Fe_2O_3
%	1.23	6.92	17.9	0.16	54.3	0.07	0.40	0.03	0.89	6.78

The head sample contains elements in various percentage as indicated in the table 1 with P_2O_5 having 17.9% composition.

Table 2: The XRF result of froth flotation

Sieve size (µm)	Product	Weight (g)	Weight (%)	Assay Value (%)		
				(P_2O_5)	(CaO)	(SiO_2)
-90+75	**Feed**	**200**	**100**	**17.90**	**54.30**	**6.92**
	Conc.	**103.26**	**51.63**	**26.00**	**41.11**	**1.90**
	Tailing	**88.54**	**44.27**	**3.50**	**24.11**	**11.32**
	Losses	**8.2**	**4.10**	**-**	**-**	**-**

Table 2, shows the concentrates and the tailings having weights of 51.63g, 103.26g respectively and the assay value of 26%P2O5 but reduction in CaO insignificant.

Table 3: The XRF result of thermal treatment (Calcination)

Product	SiO_2	P_2O_5	CaO
%	3.43	30.1	31.43

About 30.1% P_2O_5 was achieved by thermal treatment obtained from a feed sample containing 17.9%P_2O_5

Conclusion

The phosphate sample sourced from Bodinga, Sokoto State was pulverized, sieved to fraction of 75µm and then upgraded by using both froth flotation technique as well as thermal treatment (calcination) processes. Significant parameters like scrubbing, desliming, collector, depressant, pH and lime slaking process were taken care of to achieve the best recovery. The results of this study revealed phosphate concentrate of about 26% by flotation and 30% by thermal treatment obtained from a feed sample containing 17.9%P_2O_5. Thermal treatment route of upgrading proved to be better which can be ascribed to conversion of unstable lime CaO to more stable form of lime calcium hydroxide, thus;

(Limestone) $CaCO_3$ + HEAT - (Calcium Oxide) CaO + CO_2

(Calcium Oxide) CaO + (Water) H_2O - Calcium Hydroxide $Ca(OH)_2$ + HEAT

However, the minimum requirement for fertilizer production of 34%P_2O_5 has not been met. The study, therefore recommended calcining the concentrates from flotation technique.

References

Abouzeid, A.-Z. M. (2008). "Physical and thermal treatment of phosphate ores — An overview." International Journal of Mineral Processing, 85 (4): 59-84.

Anon, (2002). Food and Agriculture Organization Use of Phosphate Rock for Sustainable Agriculture, PP 54

Elgillani, D. A., Abouzeid, A.-Z.M. (1993). "Flotation of Carbonates from Phosphate Ores in. Acidic Media." Int. J. Miner. Process, 38: 235.8

El-Jalead, I.S., Abouzeid, A.Z.M., El-Sinbawy, H.A., (1980), “Calcination of phosphates: reactivity of calcined phosphate”, Powder Technology 26, 187–197 150-8

Fang, G. and L. Jun (2011). "Selective separation of silica from a siliceous–calcareous phosphate rock." Mining

Science and Technology, (China) 21(1): 135-139.

Jasinski, S. M. (2012). “Phosphate Rock”, mining engineering, USGS. 64: 81-84.

ÖZER, A. K. (2003). "The characteristics of phosphate rock for upgrading in a fluidized bed" Advanced Powder Technol, 14 (1): 33–42.

Sis, H. and S. Chander (2003). "Reagents used in the flotation of phosphate ores: a critical review." Minerals Engineering, 16 (7): 577-585.

Umar A.H, Yaro S.A, Abdulwahab M, and Dodo M.R. (2016). Characterization of Sokoto Phosphate Rock for Beneficiation, Journal of Raw Material Research, page 74-93.

Akindele, et al (2019) Nigerian Mining Journal, (16) 77 - 84
© Nigerian Society of Mining Engineers, ISBN 1117 - 4307

Characterization of Alawa Graphite, North-Central Nigeria

***Usman M. Akindele, **Shehu A. Yaro, and *Usaini, M.N.S**
*Department of Mineral and Petroleum Resources Engineering, Kaduna Polytechnic, Kaduna
**Department of Metallurgical and Materials Engineering, Ahmadu Bello University, Zaria
Corresponding Author: usmanakindele4mre@gmail.com.

Abstract
Bulk Alawa graphite sample were collected at three different locations, crushed and pulverized. A representative sample was obtained by coning and quartering method. Mineralogical study by XRD revealed graphite, quartz, muscovite and cronsdtetite as principal mineral phases. The head sample was analyzed and gave the average fixed carbon content of the deposit as 36.21% by proximate analysis other elemental composition revealed to be 67.14 % Si, 7.036% Fe, Calcium of 4.09%, Aluminum of 4.35% and 3.70% Potassium using XRF machine. Liberation study shown that 45 µm sieve size as the liberation size, having the highest-grade value of 35.39% fixed carbon (FC) fall within acceptable size for pencil making. The specific gravity of 2.178 on the average was obtained for the Alawa graphite. Also, an average work index determined to be 12.07kwh/ton. The mineralogical study, chemical analysis (proximate and XRF), specific gravity and work index determination indicated that Alawa graphite could be beneficiated to meet up various applications most especially to pencil grade for the greatest problem is that Nigeria still imports pencil even though the raw materials (graphite) required is much available in the country.
Keywords: Alawa graphite, characterization, Beneficiation, pencil grade.

Introduction

The key to the exploitation of minerals lies on the nation's ability to fully characterize her mineral deposits in such a manner that would expose their potentials, thereby attracting the much-needed investors. The identification and characterization of minerals is of fundamental importance in the development and operation of mining and mineral processing systems (Hope *et al*., 2001), and it is very important in choosing a suitable flowsheet for recovering the valuable constituents. It is also critical in optimizing actual plant for improving performance (Xiao and Laplante, 2004). According to Cook (2000), the growing need for detailed information about the mineralogical composition of a mineral deposit is an integral part of investigations. Knowledge of mineralogical/chemical composition, size, morphology and association with other minerals is therefore expected to provide insights and information on the characteristics, type, nature and amount of minerals and elements present within the ore at different locations. This would permit an assessment and determination of the optimal processing route for its constituent minerals/metals.

Graphite, a natural form of carbon, is characterized by its hexagonal crystalline structure. It occurs naturally in metamorphic rocks such as marble, schist and gneiss due to reduction of sedimentary carbon

compounds during metamorphism. It also occurs in igneous rock and in meteorites. The same element crystallizing in an octahedral system becomes a diamond. It is a lustrous black carbon mineral, unctuous, and relatively soft with a hardness of 1-2 on the Mohr's scale (Slodkevich, 2009). It occurs naturally in the earth's crust and is the most abundant form of pure carbon. Graphite exhibits the properties of metals and non-metals which makes it suitable for many industrial applications. The metallic properties include thermal and electrical conductivity while non- metallic properties are inertness, high thermal resistance and lubricity and a high melting temperature of about 3,500^{o}C (Tagiri, 2007).

The formation of graphite is a result of contact or regional metamorphism of sedimentary organic matter (e.g. organic material is transformed into graphite in response to increasing temperature and/or pressure in the Earth's crust) (Mitchell 1993; Kwiecińska and Petersen 2004). With the gradual increase of metamorphism, sedimentary carbonaceous material transforms first into an amorphous form of carbon (Landis, 1971; Wakamatsu and Numata, 1991). For certain industrial applications (see below) this amorphous carbon may substitute for crystalline graphite. Amorphous carbon resources are hosted by moderately metamorphosed marine sedimentary rocks, such as quartzites or phyllites, but also represent former coal beds. The "grain" size of this amorphous graphite is typically between +40–70 μm in diameter. Natural graphite may occur in metamorphosed siliceous rocks (typically quartzite) as well as metamorphosed carbonate rocks. Associated minerals with graphite occur as quartz, rock-forming silicates such as amphiboles and feldspars, also calcite, sulfides, or magnetite (Mitchell, 1993; Bulatovic, 2014).

Graphite, being one of the important non-ferrous minerals, finds applications in various important industries. More sophisticated applications of graphite are in refractories, expanded graphite-based sealing gaskets, graphitized grease, braid, brushes, brake lining, etc. It is also used in minor amounts as a vital additive for producing foundry coatings to prevent fusion of liquid metal with sand at the mould or core face. Such coatings are either applied by spraying or painting in the form of suspension or by dusting or rubbing as dry powders. Graphite used for coating is of high quality which does not peel off as flakes on drying and imparts a smooth surface to the casting. Graphite, a major additive to many coating systems, is known for its multifarious functions, in refractories, lubricants, thermal conductors, electrical conductors, UV shields, electromagnetic pulse shields, corrosion shields and pigments. It is also used as moderator in nuclear reactors. Traditional uses of graphite are found in crucibles, foundries, pencils, etc. (Indian Mineral Review, 2015).

Table 1: Importation of graphite by United States from 2011 to 2015

Items	**Years**				
	2011	**2012**	**2013**	**2014**	**2015**
Production, mine	-	-	-	-	-
Imports for consumption	72	57	61	61	66
Export	6	6	9	12	12
Consumption, apparent	65	50	52	53	54

Price of imports flake (dollars per ton)	1,180	1,370	1,330	1,270	1,240
Lump and chip (dollars per ton)	1,820	1,960	1,720	1,870	1,890
Amorphous (per ton)	301	339	375	360	370
Net import reliance as a percentage of apparent consumption	100	100	100	100	100

From table 1 above, USA imported 66,000 tons of natural graphite in 2015 at an average price of $1,240 per ton, while, world graphite production has risen to an estimated 1.2 million tons in 2016 at a compound annual growth rate of over 2% (USGS, 2016; SRG Graphite Inc., 2017).

According to the variety of applications, graphite demand has markedly increased in the last decade (Chelgani et al., 2016). Graphite is one of the main resources of graphene. Graphene obtained from high-grade graphite usually has good quality and is highly conductive (Jagiello et al. 2014). Global consumption of natural graphite has increased from ~600,000 tons in 2000 to 1.6 M tons in 2015 (Cowie 2012; Graphite One Resources 2015).

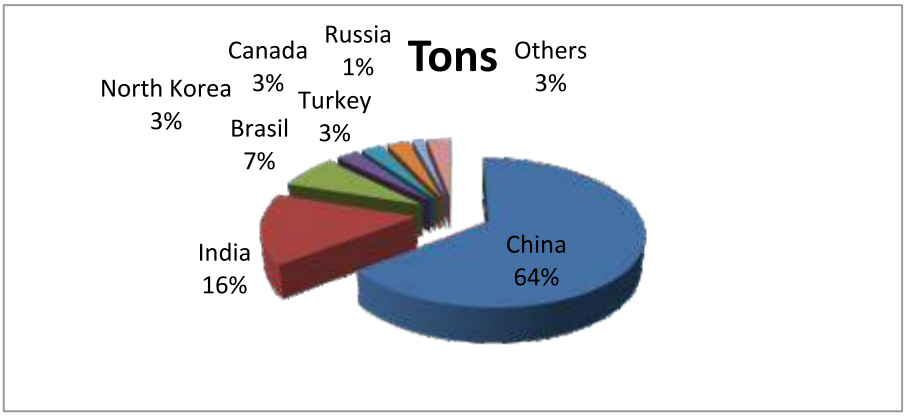

Figure 1: World natural graphite production estimated at 1.17million tonnes in 2014 with most of it originating in China (67%), India (15%), Brazil (7%), Canada (3%), Turkey (3%), and North Korea (3%) (George *et al*., 2015).

Raw Materials Research and Development Council (2010) reported an estimated reserve of Alawa graphite to be 1.1-3.3Mt thus makes the graphite stand as fundamental mineral to Nigeria's economy. Hence, the need to characterize Alawa graphite to determine metallurgical grade that can be used as feed for the production of pencil (The greatest problem is that Nigeria still imports pencil even though the raw materials (graphite) required is much available) and other graphite based products.

.

Materials and Methods

Sample Collection

Representative sample (50 Kg) was obtained from three points around the study area; Alawa, Rafi local government area of Niger state were used for the test work

Figure 2: Topographical Map of Alawa showing the sampling points

Equipment and Materials

Laboratory Jaw crusher, Pulverizer, Set of sieves, Laboratory sieve shaking machine, Weighing balance, Specific gravity bottle (Pycnometer), X-ray fluorescence machine, X-ray diffractometer machine, Furnace, Graphite sample.

Methodology

Alawa graphite lumps were crushed, pulverized, coned and quartered to yield a representative sample. The specific gravity was determined using pycnometer (density bottle) method, chemical compositions analyzed by XRF and proximate analyses while, XRD conducted for various associating mineral grains. Size – assay analysis of the Alawa graphite using a set of sieves mounted on a sieve shaker was carried out. The various size fractions retained on the various sieves were then weighed and assayed for fixed carbon (FC) content using proximate analysis.

Results and Discussion

Proximate/XRF

Table 2a: Result of Proximate Analysis

	Content %			
Head Sample	MC	VM	AS	FC
	14.11	18.26	31.42	36.21

Table 2b: Result of XRF Analysis

Element	Al	Si	K	Ca	Ti	V	Cr	Mn	Fe	Mg	Pb	Zn	Ba
%	4.35	67.14	3.70	4.09	0.40	0.38	0.06	0.86	7.03	0.15	0.19	0.42	0.26

The head sample was obtained by putting the entire sample from different pits together, mixed properly and a representative sample generated as head sample. The head sample was analyzed and gave the average fixed carbon content of the deposit as 36.21% by proximate analysis (Table 2a), other elemental composition revealed to be 67.14 % Si, 7.036% Fe, Calcium of 4.09%, Aluminum of 4.35% and 3.70% Potassium by XRF (Table 2b).

Sieve Size/ Assay Analysis

Table 3: Particle Size Analysis of Alawa Graphite

Sieves (um)	Wt (g)	Wt (%)	Cum wt(%) retained	Cum wt (%) passing	FC(%)
180	173.8	17.38	17.38	82.62	25.23
125	275.0	27.5	44.88	55.12	28.11
90	202.2	20.22	65.10	34.90	29.42
63	100.4	10.04	75.14	24.86	29.87
45	209.8	20.98	96.12	3.88	35.39
pan	38.8	3.88	100	0	

Table 3 shows the results of Sieve analysis of the head sample and the assay grade of carbon in the various sieve sizes. The first column shows the various sieve size in µm used in the sieve test. The coarsest sieve size used was 180 µm and the finest was 45 µm. The results had shown the 45 µm sieve size as the liberation size, having the highest grade value of 35.39% fixed carbon, followed by 63 µm of 29.87% FC, 90 µm of 29.42%, 125 µm of 28.11% and 1180 µm with the least having 25.23%.

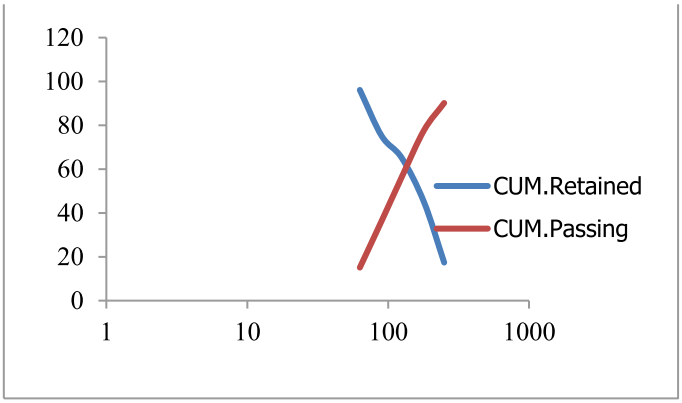

Figure 3: Graphical presentation of Alawa Graphite sieve analysis results

XRD Diffraction

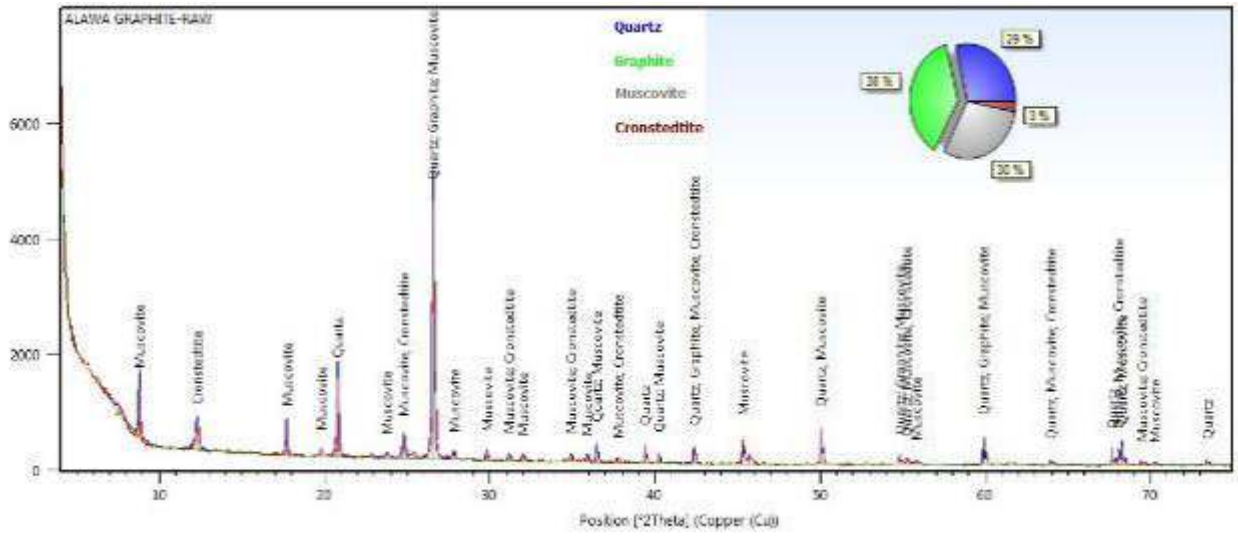

Figure 4: XRD diffraction pattern of Alawa Graphite

Table 4: Mineralogical composition of the Alawa Graphite as determined from XRD

Mineral name	Compound name	Empirical formula	Chemical formula
Graphite	Graphite	$C_{4.00}$	C
Muscovite	Phylosilicate mineral of Aluminum and Potassium	$KAl_3SiO_{10}(OH)_{1.8}F_{0.2}$	$KAl_2(AlSi_3O_{10})(FOH)_2$
Cronstedtite	Iron silicate mineral	$Fe^{2+}2Fe^{3+}2SiO_5(OH)_4$	$Fe{+}{+}2Fe{+}{+}{+}(SiFe{+}{+}{+})O_5(OH)_4$
Quartz	Silica mineral	Si_3O_6	SiO_2

The X-ray diffractometer result as shown in table 4 and figure 4, revealed the presence of four mineral phases. These are graphite, (38%), as the valuable mineral, quartz (29%), Muscovite (30%) and Cronstedtite (3%) as major and minor minerals present. The XRD result has agreed significantly with the results of proximate analysis.

Specific Gravity Determination

Specific Gravity is an essential mineral parameter needed to facilitate the assessment of the feasibility of separating mineral assemblage using gravity separation methods and computation of processing plant throughputs (Wills, 2006). It is mostly determined using the pycnometer method (Jones, 1987)

S.G. = $(w_1 – w)/ [(w_3 – w) – (w_2 – w1)]$

- Empty dried density bottle was weighed dried (w)
- Dried graphite sample plus empty density bottle was weighed (w_1)
- Density bottle + Alawa graphite sample + filled with water was weighed (w_2)
- Empty density bottled filled with water was weighed (w_3)

Table 11: Result of Specific gravity determined of Alawa graphite

	Test 1 (g)	Test 11 (g)
Wt of empty density bottle	23.3	23.3
Wt of empty density bottle + sample	28.3	28.3
Wt of empty density bottle + sample + water	73.4	73.2
Wt of density bottle + water	70.6	70.6

$$S.G\,(1) = (28.3 - 23.3)/[(70.6 - 23.3) - (73.4 - 28.3) = 2.273$$
$$S.G\,(11) = (28.3 - 23.3)/[(70.6 - 23.3) - (73.2 - 28.3)] = 2.083$$
$$\text{Average } S.G. = 2.178$$

The specific gravity of 2.178 on the average, was obtained for the Alawa graphite. The value obtained is within 2.1 – 2.3 for graphite minerals sighted in literature (Anon, 2017).

Conclusion

It is imperative that the key to successful beneficiation is greatly attached to the amount of information available on the nature and properties of the various components making up the mineral. The mineralogical studies carried out with XRD phase patterns, confirmed the availability of minerals such as graphite, quartz, muscovite and cronstedtite with percentage distribution of 38, 29, 30 and 3 respectively. The chemical composition determined by proximate analysis reveal average fixed carbon content of the deposit as 36.21%, other elemental composition revealed to be 67.14 % Si, 7.036% Fe, Calcium of 4.09%, Aluminum of 4.35% and 3.70% Potassium by XRF

Also, liberation study has shown that 45 µm sieve size as the liberation size, having the highest grade value of 35.39% fixed carbon (FC) fall within acceptable size for pencil making sighted in the literature (Indian Mineral Review, 2015), though require beneficiation to meet up the pencil grade.

Furthermore, the specific gravity of 2.178 on the average was obtained for the Alawa graphite. The value obtained is within 2.1 – 2.3 for graphite minerals.

References

Anonymous (2017). *Graphite and its properties*, free encyclopedia. Retrieved November 23.

Bulatovic, S. M., (2014), *"Beneficiation of graphite ore."* In Handbook of Flotation Reagents: Chemistry, Theory and Practice. Volume 3: Flotation of Industrial Minerals, Oxford, UK: Waltham, pp. 163–171.

Cook, N.J., (2000) Mineral characterisation of industrial minerals deposits at the Geological SurveyNorway: A Short Introduction. *Norges geologiske undersekelse Bulle tin,* 436, 189-192.

Cowie, A., (2012), The Biggest Graphite Find in Decades Comes With a Catch. Retrieved from http://moneymorning.com/

Chehreh Chelgani .S, Rudolph M., Kratzsch .R Sandmann D and Gutzmer G. (2016) A Review of Graphite Beneficiation Techniques Mineral Processing And Extractive Metallurgy Review, Vol. 37, NO. 1, 58–68

European Union, Report on critical raw materials for the EU, (2014), Report of the Ad hoc Working Group on defining critical raw materia, European Commission, pp. 1–41.

George J.S, Suzanne P, Carlee A (2015) Graphite deposit, types, their region and economic significance; *Symposium on strategic and critical materials procedings*. V3, pp 163-171

Graphite One Resources, (2015), Graphite 101. Retrieved from http://graphiteoneresources.com/

Hope, G.A., Woodsy, R., Munce, C.G., (2001). Raman microprobe mineral identification. Miner. Eng. 14 (12), 1565–1577.

Indian Mineral Review (2015) Graphite, Government of India, Ministry of Mines. 53rd Edition.

Jagiello, J., Judek, J., Zdrojek, M., Aksienionek, M., and Lipinska, L., (2014), "Production of grapheme composite by direct graphite exfoliation with chitosan." Materials Chemistry and Physics, 148, pp. 507–511.

Jones, M. P (1987). Applied Mineralogy, A quantitative Approach, pp 13 – 69, 150 - 176

Kwiecińska, B. and Petersen, H. I., (2004), "Graphite, semi-graphite, natural coke, and natural char classification-ICCP system." International Journal of Coal Geology, 57, pp. 99–116.

Landis, C. A., (1971), "Graphitization of dispersed carbonaceous material in metamorphic rocks." Contributions to Mineralogy and Petrology, 30, pp. 34–45.

Mitchell, C. J., (1993), Industrial Minerals Laboratory Manual: Flake Graphite, Technical Report WG/92/30, British Geological Survey, 35 pp.

Raw Materials Research and Development Council (2010), Non- Metallic Mineral Endowment in Nigeria.

Slodkevich, V.V., (2009); Graphite paramorphs after diamond. International Geology Reviews 25, 497–514.

SRG Graphite Incoperation, (2017) The Lola graphite deposit Eastern Guinea, West Africa, corporate presentation, Slide 19

Tagiri, M., (2007). A measurement of the graphitizing-degree by the X-ray powder diffractometer. Journal of the Japanese Association of Mineralogists, Petrologists and Economic Geologists 76, 345–352.

Yaro, S. A. and Thomas, D. G., (2013): Mineral Processing Engineering Practical Manual (Some Aspects), Department of Metallurgical and Materials Engineering, A.B.U Zaria: unpublished.

Wakamatsu, T. and Numata, Y., (1991), "Flotation of graphite." Minerals Engineering, 4, pp. 975–982.

Xiao, Z., Laplante, A.R., (2004). Characterizing and recovering the platinum group minerals—a review. Miner. Eng. 17, pp 961–979.

NIGERIAN MINING JOURNAL

INFORMATION FOR AUTHORS

Scope
NIGERIAN SOCIETY OF MINING ENGINEERS presents technical papers covering the fields of mining, mineral processing and extractive metallurgy. The papers provide in-depth information on research findings from various aspects of actual exploitation of minerals and related engineering practice. Researches based on local technology are particularly welcome.

Manuscripts
Manuscripts submitted for publication must represent original contributions and should not have been proposed for publication elsewhere. The papers should be based on original research, innovations and field experience in Mining, Mineral Processing, Extractive Metallurgy and Equipment Maintenance relevant to the minerals industry. Three copies of each manuscript must be submitted together with the electronic copy containing the author(s) papers, preferably in Microsoft Word environment

Abstract
The manuscript must include an abstract summarizing the main aspects of the paper in not more than 200 words. The main results must be stated clearly.

Text
Papers should be typewritten with double line spacing and wide margins on one side only. Each page should be numbered. The first page should include a concise title of the paperand the author(s) name(s), affiliation(s) and addressees). In order to maintain consistency, titles such as Engr, Dr, Prof, should be avoided as they frequently change. The authors have to secure the right of reproduction of any material that has already been published elsewhere.

Units
The S.I. unit is mandatory. However in isolated accepted cases authors should insert conversion factors or monographs.

Mathematical symbols and formulae
All characters available on a normal typewriter must be typewritten in the text as well as in the equation. Symbols that must be drawn by hand should be identified on the margin. Subscripts and superscripts should all be clear. Equations referred to in the text should be placed between parentheses at the right hand margin.

Figures
All illustrations should be drawn using black ink or AutoCAD on good quality paper. The originals or good quality photographic prints (maximum 210 x 297mm) should be submitted together with the manuscript. Each figure must be referred to in the text with the number clearly written on the back of the photograph or drawing. Lettering or figures should be large enough to enable clarity of reproduction after reduction.

Tables
Each table should be typed on a separate sheet as the authors expect it to appear in print. They should carry a brief title on top. They should be numbered and referred to in the text. .

Reference
References should be in APA system or listed in alphabetical order of the first author. Quotation of papers in the reference list should be as follows:

Books: Jaeger, J.C and Cook N.G.W. (1979) Fundamental of Rock Mechanics: Chapman and Hall London

Journals: Ojo, O and Brook, N: (1990) The effect of moisture on some mechanical properties of rock. Mining' Science and Technology, 8(2), 14-26

Unpublished work: Umoru, E.E. (1996) Re-appraisal of mining methods of Ameka Lead/zinc deposit. Unpublished HND project, Kaduna Polytechnic Kaduna, Nigeria.

Proceedings: Bello,S.B. (1996) Optimisation of mning parameters of sub-basalt underground mine development of solid mineral for national self-reliance and economic growth. Edited by E.O.A. Damisa, Engineering Conference Series, pp 202-215

Assignment of Copyright Ownership
Submission of a manuscript for possible publication in the Nigerian Mining Journal carries with it the understanding that the manuscript has not been *published* nor is being simultaneously considered for publication elsewhere. On submission of a manuscript, the author(s) agree that the copyright to their articles is assigned to the Nigerian Society of Mining Engineers (NSME) if and when the articles are accepted for publication.